

**Identification of Mouse Cytomegalovirus Factors that  
Determine the Tropism for Epithelial Cells and that  
Induce Morphological Changes in Infected Cells**

Von der naturwissenschaftlichen Fakultät der  
Gottfried Wilhelm Leibniz Universität Hannover

zur Erlangung des Grades einer

**DOKTORIN DER NATURWISSENSCHAFTEN**

**Dr. rer. nat.**

genehmigte Dissertation

von

Dipl. Biol. Sarah Sengstake

geboren am 24.06.1978 in Bremen

Referent: Prof. Dr. Martin Messerle  
Korreferent: Prof. Dr. Georg Herrler  
Tag der Promotion: 2. Juni 2009

# 1 Abstract

Cytomegaloviruses (CMVs) infect different cell types, such as epithelial cells. Epithelial cells are of particular importance for CMV infections, since they are exposed first to infectious virus and therefore are first targets for CMV. Cytomegaloviruses are transmitted by bodily fluids that are secreted by epithelial cells. The broad cell tropism of CMV results from the acquisition of cell tropism factors. Viral factors that determine the tropism of mouse CMV (MCMV) for endothelial cells or macrophages have been described. Viral factors that determine the tropism of MCMV for epithelial cells, however, remain to be identified. CMVs induce cell rounding that causes the formation of characteristic plaques in the cell monolayer. This cytopathic effect is only poorly characterised for MCMV.

The present study aimed to identify factors of MCMV that determine the tropism for epithelial cells and the induction of cell rounding during infection. To this end, a library of MCMV mutants was generated. Genes were deleted that are dispensable for viral growth in fibroblasts. Subsequently, the growth properties of the MCMV deletion mutants were investigated in epithelial cells and fibroblasts. In parallel, the infected fibroblasts were screened for a loss of cell rounding.

A virus mutant, lacking the gene region of m106 to m108, yielded strongly reduced titres in epithelial cells compared to those of the wild type MCMV. By contrast similar titres were measured in fibroblasts. Therefore, the presence of tropism factors for epithelial cells in this region of the MCMV genome was assumed. The analysis of additional mutants excluded the m106 gene and a stable intron RNA as potential epithelial tropism factors. The prevention of potential m107 or m108 protein synthesis did not, however, inhibit the growth of the respective mutants in epithelial cells. These results demonstrated that neither proteins nor RNA account for the impaired growth of the m106-m108 deletion virus. DNA sequences within the m106-m108 region of the MCMV genome that are as yet undetermined possibly bind epithelial cell-specific transcription factors and are a prerequisite for the productive infection of epithelial cells. The analysis of the morphology of infected fibroblasts revealed that M25-deficient MCMV mutants lost their ability to induce cell rounding. This could be restored with inserting M25 in the mutant genome. M25 induced cell rounding in the absence of other MCMV genes. The synthesis of M25 mRNAs and their translation into proteins correlated with the kinetics of MCMV-induced cell rounding. In this study, M25 was identified as the MCMV gene that is necessary for the induction of cell rounding.

**mouse cytomegalovirus, cell tropism, cytopathic effect**

# Zusammenfassung

Zytomegaloviren infizieren verschiedene Zelltypen, darunter auch Epithelzellen. Epithelzellen spielen eine besondere Rolle für die Zytomegalovirus-Infektion. Sie sind vermutlich die ersten Zellen, die infiziert werden und Zytomegaloviren werden in Körperflüssigkeiten übertragen die von Epithelzellen sezerniert werden. Der breite Zelltropismus der Zytomegaloviren beruht auf dem Erwerb von Zelltropismusfaktoren. Bisher konnten für das murine Zytomegalovirus (MCMV) Gene für den Endothelzell- und den Makrophagentropismus gefunden werden. Gene, die den Epithelzelltropismus des MCMV bestimmen, sind hingegen unerforscht. CMV-infizierte Zellen runden sich ab was zu einem charakteristischen Plaque im Zellrasen führt. Dieser zytopathische Effekt ist für MCMV bisher wenig charakterisiert.

Das Ziel der Arbeit war die Identifizierung von viralen Genen, die den Epithelzelltropismus des MCMV bestimmen und das Abrunden der Zellen während der MCMV-Infektion induzieren. Zu diesem Zweck wurde eine Bibliothek von MCMV-Mutanten hergestellt, in denen Gene deletiert wurden, die nicht essentiell für das Wachstum in Fibroblasten sind. Die Deletionsmutanten wurden anschliessend auf ihre Wachstumseigenschaften in Epithelzellen und Fibroblasten hin überprüft. Die infizierten Fibroblasten wurden ausserdem auf einen Verlust der Zellabrundung hin untersucht.

Für das Virus, in dem die Gene m106-m108 deletiert sind, wurden stark reduzierte Titer in Epithelzellen im Vergleich zu denen des Wild-Typ MCMV festgestellt. Die Titer der beiden Viren in Fibroblasten waren hingegen vergleichbar. Daraus wurde geschlossen, dass in der m106-m108 Gen-Region Faktoren für den Epithelzelltropismus kodiert sind. Mit Hilfe von weiteren Deletionsmutanten konnten das m106-Gen und eine stabile Intron RNA als mögliche Epithelzelltropismusfaktoren ausgeschlossen werden. Auch die Verhinderung einer möglichen Synthese der m107- oder m108-Proteine schränkte das Wachstum der Viren auf Epithelzellen nicht ein. Diese Ergebnisse zeigten, dass weder Proteine noch RNA in der m106-m108 Region des Genomes Tropismusfaktoren für Epithelzellen darstellen. Möglicherweise funktionieren noch nicht identifizierte DNA-Sequenzen in dieser Region als Bindeelemente für epithelzell-spezifische Transkriptionsfaktoren und sind somit eine Voraussetzung für die effiziente Vermehrung des MCMV in Epithelzellen.

Die Überprüfung der Morphologie der infizierten Fibroblasten zeigte, dass ein Fehlen des M25-Gens im Virusgenom zu einem Verlust der Zellabrundung führt. Diese Eigenschaft konnte mit der Insertion des M25-Gens in die Mutante wiederhergestellt werden. Die Funktion des M25-Gens war unabhängig von anderen MCMV-Genen. Die Synthese von M25 mRNAs und deren Translation in Proteine korrelierte zeitlich mit dem MCMV-induzierten Zellabrunden. Somit wurde M25 als das MCMV-Gen identifiziert, welches für die Abrundung von MCMV-infizierten Zellen notwendig ist.

**Murines Zytomegalovirus, Zelltropismus, Zytopathischer Effekt**

# Contents

<b>1</b>	<b>Abstract</b>	<b>1</b>
<b>2</b>	<b>Introduction</b>	<b>5</b>
2.1	The Biology of Cytomegaloviruses . . . . .	5
2.2	The Mouse Model of CMV Infection . . . . .	7
2.3	The Herpesvirus Life Cycle . . . . .	8
2.4	Organisation of the MCMV Genome . . . . .	11
2.5	Cytomegalovirus Gene Expression . . . . .	12
2.6	Cytomegalovirus Cell Tropism . . . . .	14
2.7	Cytomegalovirus-Induced Cell Rounding as a Cytopathic Effect . . . . .	17
2.8	Genetic Manipulation of Cytomegaloviruses . . . . .	20
2.9	Aims of the Study . . . . .	23
<b>3</b>	<b>Material</b>	<b>25</b>
3.1	Chemicals and Reagents . . . . .	25
3.2	Cells and Bacteria . . . . .	27
3.3	Antibodies, Probes and Antibiotics . . . . .	28
3.4	BACs and Plasmids . . . . .	28
3.5	Laboratory Equipment . . . . .	29
<b>4</b>	<b>Methods</b>	<b>31</b>
4.1	Eukaryotic Cell Culture . . . . .	31
4.2	Mutagenesis of BACs using linear PCR Fragments . . . . .	31
4.3	Culture of Bacteria . . . . .	33
4.4	Virological Methods . . . . .	33
4.5	DNA Methods . . . . .	35
4.6	RNA Methods . . . . .	41
4.7	Protein Methods . . . . .	43
4.8	Cell Tropism Assay . . . . .	45
4.9	Infection of Cells for the Screening of the Cellular Morphology . . . . .	46
4.10	Analysis of the Cellular Morphology after Transfection of the pIRES vectors . . . . .	46
4.11	Bioinformatic Tools . . . . .	47

<b>5</b>	<b>Results</b>	<b>49</b>
5.1	Generation of a Library of Mouse Cytomegalovirus Mutants . . . . .	49
5.2	Searching for Viral Factors determining the Epithelial Cell Tropism of MCMV .	52
5.2.1	Establishment of a Cell Tropism Assay and Screening of a Library of MCMV Mutants . . . . .	53
5.2.2	Analysis of the $\Delta$ m106-m108 Virus Mutant . . . . .	58
5.2.3	Does the 7.2 kb Stable Intron RNA Function as a Tropism Factor for Epithelial Cells? . . . . .	61
5.2.4	Analysis of the m107 and m108 Genes as Viral Factors Determining the Epithelial Cell Tropism of MCMV . . . . .	66
5.3	Identification of a Viral Gene Involved in MCMV-Induced Cell Rounding . . . .	73
5.3.1	MCMV M25 plays a Major Role in Changing Cellular Morphology after CMV Infection . . . . .	73
5.3.2	Re-Insertion of the M25 Gene . . . . .	77
5.3.3	Analysis of the Growth Properties of the $\Delta$ M25 Virus . . . . .	77
5.3.4	Morphological Changes are Induced at Early Stages of Infection and are M25 Dependent . . . . .	80
5.3.5	Investigation of M25-Induced Cell Rounding Outside the Context of the Viral Genome . . . . .	83
5.3.6	The M25-Derived 105 kDa Protein is the Predominate Species Ex- pressed During Early Stages of MCMV-Infection . . . . .	85
5.3.7	Analysis of M25 Transcripts . . . . .	86
5.3.8	Identification of Proteins Expressed from M25 Transcripts . . . . .	87
5.3.9	Subcellular Localisation of M25 Proteins . . . . .	93
<b>6</b>	<b>Discussion</b>	<b>97</b>
6.1	Generation of a Library of Mouse Cytomegalovirus Mutants . . . . .	97
6.2	Searching for Mouse Cytomegalovirus Epithelial Cell Tropism Factors . . . . .	99
6.3	Identification of a Viral Gene Involved in MCMV-Induced Cell Rounding . . . .	108
	<b>Bibliography</b>	<b>121</b>
<b>A</b>	<b>Anhang</b>	<b>139</b>

# Abbreviations

aa	amino acid
ATP	adenosine triphosphate
BAC	bacterial artificial chromosome
bp	base pairs
cDNA	complementary DNA
cAMP	cyclic adenosine monophosphate
cdc	cell division cycle
Da	Dalton
DNA	desoxyribonucleic acid
F-actin	filamentous actin
GFP	green fluorescent protein
HCMV	human cytomegalovirus
IE	immediate-early
IRES	internal ribosome entry site
kbp	kilo basepairs
KnR	kanamycin resistance cassette
MCMV	mouse cytomegalovirus
MEF	mouse embryonic fibroblasts
MOI	multiplicity of infection
mRNA	messenger RNA
ORF	open reading frame
PFU	plaque forming units
PCR	polymerase chain reaction
p.i.	post infection
RNA	ribonucleic acid
rpm	rounds per minute
SDS-PAGE	sodium dodecyl-polyacrylamide gel electrophoresis
$\mu\text{g}$	microgram
$\mu\text{l}$	microliter





## 2 Introduction

### 2.1 The Biology of Cytomegaloviruses

The Herpesviridae are categorised into three subfamilies, Alpha-, Beta-, and Gammaherpesvirinae [Pellett and Roizman, 2007]. Alphaherpesviruses infect reptiles, birds and mammals whereas betaherpesviruses and gammaherpesviruses only infect mammals. The further classification within a herpesvirus subfamily is based on the similarity of the DNA sequence, the genome arrangement and the expression of characteristic proteins. Cytomegaloviruses (CMVs) belong to the subfamily of betaherpesviridae. Members of the betaherpesviruses are species-specific, i.e. they productively replicate only in cells of one species. All herpesviruses establish a latent infection in their host.

Human CMV (HCMV) infects the human population worldwide [Britt, 2008, Mocarski et al., 2007]. Evidence of a previous HCMV infection is present in nearly 100% of children and adults from developing countries in Africa, Asia and South America whereas less than 30% of adults in some areas of North America and Northern Europe have been infected with HCMV.

The clinical symptoms and the severity of disease caused by an acute HCMV infection depend on the immune status of the host. In the healthy, immune competent host HCMV manifests, if at all, in low-grade fevers, fatigue and headache. Rarely, HCMV infection in the immune competent host leads to severe disease such as encephalitis, myocarditis, or ocular disease. Transplant patients, who are immune suppressed, or people suffering from Acquired Immune Deficiency Syndrome (AIDS) develop more severe diseases. HCMV is the most common viral infection after transplantation and is one of the first opportunistic pathogens identified in patients with AIDS. HCMV infection in these immune suppressed patients often manifests as hepatitis, retinitis, pneumonia or enteritis.

Attempts to investigate the course and the pathogenesis of HCMV employ animal models such as the mouse model of CMV [Mercer and Spector, 1986, Baltesen et al., 1993, Collins et al., 1994]. Mouse CMV (MCMV) infection is characterised by an acute phase with the highest amounts of virus (titres) typically found in liver and spleen around day four and day sixteen after infection [Mercer and Spector, 1986]. Thereafter, the virus persists at low titers in these organs. In the salivary glands, the organs in which MCMV replicates to the highest titres, the peak virus titres occur around day eight after infection declining thereafter indicating the switch to the persistent phase. At day thirty-nine after infection, infectious virus can still be

measured in the salivary glands whereas the titres remain under the detection limit in spleen and liver. Virus can still be detected in the salivary glands after four months of infection but is not detectable in spleen, liver and salivary glands around six months after infection indicating latency [Baltesen et al., 1993]. During latency, viral gene expression is thought to be restricted to genes that ensure the maintenance of the viral genome. MCMV latency is further characterised by a reduced viral genome number in comparison to the acute infection and the absence of CMV-specific antigens [Baltesen et al., 1993].

During an acute infection, CMV is continuously shed into bodily fluids such as saliva, breast milk or genital secretions. Transmission of CMV between individuals occurs by close contact with these fluids. Primary CMV infection often takes place at a young age, via breast milk or during childhood via the saliva of acutely infected children. Most infants that have been exposed to infectious bodily fluids such as breast milk from mothers with an acute HCMV infection become infected with HCMV [Dworsky et al., 1983]. Virus shed from acutely infected children also represents a source of infection for HCMV negative adults. In sexually active adolescents, infection is presumed to occur via exposure to genital secretions bearing infectious virus particles. Other routes of infection that do not include direct human-to-human contact are blood transfusions or organ transplants from HCMV-positive donors.

Most HCMV infections are thought to occur as a result of exposure of the epithelium at mucosal surfaces to infectious HCMV. Studies in primates have demonstrated that infection of the oral mucosa leads to dissemination of the virus and subsequent infection of organs such as the liver and spleen [Lockridge et al., 1999]. Oral or intravenous inoculation of rhesus macaques with rhesus CMV both lead to virus dissemination and infection of liver and spleen. However, dissemination after oral inoculation was delayed suggesting that the virus replicates in the mucosal epithelium before it then spreads to secondary organs such as liver and spleen [Lockridge et al., 1999]. Studies in mice are consistent with this mode of spread in the host. MCMV is first detected in blood leukocytes after intraperitoneal inoculation of mice with MCMV, representing the first viremia. The virus is then disseminated to liver and spleen where it again replicates to high titres thereby causing the second viremia [Collins et al., 1994]. These organs may serve as reservoirs for infectious virus during acute infection allowing the spread to other organs. The salivary gland has been shown to be a site of persistent infection where the virus continuously replicates to high titres after the virus has been cleared from liver and spleen [Jonjic et al., 1989]. MCMV replicates in a specialised cell type of the salivary gland, the acinar glandular epithelial cell. This cell type provides a niche for CMV, delaying its elimination by immune cells, predominately mediated by CD4<sup>+</sup> T cells [Jonjic et al., 1989]. The salivary gland is also the first organ from which MCMV was isolated and propagated in cell culture [Smith, 1954] and the reason why CMV is also called salivary gland virus.

## 2.2 The Mouse Model of CMV Infection

Cytomegaloviruses are species-specific, thus human CMV pathogenesis can not be studied in other animals. In order to analyse various aspects of CMV infection one has to make use of animal CMV models such as the mouse model of CMV infection. MCMV and HCMV have colinear genomes meaning that their genomic organisation is very similar [Rawlinson et al., 1996]. The MCMV and HCMV genomes contain a core of gene blocks that are conserved in order and gene content among all herpesviruses (Fig.2.2). These conserved gene blocks are flanked with genes that have homologs in all CMVs. However, there are also differences between the two viruses as their genomes contain genes that are unique for MCMV or HCMV [Rawlinson et al., 1996]. Despite their genetic differences, the similar courses of infection in their respective hosts with respect to the cell types, tissues and organs infected makes MCMV a valuable animal model for HCMV.

The CMV mouse model has been useful in studying CMV-directed immune responses and CMV dissemination [Holtappels et al., 2008, Bale and O'Neil, 1989, Collins et al., 1994, Noda et al., 2006, Saederup et al., 2001, Sacher et al., 2008]. The fact that CD8<sup>+</sup> T cells are antiviral effector cells which prevent virus dissemination and organ disease during MCMV infection was concluded from in vivo mouse experiments [Holtappels et al., 2008]. The adoptive transfer of CMV-specific CD8<sup>+</sup> effector and memory T cells not only limited CMV infection but also prevented the manifestation of CMV-infection in tissues. These results were fundamental for the establishment of clinical trials using CMV-specific CD8<sup>+</sup> T cells and supported the establishment of a T cell based immunotherapy in CMV-disease [Riddell et al., 1991].

Leukocytes are believed to be the source of CMV dissemination within the human or murine host. All leukocyte subsets isolated from peripheral blood of immunocompromised patients with acute CMV infection were positive for HCMV DNA, arguing that these cells play a role in CMV dissemination [Gerna et al., 1992]. The role of leukocytes during CMV infection was investigated in the mouse model. The detection of infectious virus or viral DNA in blood leukocytes isolated from both immune competent and immune deficient mice indicated that leukocytes may also be the major source for dissemination of MCMV, thereby further emphasising the biological similarities between MCMV and HCMV [Bale and O'Neil, 1989, Collins et al., 1994]. Virus dissemination using leukocytes is actively stimulated by the virus itself, exploiting host adaptive immune cells. A MCMV-secreted viral chemokine, MCK-2, attracts and recruits leukocytes to sites of infection [Saederup et al., 2001, Noda et al., 2006]. A MCK-2 deletion virus showed less infiltration of leukocytes into the infected tissue and an impaired dissemination to the salivary glands.

In order to shed light on CMV dissemination, the contribution of virus spread from infected hepatocytes was investigated in transgenic mice using a genetically modified MCMV. Sacher et al. constructed a MCMV virus with a marker gene which is exclusively expressed in hepatocytes

following activation by Cre-recombinase [Sacher et al., 2008]. Viruses that infected hepatocytes and also progeny viruses expressed the marker protein, GFP, in order to follow virus spread from the liver to other organs. The authors could show that hepatocytes are among the first cells in which the virus grows to high titers during the course of infection. Surprisingly, however, these cells are not the main source of MCMV dissemination since MCMV did not spread from the liver to other organs.

In general, to study CMV pathogenesis, the use of mice is advantageous over other animals such as guinea pigs, rats, or primates, in that a wide variety of genetically modified mice that are applicable in CMV research are available. In addition, a humanised mouse model has been established in order to study HCMV replication in human implants. SCID-hu mice, severe combined immunodeficient (SCID) mice carrying a human tissue implant, were used to investigate human CMV replication *in vivo* [Mocarski et al., 1993]. Implanted human fetal liver or thymus tissue allowed the *in vivo* growth of HCMV in these mice. The restricted host range of CMV was maintained since virus was only found in the implanted tissues. In addition, virus replication could also be controlled in these implants by applying antiviral treatment and thus provided a tool to study the efficacy of antiviral therapeutics. Further, the model system was also used to study the growth properties of low-passaged or high-passaged HCMV isolates in human implants [Brown et al., 1995]. However, this humanised mouse model is of limited use since HCMV pathogenesis or any other question related to the immune response directed against HCMV cannot be studied.

### 2.3 The Herpesvirus Life Cycle

Viral productivity and fitness is a function of the ability of the virus to enter, replicate and exit from a cell in an efficient way. The architecture of the mature virion is common to all members of the herpesviruses [Pellett and Roizman, 2007]. The size of a herpesvirus virion varies between 120 and 260 nm, and consists of an icosahedral (20 faces) nucleocapsid containing the capsid with the viral dsDNA, the tegument which is an amorphous protein layer surrounding the capsid, and the lipid envelope containing viral glycoproteins.

In HCMV infection, the envelope glycoprotein complexes consisting of gB or gM/gN or gH/gL bind to cell surface receptors such as integrins or heparan sulfate proteoglycans (HS) (Fig.2.1, (1)) [Feire et al., 2004, Wang et al., 2005, Compton et al., 1993]. For viral entry, virions either fuse with the plasma membrane thereby releasing virus capsids into the cytoplasm or virions are endocytosed (Fig.2.1, (2)). The cellular transport machinery is exploited to deliver the herpes genome towards the nucleus [Radtke et al., 2006]. In fact, microtubules are required for efficient transport of HCMV capsids towards the nucleus (Fig.2.1, (3)) [Ogawa-Goto et al., 2003]. The release of HCMV viral capsids from endocytic vesicles into the cytoplasm occurs



Figure 2.1: **Summary diagram of the herpesvirus life cycle.** Details of the different steps are described in the text. Modified from Mettenleiter et. al, 2006

via low pH-dependent fusion of the viral envelope with the endosomal membrane (Fig.2.1, (4)) [Ryckman et al., 2006]. The viral DNA is released into the nucleus after the viral capsids have reached the nuclear pore. Viral gene expression, viral replication and packaging of the newly replicated viral genomes into preformed capsids, takes place in the nucleus (Fig.2.1, (5-6)).

The analysis of herpesvirus capsids by cryo-electron microscopy and 3D image reconstitution revealed that herpesvirus capsids have a unique structure [Zhou et al., 1994, Butcher et al., 1998, Trus et al., 2001]. The capsid shell consists of protein complexes called capsomers that are formed by 150 hexons and 12 pentons which are connected by proteins organised in triplexes. The HCMV capsid proteins that assemble into these capsomers are the major capsid protein (MCP, UL86) the triplex monomer and triplex dimer protein (TR1, UL46, TR2, UL85), and the smallest capsid protein (SCP, UL48/49) [Gibson, 2006]. The CMV nucleocapsid has a diameter of approximately 130 nm in which the viral genome is tightly packaged [Butcher et al., 1998].

The current model for the egress and the release of herpesviral viral particles at the plasma membrane is the two-step envelopment process [Mettenleiter et al., 2006, Mocarski et al., 2007]: Primary envelopment describes mature nucleocapsids that bud through the inner nuclear membrane into the perinuclear cleft.

The primary envelope fuses with the outer nuclear membrane thereby releasing the viral capsid into the cytoplasm (Fig.2.1, (7)).

The tegumentation of nucleocapsids takes place in the cytoplasm and is initiated at two sites, the virus capsid and outer tegument proteins assemble at vesicles for final envelopment (Fig.2.1, (8)) [Mettenleiter et al., 2006]. The surface of the capsid provides anchor points for tegument proteins and the binding of additional tegument proteins requires specific and direct interaction with capsid proteins as was revealed from electron cryomicroscopy of herpesviral capsids and image reconstitution [Trus et al., 1999]. Close-up views of reconstituted images of herpesviral capsids demonstrate binding of tegument proteins to pentons and hexons [Chen et al., 1999]. Thus, the viral capsid provides a surface to which tegument proteins are consecutively added in a defined order via protein-protein interactions.

Tegument proteins constitute the layer that surrounds the nucleocapsid and play a role during entry or maturation of the virion. They are involved in the assembly of the virion or the uncoating of the virus particle during entry and are packaged into the virion to ensure their presence upon infection of a new host cell [Mocarski et al., 2007]. Other tegument proteins alter the host cell cycle and stimulate the host cell metabolism to produce optimal conditions for replication. As many as fifty-nine viral proteins were found in purified HCMV virions by mass-spectrometry [Varnum et al., 2004]. The functions or predicted functions of a total of 17 tegument proteins have been described, fourteen of which have been identified in purified virions [Gibson, 2006]. Among the most abundant proteins purified from HCMV-infected cell cultures are the major tegument protein pp65 (UL83), and the basic phosphoprotein BPP (pp150, UL32) which is also a tegument protein. The latter protein has the highest immunogenic potential, since the strongest reactivity in human sera was found directed against pp150 [Jahn et al., 1987]. The UL32 and UL82 homologs in MCMV, M32 and M82, have been identified in purified MCMV virions among other tegument proteins with unknown function such as M25 [Kattenhorn et al., 2004]. Six HCMV envelope glycoproteins have been identified that are conserved among all herpesviruses and are essential for viral replication in cell culture [Eickmann et al., 2006, Britt, 2007]. These glycoproteins form the gI (gB), gII (gM/gN) and gIII (gH/gL/gO) membrane-anchored glycoprotein complexes.

The site in the cytoplasm at which the nucleocapsid and the surrounding tegument become enveloped is not well defined. Electron microscopy analysis of herpesvirus assembly showed that nucleocapsids obtained their membranous envelope by budding into cytoplasmic vesicles [Tooze et al., 1993, Mettenleiter et al., 2006]. Based on the findings that envelope glycoproteins are recycled from the plasma membrane to the trans-golgi-network in HCMV-infected cells and that nucleocapsids bud into the cisternae of the trans-golgi-network, the capsid envelopment is thought to occur in an intermediate compartment consisting of vesicles of early/recycling endosomal vesicles and cisternae of the trans-golgi-network (Fig.2.1, (9)) [Schmelz et al.,

1994, Homman-Loudiyi et al., 2003, Tooze et al., 1993]. The final egress of mature virions resembles the exocytosis of secretory vesicles as the release of herpesvirus particles occurs via fusion at the plasma membrane (Fig.2.1, (10)) [Mettenleiter et al., 2006].

In addition to infectious viral particles, non-infectious enveloped viral particles are released in superior numbers during HCMV infection (Fig.2.1, (11)). These particles do not contain viral DNA and have either no capsid at all (dense bodies) or have an immature capsid (non-infectious enveloped particles) [Irmiere and Gibson, 1983]. In both types of non-infectious particles, the tegument composition is different from that of the infectious particles and their presence indicates that neither the packaging of the viral genome nor capsid assembly is required for secondary envelopment. During infection *in vivo*, it is possible that these particles impede the immune response by binding to immune effector cells thereby allowing the infectious viral particles to reach their targets.

## 2.4 Organisation of the MCMV Genome

MCMV, as do all herpesviruses, possesses a linear double stranded DNA genome that circularises immediately upon its release from capsids into the nuclei of infected cells [Pellett and Roizman, 2007]. Sequence analysis of the MCMV Smith strain revealed a genome length of 230 kbp that is similar to that of HCMV (230 kbp) but larger than the genome size of the alphaherpesvirus herpes simplex virus type-1 (152 kbp) and the gammaherpesvirus Karposi's sarcoma-associated herpesvirus (170 kbp) [Rawlinson et al., 1996, Pellett and Roizman, 2007].

A total of 170 ORFs were predicted for MCMV, based on the analysis of the genomic sequence of the Smith strain [Rawlinson et al., 1996]. However, this prediction of ORFs had limiting criteria such as a minimum length of 300 bp and less than 60% overlap with adjacent ORFs. Thus, the prediction excluded ORFs that might encode proteins but that are shorter in length. In addition, this was only a prediction based on the genomic sequence and did not include an analysis of viral gene expression. Lowering the criteria for an ORF to a minimum length of 150 bp led to the prediction of 14 additional ORFs within the MCMV sequence and further analysis of viral gene expression in cells confirmed the existence of the majority of all predicted ORFs [Tang et al., 2006]. Sequence analysis of the Smith strain without restriction to the degree of overlap between putative protein-coding regions and with a focus on ORFs with more than 60 bp predicted several additional ORFs [Brocchieri et al., 2005]. The newly annotated ORFs, such as m106.1, m106.2, m107.1, m107.2 and m107.3 are partly located inside previously predicted ORFs.

The MCMV genome contains genes that are conserved across the herpesviruses and which are clustered in seven core gene blocks in the central part of the MCMV genome (Fig.2.2). The block arrangement and the gene order differs across the herpesvirus families but is conserved

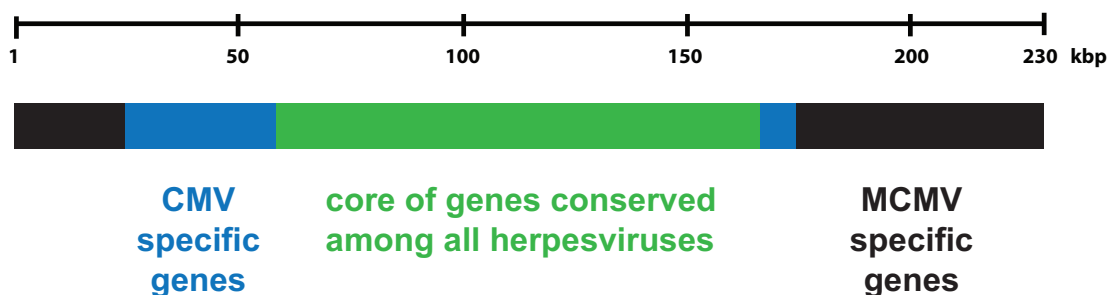


Figure 2.2: **Organisation of the MCMV genome.** The core of genes that are conserved among all herpesviruses is located in the center of the MCMV genome. This region is flanked by genes that are common within the betaherpesvirus family. MCMV-specific genes are located at the termini of the genome. A kbp scale is given for the orientation of the gene regions within the genome.

within a subfamily [Pellett and Roizman, 2007]. Thus, the position and the orientation of the MCMV gene blocks are identical to those of HCMV. The core of conserved genes contains the genes from M44 to M115 that encode mainly proteins that are essential for the viral replication machinery and for the assembly of the virus particle. It also encompasses the origin of lytic replication, *oriLyt*, which is required for replication of the viral DNA [Masse et al., 1997]. In addition to the core conserved genes, MCMV contains genes that are HCMV homologs and are distributed within the central part of the genome. In contrast, genes present in the left and right termini of the sequence are unique to MCMV [Rawlinson et al., 1996].

The comparison of the genomic sequences of different MCMV isolates identified the highest variability across the genome in these termini [Mocarski et al., 2007, Smith et al., 2008]. The left and right termini of the MCMV genome consist of 31 bp direct repeats that contain cis-acting signals for the cleavage and packaging of viral DNA during viral replication. The presence of viral genes that show homology to cellular genes suggests that herpesviruses have captured cellular genes during co-evolution with their host. These genes are likely to be insertions of a cDNA copy from cellular mRNA or pre-mRNA species [Davison and Bhella, 2007]. These cellular homologs are predominately located towards the genomic termini and between the core gene blocks [Pellett and Roizman, 2007]. MCMV ORFs with homology to cellular genes include the M33 and the m144 genes that have been shown to have sequence homology to G protein-coupled receptors and to a class I MHC heavy-chain homolog, respectively [Davis-Poynter et al., 1997, Chapman and Bjorkman, 1998].

## 2.5 Cytomegalovirus Gene Expression

Herpesviral gene expression is a regulated process [Stinski and Meier, 2007, White and Spector, 2007, Anders et al., 2007]. Viral proteins of different kinetic classes are synthesised during



infection. After the viral genome is released into the nucleus the transcription of viral genes takes place. Transcription of viral genes is dependent on the cellular RNA polymerase II. In addition, the virus exploits the cellular basic transcription machinery and cellular translation factors [Mocarski et al., 2007]. The application of inhibitors of protein synthesis alone or in combination with inhibitors of DNA synthesis prior to viral infection and the subsequent analysis of viral gene expression revealed that herpesvirus gene expression can be divided into three phases. Viral genes are expressed with immediate early (IE), early (E) or late kinetics (L) [Honess and Roizman, 1974].

The immediate early genes are the first genes transcribed after infection. In contrast to the early or late genes, their transcription does not require de novo viral protein synthesis. Transcripts of MCMV immediate early genes can be detected immediately after infection within a period of four hours [Keil et al., 1984, Messerle et al., 1991]. Early viral gene transcripts are detected from two hours until ten hours post infection showing peak levels at four hours after infection [Bühler et al., 1990]. Late transcripts are detected around sixteen hours post infection and reached maximum levels at 20 to twenty-four hours post infection [Keil et al., 1984]. Late viral gene expression is concomitant with viral DNA replication and the first new MCMV virions are released 24 hours after infection.

The best characterised immediate early genes in MCMV or HCMV are the ie1, ie2 and ie3 genes, expressed under the control of the major IE promoter, MIEP. The IE1 and IE3 proteins affect viral gene expression and viral replication and thus are critical determinants of productive virus infection. A MCMV ie3 deletion mutant is unable to grow in cultured cells due to a block in early and late gene expression indicating the significance of a transactivating role of the corresponding IE3 protein [Angulo et al., 2000]. The MCMV IE1 protein has been shown to interact with cellular factors in the nuclei of infected cells that otherwise repress the transcription of viral genomes [Tang and Maul, 2003]. The MIEP region is located outside of the core region and is a complex regulated unit. HCMV IE gene expression can be activated by binding of the tegument protein pp71 to the enhancer region of the MIEP [Liu and Stinski, 1992]. An autoregulatory function of ie3 or the HCMV equivalent ie2, by repression of the major IE promoter of MCMV and HCMV, respectively, has been described [Messerle et al., 1992, Pizzorno and Hayward, 1990].

Early and late gene expression in herpesviruses requires de novo protein synthesis. For example, the MCMV IE3 protein not only autoregulates its own promoter but also activates the promoters regulating the expression of early genes [Messerle et al., 1992]. Many of the viral genes that are expressed with late kinetics encode structural proteins for virus assembly or egress [Anders et al., 2007].

The kinetic expression profile of HCMV genes was investigated by the detection of viral transcripts in the presence of protein synthesis or DNA synthesis inhibitors. This revealed that

genes that are expressed with early or late kinetics are distributed over the HCMV genome whereas genes expressed with IE kinetics are clustered in few loci on the genome and further, most HCMV genes are expressed during the early phase of infection [Chambers et al., 1999].

## 2.6 Cytomegalovirus Cell Tropism

The ability of a virus to productively infect a certain cell type is referred to as its cell tropism [Mahy and van Regenmortel, 2008]. The broad cell tropism of MCMV and HCMV enables the establishment of a systemic infection in the host, targeting multiple organs. Fibroblasts, epithelial cells, endothelial cells and smooth muscle cells are the main target cells of HCMV according to immunohistological stainings of various organ tissues from acutely infected patients [Sinzger et al., 1995]. Explanations for this broad cell tropism are the expression of CMV receptors on the surface of various cell types and also permissiveness to viral replication.

The cell surface receptors discovered to date for CMV attachment or entry are glycosaminoglycans, i.e. heparan sulfate and integrins such as  $\alpha$ -V- $\beta$ 3 and also the platelet-derived growth factor- $\alpha$  receptor (PDGF- $\alpha$ ) [Compton et al., 1993, Feire et al., 2004, Wang et al., 2005, Soroceanu et al., 2008]. Heparin competition or enzymatic digestion with heparinase block virus attachment and viral gene expression whereas antibodies specific for integrins such as  $\alpha$ V and  $\beta$ 3 inhibit virus entry but not virus binding [Feire et al., 2004]. Recently, HCMV entry was found to depend on the surface expression of the growth factor receptor PDGF- $\alpha$ . Virus particle internalisation and viral gene expression is absent in PDGF- $\alpha$  null cells and the authentic PDGF- $\alpha$  ligand decreases HCMV entry [Soroceanu et al., 2008]. Thus, HCMV is most likely to attach to heparan sulfates before its subsequent binding to integrins and/ or growth factor receptors. All of the identified HCMV-receptors are suggested or have been shown to bind either glycoprotein gB or gH.

However, virus replication only occurs if a cell is permissive. Based on cross-species experiments, it is assumed that viral factors interact with other cellular factors at the post-entry step to promote productive infection. A number of studies have shown that cells of species other than mouse or human are susceptible for MCMV or HCMV, respectively, but only few are permissive [Fioretti et al., 1973, Lafemina and Hayward, 1988, Nowlin et al., 1991, Jurak and Brune, 2006]. The replication of MCMV in cells of other species is not productive, partly due to infection-induced programmed cell death [Jurak and Brune, 2006]. In general, inside the cell, the interference with cellular defense mechanisms is critical for the virus to be able to replicate and spread efficiently. Due to their slow replication cycles, CMVs are particularly reliant on suppressing cellular defence mechanisms including cell death and the interferon response [Goldmacher, 2005, Zimmermann and Hengel, 2006].

Viral cell tropism factors are suggested to interact with intracellular factors thereby ensuring replication of the virus. The identification of cell tropism genes of CMVs was pioneered by Brune et al. who showed that productive infection of endothelial cells is only possible in the presence of M45 [Brune et al., 2001]. A number of viral genes of different CMV species have since then been identified that determine the tropism for endothelial cells, epithelial cells or macrophages [Brune et al., 2001, Ménard et al., 2003, Dunn et al., 2003, Hahn et al., 2004, Lilja et al., 2008]. To date, modes of action have only been identified for the MCMV M36 and M45 proteins. In the absence of the M36 protein infected macrophages and hepatocytes undergo apoptosis, whereas the effect is less pronounced in fibroblasts. The survival of CMV-infected macrophages and hepatocytes is obviously necessary for viral fitness since the  $\Delta$ M36 virus does not reach comparable titres to the wild type MCMV in the salivary glands. The M36 protein interferes with Fas-associated death domain (FADD) function and thereby inhibits the death receptor mediated pathway of apoptosis [Cicin-Sain et al., 2008]. The M45 protein binds to the cellular receptor-interacting protein RIP1 and prevents the TNF $\alpha$ -induced death of endothelial cells [Mack et al., 2008, Upton et al., 2008]. The finding that mutant viruses that do not express M45 are avirulent in immunodeficient mice and do not replicate in their target organs highlights the relevance of endothelial cells for MCMV pathogenesis [Lembo et al., 2004]. The cell type-dependent sensitivity to cell death in the absence of M45 has been suggested to depend on the cellular expression level of RIP1.

The majority of the identified CMV cell tropism factors exert their functions after the virus has entered the cell. Even in the absence of cell tropism factors gene expression under the control of the major IE promoter is observed [Brune et al., 2001, Lilja et al., 2008] implying that cellular permissiveness to a virus is determined by cell tropism factors acting at a post-entry step. However, the tropism of HCMV for endothelial and epithelial cells is determined prior to viral gene expression. Laboratory-adapted HCMV strains have lost their tropism for epithelial and endothelial cells due to mutations in the UL128-131 locus of the viral genome [Hahn et al., 2004]. The formation of a complex consisting of the glycoproteins gH/gL together with the UL128-UL131 gene products on the surface of HCMV virions is required for entry in epithelial and endothelial cells via pH-dependent fusion at endocytic vesicles prior to viral gene expression [Wang and Shenk, 2005a, Ryckman et al., 2008]. In contrast, the glycoprotein complex gH/gL/gO mediates entry into fibroblasts via fusion at the plasma membrane.

The two cell types that were used in the present study for the investigation of MCMV cell tropism and the induction of cell rounding are epithelial cells and fibroblasts. Fibroblasts are commonly used for the propagation of CMV in cell culture since CMV produces high amounts of progeny virus in this cell type [Kim and Carp, 1971, Smee et al., 1989, Furukawa et al., 1973]. Fibroblasts and smooth muscle cells belong to the family of connective tissue cells and are dispersed throughout the body [Alberts et al., 2002]. It can be speculated that this cell

type is also a source for the production of progeny virus and virus spread *in vivo*. Several studies, examining the growth properties of MCMV deletion viruses, demonstrate that the tropism of MCMV for fibroblasts is not determined by ORFs that are located outside of the herpesviral core region [Zhan et al., 2000, Ménard et al., 2003, Brune et al., 2001, 2006]. This indicates that the core of conserved genes are sufficient for the productive infection of fibroblasts.

### **Infection of Epithelial Cells**

Epithelial cells of mucosal surfaces are exposed first to infectious virus and therefore have been suggested to be the first targets for CMV. During the course of infection CMV is disseminated to sites that have been postulated to support persistent infection *in vivo*. These include the salivary gland and breast secretory epithelium, prostatic epithelium and renal tubule epithelium [Britt, 2007]. Further, HCMV persistence in retinal epithelial cells of immunocompromised individuals has been reported [Scholz et al., 2003]. Glandular epithelial cells are the main secretory cells of the salivary and the mammary glands [Welsch, 2006]. Consistent with the fact that CMV is transmitted via bodily fluids such as saliva virus particles have been found in acinar glandular epithelial cells of the salivary gland in persistently infected mice [Jonjic et al., 1989]. Further, glandular or ductal epithelial cells in kidney, breast milk duct and genital organs are thought to be major sites for shedding of infectious virus into urine, mothers breast milk and cervical secretions [Britt, 1996].

Viral factors that are necessary for the productive infection of epithelial cells have only been identified to date for HCMV and rhesus CMV [Hahn et al., 2004, Lilja et al., 2008]. The rhesus CMV Rh01-deletion mutant grows to reduced titres in epithelial cells compared to those in fibroblasts whereas similar titres of the wild type CMV were obtained from both cell types [Lilja et al., 2008]. Although the mechanism remains unknown, the failure to produce similar titres must be due to a post entry-step since epithelial cells infected with the mutant expressed similar levels of all kinetic classes of viral proteins.

The impact of epithelial cells for the dissemination and pathogenesis of CMV has not been studied to date. The identification of epithelial cell tropism factors of MCMV could be useful for answering this question. Their deletion and the analysis of the *in vivo* growth properties of the respective mutants in the *in vivo* mouse model would be suitable to clarify the role of epithelial cells during MCMV infection.

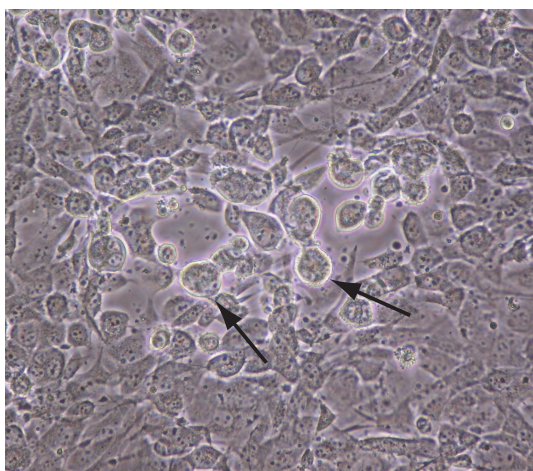


Figure 2.3: **CMV-induced plaque formation.** CMV infection results in cell rounding leading to the formation of holes in the cell monolayer, so called plaques. Arrows point to CMV-infected primary fibroblasts.

## 2.7 Cytomegalovirus-Induced Cell Rounding as a Cytopathic Effect

Cell rounding is a cytopathic effect induced by CMV [Furukawa et al., 1973, Fioretti et al., 1973, Ihara et al., 1982, Albrecht et al., 1983, 1980]. During the early stages of infection the morphology of fibroblasts changes from a typical fibroblast shape to a round cell shape. Characteristic holes in the cell monolayer, so-called plaques, are formed during CMV infection and are caused by rounded CMV-infected cells (Fig.2.3). Although CMV replication is species-specific, cell rounding can be induced in cells of other species. MCMV and HCMV can enter human cells and guinea pig cells respectively and express a set of genes that are sufficient to induce cell rounding [Jurak and Brune, 2006, Fioretti et al., 1973].

The onset of cell rounding is observed at 5-6 hours after infection in single HCMV-infected fibroblasts and most infected cells are rounded at 24 hours after infection [Furukawa et al., 1973, Fioretti et al., 1973, Ihara et al., 1982, Albrecht et al., 1983, 1980]. The application of inhibitors affecting protein synthesis, transcription, or DNA synthesis in combination with HCMV infection and UV-irradiation of virus particles indicates that viral induced cell rounding is not induced by a constituent of the virion but requires *de novo* synthesis of an early virus protein. Cell rounding was completely inhibited when the protein synthesis inhibitor cycloheximide or the transcription inhibitor actinomycin D were added before or within two hours of HCMV-infection, indicating that early viral protein synthesis is required for this process [Furukawa et al., 1973]. Further, the inhibition of viral DNA replication does not inhibit the induction of cell rounding [Albrecht et al., 1983]. The requirement of *de novo* gene expression and protein synthesis for the induction of cell rounding is further confirmed by the fact that UV-irradiated virus particles are unable to induce cell rounding [Hirai et al., 1977].

Possible explanations of HCMV-induced cell rounding include virus-induced integrin signalling, cellular  $\text{Ca}^{2+}$  accumulation and ATP depletion. The latter was attributed to a single HCMV-gene whereas MCMV-induced cell rounding has not been characterised to date nor has the responsible gene been identified. The reduction of the cellular adhesion molecule integrin  $\alpha1/\beta1$  correlates with the onset of cell rounding in HCMV infected cells, indicating that the early events that induce the morphological changes also influence integrin signalling or vice versa [Warren et al., 1994]. HCMV-induced cell rounding is inhibited in smooth muscle cells by calcium influx blockers suggesting that virus-induced cell rounding resembles a contractile-like process and that an influx of cations triggered through an early viral protein causes this initial contraction of actin filaments [Albrecht et al., 1983]. Recently, a single HCMV gene, vMIA, has been implicated in HCMV-induced cell rounding [Poncet et al., 2006]. This gene was initially described encoding an inhibitor of apoptosis and is expressed with immediate early kinetics [Goldmacher et al., 1999]. However, the influence on cell rounding is not related to its anti-apoptotic function but to the inhibition of the phosphate supply for the generation of ATP, thereby reducing cellular ATP levels [Poncet et al., 2006].

Since the cytoskeleton is required for the maintenance of the spatial organisation and the structural framework of a cell, cell rounding must correlate with cytoskeletal reorganisation. Cellular proteins that regulate the microtubule architecture or the actin cytoskeleton might represent potential targets for viral proteins to induce cell rounding. Regulatory proteins of the actin cytoskeleton, Rho, Rac and Cdc42 are members of the guanosine triphosphatase (GTP) family. GTPases control the assembly and the organisation of the actin cytoskeleton and are required for the maintenance of cell polarity and cell contraction [Etienne-Manneville and Hall, 2002]. Activation of Rho in NIH 3T3 fibroblasts leads to the contraction of actin-myosin filaments (Fig. 2.4) [Hall, 1998]. The formation of lamellipodia and membrane ruffles is induced when Rac is activated, for example by platelet-derived growth factor and activated Cdc42 induces actin-rich surface protrusions called filopodia. The effects of Rho, Rac or Cdc42 activation are not restricted to fibroblasts but have been observed in other cell types including epithelial and endothelial cells and macrophages [Hall, 1998].

Microbial pathogens exploit the involvement of Rho GTPases in multiple cellular functions in order to induce cytopathic and cytotoxic effects [Aktories and Barbieri, 2005]. The Gram-positive bacterium *Clostridium difficile* effects morphological changes in its target cells resulting in cell rounding concomitant with the induction of apoptosis. The *Clostridium difficile* toxin A and toxin B glycosylate and thereby inactivate Rho/Rac proteins. This modification induces the cytopathic effect as well as the cytotoxic effect in infected cells [Gerhard et al., 2008, Halabi-Cabezón et al., 2008].

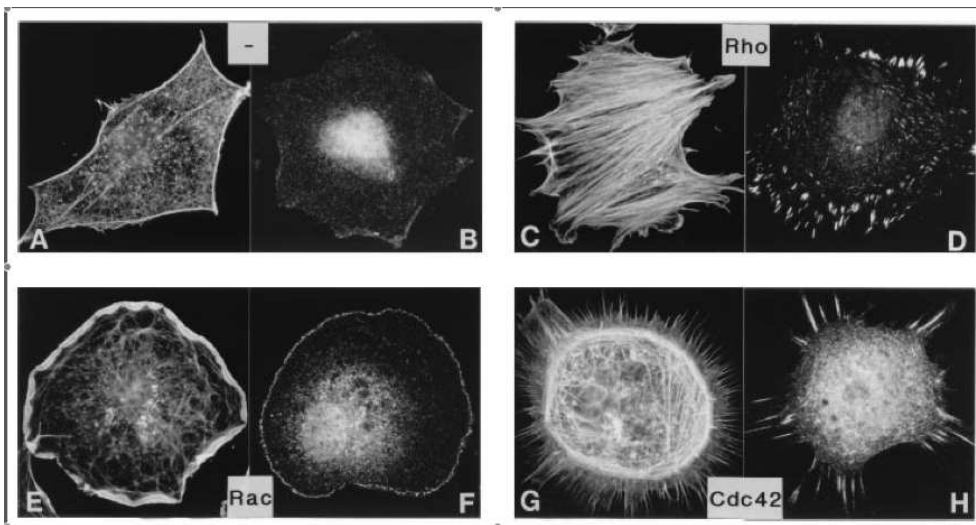


Figure 2.4: **Rho, Rac, and Cdc42 control the assembly and organisation of the actin cytoskeleton.** (A) Quiescent fibroblasts contain very few organised actin filaments. (C) Rho activation leads to the formation of actin stress fibers effecting a morphology with prominent focal adhesions. Microinjection of constitutively active Rac induces lamellipodia (E), whereas active Cdc42 leads to the formation of filopodia (G). In (A), (C), (E), and (G), actin filaments were visualised with rhodamine phalloidine; in (B), (D), (F), and (H), the adhesion complexes were visualised with an antibody to vinculin. Scale: 1 cm = 25  $\mu$ m, taken from Hall, 1998.

In two members of the alphaherpesviruses, pseudorabies virus and Marek's disease virus, the viral US3 protein kinase has been identified as manipulating the actin cytoskeleton [Van Minnebruggen et al., 2003, Schumacher et al., 2005]. An impressive actin stress fibre breakdown is observed in cells at six hours after infection with pseudorabies virus. This actin stress fibre breakdown is dependent on the presence of the US3 protein kinase [Van Minnebruggen et al., 2003]. Although the exact mechanism remains elusive, it is speculated that the nuclear localised US3 kinase interferes with Cdc42/Rac signalling. The US3 protein kinase of Marek's disease virus contributes only partially to actin stress fibre breakdown since this effect is also observed in  $\Delta$ US3-infected cells indicating that additional viral proteins are involved [Schumacher et al., 2005]. The US3-induced stress fibre breakdown leads to morphological changes but does not disrupt cell-to-cell contacts and so is unable to produce totally rounded cells as observed during CMV infection. Thus, actin stress-fibre breakdown alone does not lead to cell rounding and other additional factors must be required to drive these morphological changes.

The US3 protein kinase is also present in HSV-1 and HSV-2. The importance of US3 for HSV-induced cell rounding has so far only been investigated in a cell line expressing HSV-2 US3 [Murata et al., 2000]. Here, cell rounding is observed upon the expression of US3. Notably, the finding that co-expression of dominant active forms of Cdc42/Rac inhibit cell rounding is indicative of an interference of US3 with GTPase-signaling. No US3 homologs were found in HCMV or MCMV [McGeoch et al., 1988, Chee et al., 1990, Rawlinson et al., 1996]. Thus, it

is possible that cell rounding during MCMV infection is induced by another viral kinase.

Cells that are transformed with rous sarcoma virus exhibit a loss of contact between neighbouring cells and a round cell morphology [Rohrschneider and Reynolds, 1985]. This transformation is ascribed to the interaction of the virally expressed kinase v-src and the Rho protein [Mayer et al., 1999]. Expression of a constitutively active Rho-protein in trans, in rous sarcoma virus-transformed fibroblasts, partly restored the typical fibroblast shape with the formation of stress fibres and focal adhesions. This suggested that the cytoskeletal rearrangements in rous sarcoma virus-transformed cells are induced through phosphorylation of the cytoskeletal regulator protein Rho.

The in vivo relevance of virally-induced cell rounding, if any, is unclear. Manipulation of the cytoskeleton by cytomegaloviruses may facilitate the dissemination of the virus. Circulating CMV-infected endothelial cells (CCIC) are found in blood from immunocompromised patients with symptomatic or asymptomatic CMV-disease [Percivalle et al., 1993, Salzberger et al., 1997]. In one study increased numbers of CCIC corresponded to peak levels of antigenemia and viremia [Percivalle et al., 1993]. The findings support the view that endothelial cells detach from the vessel wall as a result of HCMV-induced cytopathic effect. These cells then enter the blood stream leading to dissemination of the virus in peripheral blood. Notably, CCIC that are in close contact to surrounding leukocytes has been reported [Salzberger et al., 1997] suggesting virus transmission between these cells.

Bentz et al. reported of increased expression of cell surface adhesion molecules in endothelial cells after HCMV infection [Bentz et al., 2006]. This was shown to be sufficient for the adherence of naïve monocytes to the endothelial surface and virus transmission. Further, CMV-induced morphological alterations in endothelial cells lead to a permeable endothelium that enables traversing of infected monocytes and hence virus dissemination.

Thus, the identification of the MCMV gene that induces cell rounding during infection and the examination of a mutant virus lacking the ability to induce cell rounding may exhibit an excellent tool to study the relevance of cell rounding for the infection process. The elucidation of the mechanism of CMV-induced cell rounding may further provide insights into cellular processes that are as yet poorly understood e.g. cell rounding during mitosis.

## 2.8 Genetic Manipulation of Cytomegaloviruses

Manipulation of the large CMV genomes with the aim of the identification of viral gene functions was first achieved by mutagenesis of isolated virus using UV-irradiation [Hirai et al., 1977, Ihara et al., 1978]. Mutagenesis by UV-irradiation of virus particles generates mutants that show temperature-sensitive viral replication [Ihara et al., 1978]. However, the identification of point mutations is laborious and only few mutated gene regions of HCMV temperature-



sensitive mutants can be mapped and associated with open reading frames [Ihara et al., 1994].

More recently viral genes have been cloned into plasmids and thus made accessible for manipulation in bacteria. This approach has been applied in particular to examine the function of already known viral genes [Manning and Mocarski, 1988]. Mutated fragments are transfected into cells together with the wild type CMV and homologous recombination replaces a genome fragment with the mutated sequence. However, homologous recombination is a rare event in eukaryotic cells, and without any selection for the mutated viral genomes reconstitution of the wild type CMV would be dominant. Therefore, selection markers were provided with the mutated viral fragments that were inserted into the viral genome.

The use of viral cosmids to reconstitute the mutated viral genome in the absence of the wild type CMV genome facilitated the isolation of mutant genomes [Kemble et al., 1996, Ehsani et al., 2000]. Viral genomes have been cloned in several fragments as a set of overlapping cosmid clones. After transfection of all the cosmid clones into eukaryotic cells, the wild type CMV genomes are reconstituted via multiple homologous recombination events. A mutation can be introduced in one of these fragments. Several viral fragments with mutations have been constructed by generating a cosmid library using transposon mutagenesis [Zhan et al., 2000]. After transfection and homologous recombination of the single cosmid clones the mutated genome is reconstituted in the absence of the wild type genome. However, the efficiency of this method is poor. Further, additional mutations can occur in the viral genome since the reconstitution of the virus out of the several cosmid clones relies on several recombination events in the cell.

With the cloning of CMV genomes as bacterial artificial chromosomes (BAC) in *E. coli*, manipulation of CMV genomes using bacterial genetics became possible and thus new opportunities were opened for the investigation of viral gene functions [Messerle et al., 1997]. After reconstitution from the BAC, the genomic sequence of the virus is indistinguishable from that of the isolated wild type CMV due to the self-excision of the BAC vector sequences in eukaryotic cells [Wagner et al., 1999]. Site-directed mutagenesis or random transposon mutagenesis of the viral genome can be used to generate libraries of virus mutants [Brune et al., 2006, 1999]. The transposon library has been used to screen for essential and non-essential herpesvirus genes by random insertions into the viral genome [Brune et al., 1999] whereas the library of mutants generated by the site-directed mutagenesis technique aims at the manipulation of the viral genome on a selected gene-by-gene basis. Site-directed mutagenesis of the viral genomes is achieved by homologous recombination between linear DNA fragments or shuttle plasmids and the viral BAC in *E. coli*. The site-directed mutagenesis technique using linear PCR fragments is probably the most frequently used method for the functional analysis of a specific viral gene. Mutant genomes with introduced deletions, insertions or point mutations can be efficiently generated [Borst et al., 2007]. The reconstituted mutants can then be

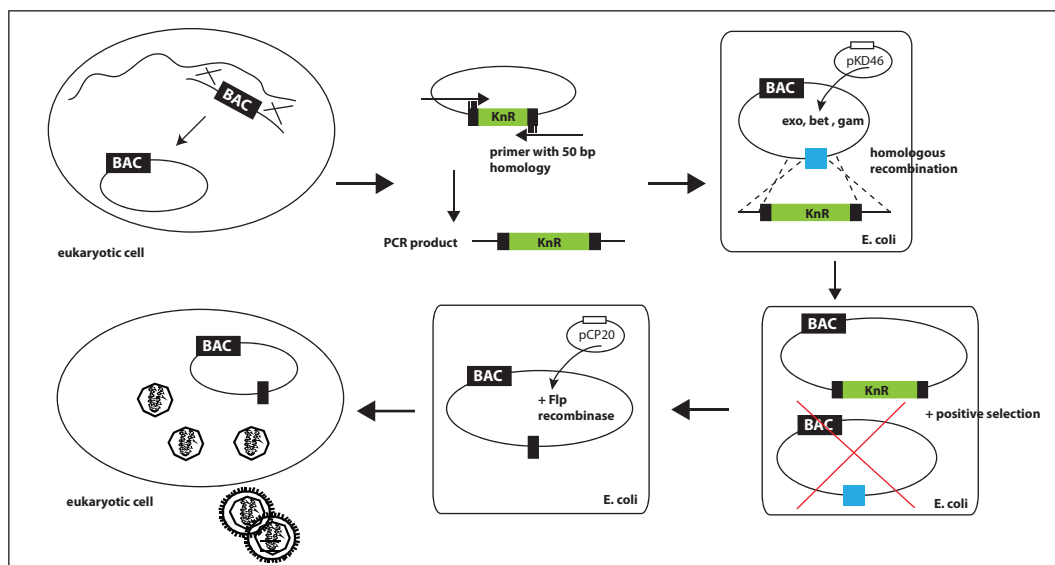


Figure 2.5: **Site-directed BAC mutagenesis using linear PCR fragments.** The MCMV Smith strain was previously cloned as a BAC [Messerle et al., 1997]. For this, the viral DNA and recombination plasmids containing the BAC were transfected into eukaryotic cells to generate a recombinant virus. A selection marker i.e. the kanamycin resistance cassette (KnR, green bar) flanked by FRT-sites (back bars) was amplified by PCR using primers with additional homology to the sequences directly upstream and downstream of the gene or gene region of interest (blue box). The linear PCR product was electroporated into E.coli containing the viral BAC and the plasmid pKD46 expressing the recombination enzymes *exo*, *bet*, *gam*. The recombination enzymes mediate homologous recombination between the PCR product and the BAC. Only those bacteria containing the mutated BAC are able to grow under selection pressure. The Flp recombinase is expressed from the pCP20 plasmid and mediates the excision of the selection marker leaving a single FRT site in the BAC (black bar). The mutated BAC is then transfected into eukaryotic cells to reconstitute mutant virus. The scheme is not drawn to scale.

screened for the appearance of a searched for phenotype in an appropriate assay. A scheme of the site-directed mutagenesis using linear PCR fragments is shown in Fig. 2.5. In this way the functions of several CMV genes have been identified, such as for cell tropism, the inhibition of apoptosis, the immunomodulation and capsid maturation [Brune et al., 2001, Ménard et al., 2003, Hahn et al., 2004, Lilja et al., 2008, Bubic et al., 2004, Hasan et al., 2005, Loewendorf et al., 2004, Mack et al., 2008, Upton et al., 2008, Borst et al., 2008].

A growing number of HCMV and MCMV strains, have been cloned as BACs to date [Brune et al., 2006] allowing the maintenance of clonal reference genomes of individual viruses. Further, several herpesvirus genomes were cloned as BACs and used to study viral gene functions [Zhou et al., 2002, Chang and Barry, 2003, Smith and Enquist, 2000, Nagel et al., 2008]. When examining viral gene function, by applying mutagenesis techniques, the observation of a phenotype upon deletion of a selected gene requires a close investigation of the phenotype-genotype connection. It is always possible that the phenotype is not caused by the deletion

of a gene but rather by the deletion of sequence elements that influence adjacent genes. A suitable tool to prove whether a viral gene is responsible for the observed phenotype is cis-complementation via integration of the missing gene into the mutant BAC [Borst et al., 2001].

## 2.9 Aims of the Study

Among the characteristic features of a cytomegalovirus infection are the broad cell tropism and the induction of cell rounding [Mocarski et al., 2007, Sinzger et al., 2008, Furukawa et al., 1973, Fioretti et al., 1973, Ihara et al., 1982, Albrecht et al., 1983, 1980]. Genes have been identified that determine the tropism of different CMV species for endothelial cells, macrophages or epithelial cells [Brune et al., 2001, Ménard et al., 2003, Hahn et al., 2004, Lilja et al., 2008]. Most of the so-called cell tropism factors interact with cellular factors at a post-entry step. This raised the hypothesis that cell tropism factors are required in addition to attachment and entry receptors for the productive infection of a specific cell type. Viral genes that determine the tropism of MCMV for epithelial cells have not been found yet. Possible explanations of HCMV-induced cell rounding have been described [Albrecht et al., 1983, Warren et al., 1994, Poncet et al., 2006] whereas MCMV-induced cell rounding is only poorly characterised.

The aim of this study was the identification of MCMV epithelial cell tropism factors and viral genes that induce cell rounding during MCMV-infection.

To this end, the construction of a library of MCMV mutants was intended. The MCMV genome was previously cloned as a bacterial artificial chromosome in *E.coli* making it accessible for mutagenesis exploiting bacterial genetics. Site-directed mutagenesis would be the method of choice to specifically target single or multiple viral genes for deletion. A cell tropism assay should be established and used to compare the growth and spread of mutants and wild type MCMV in epithelial cells and fibroblasts. Further, the mutants would be examined for their ability to induce cell rounding by analysing the cellular morphology of infected cells.



## 3 Material

### 3.1 Chemicals and Reagents

The standard chemicals and reagents were purchased from Sigma Aldrich, Steinheim; Roth, Karlsruhe and Merck, Darmstadt. Plastic labware for tissue culture was purchased from Greiner Bio-One, Frickenhausen and Sarstedt AG & Co., Nümbrecht. Further, the following chemicals, reagents and materials were used:

5'-/3'-RACE kit	Roche Diagnostics GmbH, Mannheim
1kb Plus DNA ladder	Invitrogen, Karlsruhe
100 bp DNA ladder GeneRuler	Fermentas, St. Leon-Rot
Riboruler High Range RNA marker	Fermentas
40% Acrylamide/ Bisacrylamide (19:1)	Qbiogen, Irvine, USA
Bacto-Agar	BD Biosciences, Heidelberg
Agarose	Invitrogen, Karlsruhe
Ampicillin	Roth
Ammoniumpersulfate (APS)	Merck, Darmstadt
Aqua Poly Mount	Polysciences Inc. Warrington, USA
L-(+)-Arabinose	Sigma Aldrich
Bovine Serum Albumine	Sigma Aldrich
Benzonase	Sigma Aldrich
Carboxymethylcellulose	Sigma Aldrich
Chloramphenicol	Roth
Calf Intestine Phosphatase (CIP)	New England Biolabs, Frankfurt a.M.
Cycloheximide	Roth
Electroporation Cuvettes	PeqLab, Erlangen
DecaLabel DNA labeling kit	Fermentas
Deoxynucleotide mix	Invitrogen
DMSO (Dimethylsulfoxid)	Roth
DNA-free Kit	Ambion, AppliedBiosystems, Darmstadt
Dulbeccos modified Eagles Medium (DMEM)- high glucose	Sigma Aldrich

### 3 Material

---

DMEM-high glucose	Biochrom AG, Berlin
DMEM 10 x	Sigma Aldrich
ECL Western Blotting detection reagent	Amersham Biosciences, Freiburg
Ethidiumbromid	Roth
Folic acid	Sigma Aldrich
Formamide	Roth
Formaldehyde	Merck
Fetal bovine serum (FBS)	Biochrom AG
FBS Gold	PAA Laboratories GmbH, Cölbe
HEPES	PAA Laboratories GmbH
High Fidelity Phusion DNA polymerase	Finnzymes, Espoo, FIN
Icafectin	Eurogenetec, Köln
jetPEI	Polyplus-transfection, Illkirch, France
Kanamycin	Roth
Kodak X-omat-AR X-ray films	Kodak, Stuttgart
T4 Ligase	Fermentas
Lipofectamine2000	Invitrogen
$\beta$ -Mercaptoethanol	Sigma Aldrich
Milk powder	Roth
MOPS	Roth
BD Microlance 3, needles 0,3 x 13 mm	BD Biosciences
Newborn calf serum (NCS)	Biochrom AG
Nitrocellulose membrane	Hybond-ECL, Amersham Biosciences
Nonidet P40 (NP-40)	Sigma Aldrich
Nucleobond PC 100	Macherey-Nagel, Düren
Bodyne B nylon transfer membrane	PALL, FI, USA
Opti-MEM	Invitrogen
Phenol/Chloroform/Isoamylalcohol	Roth
Phosphonoacetic acid	Sigma Aldrich
Paraformaldehyde	Sigma Aldrich
Phosphate buffered saline (PBS)	PAA Laboratories GmbH
PBS (cell culture)	CytoGen, Sinn
Penicillin/Streptomycin/Glutamine	PAA Laboratories GmbH
Protease Inhibitor Cocktail Set III	Calbiochem, SanDiego, USA
Proteinase K	Sigma Aldrich
Full range Rainbow marker (225, 150, 102, 76, 52, 38, 31, 24, 12 kDa)	GE Healthcare, München

Spectra Multicolor Broad Range Protein Ladder (260, 140, 100, 70, 50, 40, 35, 25, 15, 10 kDa)	Fermentas
QiaShredder	Qiagen, Hilden
Quick PCR purification kit	Qiagen
Restriction Enzymes	NEB
RNase A	Sigma Aldrich
RNase inhibitors	Promega, Mannheim
RNeasy kit	Qiagen
SDS	Roth
Sodium bicarbonate	Gibco, Invitrogen, Karlsruhe
Salmon sperm DNA	Invitrogen
Spin columns S200	MoBiTec, Göttingen
TEMED (Tetramethylethylenediamin)	Serva, Heidelberg
TRITC-Phalloidin	Sigma Aldrich
Trypsin/EDTA	Biochrom AG
Bacto-Tryptone	BD Biosciences
Tween-20	Roth
UltraClean™15	Mo Bio Laboratories Inc., Carlsbad, USA
VenorGeM	Minerva, Berlin
Yeast Extract	Roth

## 3.2 Cells and Bacteria

**NIH 3T3**, adherent mouse fibroblasts purchased from ATCC, CRL-1658

**C127I**, adherent mouse mammary gland derived epithelial cells purchased from ATCC, CRL-1616

**293T cells**, adherent human kidney epithelial cells purchased from ATCC, CRL-11268

**MEF**, adherent primary mouse embryonic fibroblasts prepared from 2 weeks old BALB/c mice embryos, provided by Lars Steinbrück

**E. coli, DH10B**: used for the maintenance and cloning of BACs. Genotype: F-mcrA  $\Delta$ (mrr-hsdRMS-mcrBC)  $\phi$ 80lacZ $\Delta$ M15  $\Delta$ lacX74 recA1 endA1 araD139  $\Delta$ (ara leu) 7697 galU galK rpsL nupG  $\lambda$ - (Invitrogen)

**E.coli, PIR 1**: used for the cloning of plasmid pOri6k derivatives. Express the bacteriophage  $\lambda$  pi protein. Genotype: F-  $\Delta$ lac169 rpoS(am) robA1 creC510 hsdR514 endA recA1 uidA ( $\Delta$ Mlu I)::pir-116 (Invitrogen).

## 3.3 Antibodies, Probes and Antibiotics

### Antibodies

Peroxidase-conjugated goat anti-rabbit IgG	DAKO
Peroxidase-conjugated sheep anti-mouse IgG	Amersham
Alexa 568 conjugated goat anti-rat IgG	Invitrogen
Alexa 568 conjugated goat anti-mouse IgG (H+L)	Invitrogen
Monoclonal mouse CROMA101 against the MCMV IE1 protein	provided by S. Jonjic, Rijeka, Croatia
Monoclonal mouse CROMA 103 against MCMV E1	provided by S. Jonjic
Monoclonal mouse 20/352/4, (against a yet uncharacterised late MCMV protein)	provided by B. Bühler
Rat monoclonal anti-HA (subtype IgG <sub>1</sub> ), (clone 3F10)	Roche Diagnostics, Mannheim
Rabbit polyclonal anti-HA, (recognises the amino acid residues 98-106 of the human influenza hemagglutinin (HA))	Sigma Aldrich
Rabbit monoclonal anti-GAPDH (clone 14C10)	Cell Signalling Technologies, Danvers, MA, USA
probe GFP, corresponds to the cDNA of eGFP	obtained from Jens Bohne, MHH, Hannover

### Antibiotics

Chloramphenicol: 170  $\mu\text{g}/\text{ml}$  (high copy plasmids), 17  $\mu\text{g}/\text{ml}$  (low copy plasmids)

Kanamycin: 50  $\mu\text{g}/\text{ml}$  (high copy plasmids), 25  $\mu\text{g}/\text{ml}$  (low copy plasmids)

Ampicillin: 100  $\mu\text{g}/\text{ml}$  (high copy plasmids), 50  $\mu\text{g}/\text{ml}$  (low copy plasmids)

## 3.4 BACs and Plasmids

**pSM3fr**: low copy; BAC plasmid containing the full-length sequence of the MCMV Smith strain. Cam<sup>R</sup>, [Wagner et al., 1999]

**pSM3fr-GFP**: low copy; BAC plasmid containing the full-length MCMV sequence of the Smith strain. The gene expressing the enhanced green fluorescent protein was inserted into the IE2 locus of the viral genome. Cam<sup>R</sup> (provided by M.Messerle, MHH, Hannover; described in [Mathys et al., 2003]).



**pIRES2AcGFP1:** high copy; Plasmid containing an internal ribosome entry site (IRES) between an multiple cloning site and the AcGFP1 gene.  $\text{Kn}^R$ . Clontech Laboratories Inc., Saint-Germain-en-Laye, France.

**pACYC177 HindIII A:** low copy; Plasmid containing the MCMV HindIII A fragment (provided by M.Messerle, MHH, Hannover).

**pGP704-kan:** Plasmid containing the kanamycin resistance cassette flanked by FRT-sites. Grows only in the presence of the replication factor Pi expressed from the bacteriophage  $\lambda$  pir gene.  $\text{Kn}^R$  [Borst and Messerle, 2005].

**pCP20:** low copy; Plasmid expressing the Flp recombinase. Temperature sensitive replication mode at 30°C.  $\text{Amp}^R$ ,  $\text{Cam}^R$ . [Cherepanov and Wackernagel, 1995]

**pOri6k<sub>linker</sub>:** Plasmid contains a multiple cloning site and the kanamycin resistance cassette fused to a FRT-site. Grows only in the presence of the  $\lambda$  pi protein.  $\text{Kn}^R$ . (provided by E.M. Borst, MHH, Hannover)

**pKD46:** low copy; Plasmid expressing the bacteriophage  $\lambda$  recombination enzymes *exo*, *bet*, *gam* encoded by the genes *red*  $\alpha$ ,  $\beta$ ,  $\gamma$  under the control of an L-arabinose inducible promoter. Temperature sensitive replication mode at 30°C,  $\text{Amp}^R$  [Datsenko and Wanner, 2000].

## 3.5 Laboratory Equipment

Avanti J-25 Centrifuge	BeckmanCoulter, Fullerton, CA, USA
BioPhotometer	Eppendorf
Centrifuge 5415D, 5415R	Eppendorf, Hamburg
CO <sub>2</sub> Cell Incubator	Sanyo, Wood Dale, IL, USA
Gel documentation	Alpha Innotech Corp., San Leandro, GB
Gene Pulser Xcell System	Biorad, München
Hereaus Megafuge 1.0	ThermoScientific, Waltham, MA, USA
Hereaus Multifuge 3SR+	ThermoScientific
Hoefer SE600 Ruby electrophoresis unit	Amersham Biosciences
JA-10, JA-20.1, Type-19, SW40 rotors	BeckmanCoulter
LAS-3000 Imager	FujiFilm, Düsseldorf
Mini-Protean Electrophoresis System	Biorad
Mini Trans-Blot Cell	Biorad
Nikon Eclipse T5100	Nikon GmbH, Düsseldorf
PerfectBlue™ Mini/Maxi S gel system	PeqLab, Erlangen
Sterile Hood Hereaus HeraSafe	Kendro, Rodenbach
T3 Thermocycler	Biometra, Göttingen
TE 62 Transfer Unit	Amersham Biosciences

### 3 Material

---

TL 100 Ultracentrifuge

UV-Stratalinker 2400

Zeiss Axio Observer Microscope

BeckmanCoulter

Stratagene, LaJolla, CA, USA

Zeiss MicroImaging GmbH, Göttingen

## 4 Methods

### 4.1 Eukaryotic Cell Culture

#### Cell Culture

BALB/c mouse embryonic fibroblasts (MEF) and C127I were propagated in Dulbecco's modified Eagle's Medium supplemented with 10% fetal bovine serum, 2 mM glutamine, 100 U/ml of penicillin and 100  $\mu\text{g}/\text{ml}$  of streptomycin sulfate. NIH 3T3 fibroblasts were propagated likewise MEF but with 5% newborn calf serum. 293T cells were grown in DMEM supplemented with 10% FBS gold, 2 mM glutamine, 20 mM HEPES, 100 U/ml of penicillin and 100  $\mu\text{g}/\text{ml}$  of streptomycin sulfate. Cells were monthly tested for mycoplasma contamination by PCR using Venor®GeM mycoplasma detecton kit. Cells were grown in a humid atmosphere in an incubator at 37°C and 5% CO<sub>2</sub>.

#### Cryoconservation of Cells

Cells of a confluent culture dish ( $\varnothing$  10 cm) were trypsinized and resuspended in complete growth medium. Cells were pelleted by centrifugation in 15 ml centrifugation tubes at 300 x g for 3 min and were resuspended in 2.4 ml DMEM without additives. 800  $\mu\text{l}$  of the cell suspension were provided in a cryoconservation tube. Freezing medium (DMEM supplemented with 40% FCS, 20% DMSO) was added dropwise and cells were frozen in a polystyrene box at -80°C for 1 week before longterm storage in liquid nitrogen.

Cells were thawed at 37°C in a water bath and transferred into a 15 ml centrifugation tube. 5 ml complete growth medium was added dropwise and cells were pelleted at 300 x g for 3 min before they were resuspended in complete growth medium and seeded in a cell culture dish.

### 4.2 Mutagenesis of BACs using linear PCR Fragments

MCMV genomes were mutated using *E.coli* DH10 $\beta$  containing the pSM3fr BAC or the pSM3fr-GFP BAC. Homologous recombination between linear PCR fragments and the MCMV BAC

was mediated by the bacteriophage  $\lambda$  recombination enzymes expressed by the genes red  $\alpha$ ,  $-\beta$ , and  $-\gamma$  on the plasmid pKD46.

For this, 2-5 ng of plasmid pKD46 were electroporated into bacteria containing the MCMV-BAC. The bacterial culture was incubated at 30°C for 1 h and streaked onto an agar plate containing 17  $\mu\text{g}/\text{ml}$  chloramphenicol and 25  $\mu\text{g}/\text{ml}$  ampicillin. The plate was incubated overnight at 30°C. A 100 ml liquid culture of these bacteria was grown to an  $\text{OD}_{600}$  of 0.5 to 0.6 under the same selection conditions. The expression of the recombination enzymes was induced in the presence of 0.1% L-arabinose for 1 h and electrocompetent bacteria were generated from these cultures. Purified PCR fragments (300 ng) were electroporated into electrocompetent bacteria (see DNA methods) and recombination of the PCR product into the MCMV BAC was allowed to happen by incubation for at least 1.5 h at 37°C with shaking. The transformed bacteria were streaked out on agar plates containing 17  $\mu\text{g}/\text{ml}$  chloramphenicol and 25  $\mu\text{g}/\text{ml}$  kanamycin. The plasmid pKD46 was eliminated by subsequent overnight incubation at 43°C. The integrity of the mutant BACs was analysed by small scale preparation of BAC-DNA followed by restriction analysis.

### **Generation of linear PCR Fragments for BAC mutagenesis**

For the generation of PCR fragments 2-5 ng of plasmid pGP704-kan were used as a template. Primers that were designed for the generation of the mutant genomes are listed in the appendix. The primers have a 50 bp homology directly upstream and downstream to the gene or the gene region of interest and a 20 bp homology to the kanamycin resistance cassette. For a 50  $\mu\text{l}$  PCR reaction a final concentration of 0.2  $\mu\text{M}$  of each primer, 0.01 U of the Phusion polymerase in HF buffer and 200  $\mu\text{M}$  dNTPs were used. The PCR was carried out using the following cycling conditions: Initial denaturation, 98°C, 2 min; 35 cycles of (Denaturation, 98°C, 20 sec; Annealing, 55°C, 30 sec; Extension, 72°C, 10 min); Final extension, 72°C, 10 min; hold, 4°C.

The PCR product was analysed on a 1 % agarose gel and purified using a spin column purification kit (Quick PCR purification kit) according to the manufacturers instructions and eluted in 30  $\mu\text{l}$  TE buffer (10 mM Tris/Cl pH 8.0, 1 mM EDTA).

### **Excision of the Kanamycin Resistance Cassette**

The Flp recombinase mediates recombination between FRT-sites, removing the marker gene and leaving a single FRT-site in the genome.

5 ng of pCP20, expressing the Flp recombinase, were electroporated into bacteria containing the mutated MCMV BAC. The bacterial culture was incubated at 30°C for 1 h and streaked onto an agar plate containing 17  $\mu\text{g}/\text{ml}$  chloramphenicol and 25  $\mu\text{g}/\text{ml}$  ampicillin.

The plate was incubated overnight at 30°C. A few colonies were streaked onto an agar plate containing 17 µg/ml chloramphenicol only and incubated overnight at 43°C to eliminate the pCP20 plasmid. Single colonies (up to 50) were picked on a plate containing kanamycin and in parallel on a plate containing chloramphenicol only and were incubated overnight at 37°C. The BAC DNA of kanamycin-sensitive clones was analyzed by restriction analysis.

## 4.3 Culture of Bacteria

### Cryoconservation of Bacteria

1 volume of a bacterial culture (e.g. from a liquid culture from a large scale DNA preparation) was mixed with 1 volume of 50% (v/v) glycerol and stored at -80°C.

### Preparation of Electrocompetent Bacteria

A 100 ml bacterial culture grown to an OD<sub>600</sub> of 0.5 - 0.8 was chilled on ice for 15 min. The bacteria were harvested by centrifugation at 4000 rpm for 10 min at 4°C using the 2704 rotor in a Hereaus Megafuge 1.0, washed twice with abundant ice-cold sterile ddH<sub>2</sub>O. The bacteria were washed once in 10% (v/v) ice-cold glycerol, resuspended in a volume equivalent to the pellet volume of 10% (v/v) cold glycerol and stored in aliquots at -80°C. Bacteria were thawed on ice.

## 4.4 Virological Methods

### Preparation of Virus Stocks

For the preparation of virus stocks, MEF were grown in ten tissue culture dishes (ø 14.5 mm) to 70-80% confluence. MEF were infected with approximately 0.01 PFU/cell and were cultured until complete cytopathic effect was observed. Cells were harvested together with the supernatants and intracellular virions were released by at least one freeze-thaw cycle. The mixture of cells and supernatant was transferred into 500 ml sterile centrifuge buckets. Cellular debris was separated from medium by centrifugation in a Beckmann JA-10 rotor at 6000 rpm for 20 min at 4°C. The supernatant was transferred into sterile centrifuge buckets and virus was pelleted by centrifugation in a Beckmann Type 19 rotor for 3 h at 13,000 rpm at 4°C. The virus-containing pellet was left with a small amount of residual medium on ice over night at 4°C. The pellet was resuspended in the residual medium and dounced 20 times on ice. The

suspension was loaded onto a 2 ml cushion of ice-cold 15% sucrose/virus standart buffer (50 mM Tris/Cl pH 7.8, 12 mM KCl, 5 mM EDTA pH , 15% (w/v) sucrose) in a sterile SW 40 ultracentrifuge tube and centrifuged in a Beckmann Type SW40Ti rotor for 1 h at 20,000 rpm, 4°C. The supernatant was decanted and the virus-containing pellet was resuspended in 2 ml ice-cold 15% sucrose/VSB and dounced 20 times on ice. The virus suspension was divided into 50  $\mu$ l aliquots and stored at -80°C.

### **Plaque Assay**

Supernatants or virus stocks were titrated on confluent MEF. For this, dilutions were prepared in 96-well plates. Frozen samples were quickly thawed in a 37°C water bath and diluted in ice cold DMEM without serum and antibiotics. Usually, a dilution-series from 1:10 to 1:100,000 was prepared and dilutions from 1:100 to 1:10,000 were prepared and tested. Only when titers were expected to be low, dilutions of 1:2 to 1:16 were tested. Samples were titrated in triplicates on confluent MEF seeded in 48-well plates. 100  $\mu$ l of diluted sample was applied to the cells and virus was allowed to the cells incubation for 2 h at 37°C, 5% CO<sub>2</sub> before the virus inoculum was removed and cells were covered with 500  $\mu$ l titration medium ( 0.75% (w/v) carboxymethylcellulose, 5% FBS, 10% 10 x DMEM, 2 mM glutamine, 100 U/ml penicillin, 100  $\mu$ g/ml streptomycin sulfate, 3.5 g/l D-glucose, 4 mg/l folic acid, 0.37 % sodium bicarbonate). Plaques were counted four days later using fluorescence microscopy for pSM3fr-GFP derived MCMV or phase contrast microscopy for pSM3fr-derived MCMV. The number of plaque-forming units (PFU) per milliliter of sample was calculated.

### **Reconstitution of Virus**

#### **Electroporation of BAC DNA into NIH 3T3 Cells**

Mutant viruses used for the cell tropism assays were reconstituted by electroporation of BAC DNA into NIH 3T3 fibroblasts. Confluent NIH 3T3 fibroblasts of a cell culture dish ( $\varnothing$  10 cm) were trypsinized and washed once with PBS. Cells were pelleted by centrifugation at 300 x g for 3 min at RT, resuspended in 800  $\mu$ l Opti-MEM and transferred into 4 mm electroporation cuvettes. Approximately 1  $\mu$ g of BAC DNA was added to the cell suspension. The DNA was electroporated into cells using the Gene Pulser Xcell System with the following settings: 250 V and 1500  $\mu$ F. The cells were immediately resuspended in pre-warmed complete growth medium and seeded into cell culture dishes. The medium was changed the next day. When total cytopathic effect occurred the supernatant was harvested and used to infect a cell culture dish ( $\varnothing$  10 cm) with confluent MEF. The supernatant from MEF harvested after total CPE was titrated by plaque assay and used in cell tropism assays.

### **Transfection of BAC DNA into MEF**

BAC DNA from a medium-scale DNA preparation was transfected into sub-confluent MEF in a 6-well tissue culture plate. For this, 10  $\mu\text{l}$  (approximately 1  $\mu\text{g}$ ) DNA was diluted in 40  $\mu\text{l}$  150 mM NaCl solution and 2  $\mu\text{l}$  jetPEI were diluted in 48  $\mu\text{l}$  150 mM NaCl solution. The 50  $\mu\text{l}$  jetPEI solution was then added to the 50  $\mu\text{l}$  DNA solution all at once. The solution was mixed without vortexing and incubated for 25 min. Before adding the solution dropwise to the cells, the medium was aspirated and 1 ml of new medium was provided. After the addition of the solution the tissue culture plate was centrifuged for 20 min at 300  $\times$  g. The next day, 1 ml of medium was added to the transfected cell cultures.

### **Viral Growth Kinetics**

For the analysis of virus growth kinetics, NIH 3T3 fibroblasts or MEF were seeded at a density of  $1 \times 10^5$  cells/well in 12-well plates. Cells were infected at a MOI of 0.1 or at a MOI of 0.3 with centrifugation enhancement for 20 min at 300  $\times$  g resulting in an approximately 10-fold increase of infection. Supernatants from infected cultures were harvested at different time points after infection and titrated by plaque assay on MEF. Cells were pelleted by centrifugation of 5 min at 6000 rpm and the supernatant was transferred into fresh tubes and stored at  $-80^\circ\text{C}$  until all samples were collected.

## **4.5 DNA Methods**

### **Preparation of DNA from Virus Particles**

A cell culture dish ( $\varnothing$  10 cm) with sub-confluent grown MEF or 3T3 was infected at a MOI of 0.1 or less. When total cytopathic effect was achieved cells were scraped into 15 ml centrifugation tubes and were frozen with the supernatant at  $-80^\circ\text{C}$ . Cell associated virus was released by thawing the samples at  $37^\circ\text{C}$  in a water bath. Cellular debris was pelleted by centrifugation at 923  $\times$  g for 10 min at  $4^\circ\text{C}$ . The supernatant was transferred into SW 40 ultracentrifugation tubes and virus particles were pelleted at 25,000 rpm for 1 h at  $4^\circ\text{C}$  using a Beckmann Type SW40Ti rotor. For degradation of cellular DNA the pellet was resuspended in 500  $\mu\text{l}$  Benzonase buffer (50 mM Tris/Cl pH 8.0, 1 mM  $\text{MgCl}_2$ , 100  $\mu\text{g}/\text{ml}$  BSA) and incubated with Benzonase (100 U) for 1 h at RT. Enzyme activity was deactivated by adding 20  $\mu\text{l}$  0.5 M EDTA, pH 8.0. Viral capsids were solubilized by adding 500  $\mu\text{l}$  1% SDS. Cellular and capsid proteins were degraded in the presence of Proteinase K (final concentration 400  $\mu\text{g}/\text{ml}$ ) at  $65^\circ\text{C}$  for 2-3 h thereby releasing the viral DNA.

Viral DNA was extracted once with phenol/chloroform. For this, 1 volume of phenol/chloroform/isoamylalcohol (25:24:1) was added to the aqueous solution and mixed by inverting the sample for 2 min. Subsequent centrifugation at 14,000 rpm for 5 min at 4°C in a 5417R Eppendorf table centrifuge led to the separation into three phases. The aqueous upper phase contained the viral DNA and was collected. After the addition of 1  $\mu$ l of a glyco-gen solution (35 mg/ml) and 1/10 volume 3 M NaAc pH 5.2 the viral DNA was precipitated with 0.8 vol. of isopropanol at 14,000 rpm for 30 min at 4°C in a 5417R Eppendorf table centrifuge. The DNA pellet was washed once with 70% EtOH and dissolved in 100  $\mu$ l 20  $\mu$ g/ $\mu$ l RNase A/TE buffer (10mM Tris/Cl pH 7.5, 1 mM EDTA). The DNA was analysed by restriction analysis of 10-30  $\mu$ l of the dissolved viral DNA.

RNase A stock solution: 10 mg/ ml in 10 mM Tris/Cl pH 7.5/ 15 mM NaCl

## Preparation of Plasmid or BAC DNA

### Small-scale Preparation

In the following protocol the volumes for the preparation of plasmid DNA are given without parentheses and the volumes for the preparation of BAC DNA are given in parentheses. A single bacterial colony was used to inoculate 3 ml (10 ml) LB medium (1% tryptone, 0.5% yeast extract, 1% NaCl) and were grown overnight with the respective antibiotics. Bacteria were harvested by centrifugation at 4000 rpm for 10 min at 4°C and resuspended in 100  $\mu$ l (200  $\mu$ l) Solution I (50 mM glucose, 10 mM EDTA, 25 mM Tris/Cl pH 8.0). For cell lysis the suspension was mixed and incubated with 100  $\mu$ l (200  $\mu$ l) of Solution II (0.2 M NaOH, 1 % SDS) not longer than 5 min. 200  $\mu$ l (300  $\mu$ l) of ice-cold Solution III (3 M potassium acetate, pH 4.8) was used to precipitate proteins and cellular debris on ice for 5 min. The precipitate was pelleted by centrifugation at 14,000 rpm for 5 min at 4°C. The supernatant was collected and DNA was precipitated by addition of 0.8 vol. isopropanol and centrifugation at 14,000 rpm for 5-10 min at 4°C. The DNA pellet was washed once with 70% EtOH and dissolved in 50  $\mu$ l (50  $\mu$ l) 20  $\mu$ g/ $\mu$ l RNase A/TE buffer (10 mM Tris/Cl pH 7.5, 1 mM EDTA). The DNA pattern was analysed by restriction analysis of 0.5-2  $\mu$ l (45  $\mu$ l) of the dissolved plasmid or BAC DNA .

### Medium-scale Preparation

Glycerol stocks or pre-cultures of the bacteria containing the plasmid or the viral BAC were used to inoculate 100 ml of LB medium. Cultures were grown overnight in the presence of the respective antibiotics. Bacteria were harvested by centrifugation at 4000 rpm for 10 min at 4°C. The DNA was purified using the Nucleobond PC 100 DNA purification protocol for



low copy plasmids was used according to the manufacturers instructions. The DNA pellet was dissolved in 100  $\mu$ l (100  $\mu$ l) 20  $\mu$ g/ $\mu$ l RNase A/TE buffer (10 mM Tris/Cl pH 7.5, 1 mM EDTA). The DNA pattern was analysed by restriction analysis of 1-5  $\mu$ l (10  $\mu$ l) of the dissolved DNA.

### **Electroporation of Bacteria**

2-5 ng of plasmid DNA were used to transform a 50  $\mu$ l aliquot of electrocompetent bacteria by electroporation in 2 mm electroporation cuvettes using the Gene Pulser Xcell System with the following settings: 2500 V, 15 $\mu$ F and 300  $\mu$  $\Omega$ . The bacteria were resuspended in 500  $\mu$ l of LB medium, incubated at the required temperatures for 1 h and streaked onto an agar plate with the required antibiotics.

### **Transfection of Plasmids into Cells**

For transfection 5 x 10<sup>5</sup> NIH 3T3 cells/well or 8 x 10<sup>5</sup> 293T cells/well were seeded into a 6-well plate. 2.5  $\mu$ g plasmid DNA was transfected using 6.5  $\mu$ l Icafectin according to the manufacturers instructions. Medium was exchanged 12 h after transfection, and cells were harvested for Western Blotting 24 h post transfection.

NIH 3T3 fibroblasts were transfected in 6-well plates with the pIRESM25 constructs or the empty vector using 2  $\mu$ g DNA and 10  $\mu$ l Lipofectamine transfection reagent according to the manufacturers instructions.

### **Restriction Analysis of Plasmid DNA**

The integrity of plasmid DNA was controlled by digesting 0.5 - 2  $\mu$ l of 50  $\mu$ l dissolved DNA from a small-scale DNA preparation using 5 - 10 U of enzyme in the appropriate buffer for 1 h at 37°C. The sample was supplemented with DNA loading buffer and fragments were separated in a 1 - 2% agarose gel in 1 x TAE buffer (40 mM Tris base, 40 mM acetic acid, 1 mM EDTA) at 100 V for 45 min using the PerfectBlue™ Mini S gel system. Gels were stained with ethidium bromide to visualize the DNA fragments.

### **Restriction Analysis of BAC DNA**

To analyse the integrity of the viral BACs after mutagenesis, 45  $\mu$ l of 50  $\mu$ l of dissolved BAC DNA from a small-scale preparation, 10  $\mu$ l of 100  $\mu$ l of dissolved BAC DNA from a medium-scale preparation or 10  $\mu$ l of 100  $\mu$ l of dissolved viral DNA from a virus DNA preparation were treated with 20 U of the restriction enzyme in the appropriate buffer for 1.5-3 h at 37°C.

### **Agarose Gel Electrophoresis**

The DNA sample was supplemented with DNA loading buffer (50 % (v/v) glycerol, 0.37 mM Bromphenolblue, 10 mM EDTA pH 8.0) and fragments were separated in a 0.6 % agarose gel in 1 × TBE buffer (90 mM Tris/Cl pH 8.3, 90 mM boric acid, 2 mM EDTA) at 80 V for 12-16 h using the PerfectBlue™ Maxi S gel system. Gels were stained with ethidium bromid to visualize the DNA fragments.

### **Extraction of DNA from Agarose Gels**

DNA was extracted from agarose gels using the UltraClean™15 DNA purification kit according to the manufacturers instructions. The DNA pellet was dissolved in 30 µl elution buffer.

### **Phosphatase Treatment of Vector DNA**

To prevent religation of linearized vector DNA the 5'-phosphate groups can be removed from vector DNA using the alkaline phosphatase (CIP). For this, the vector is treated with alkaline phosphate (0.5 U/µg DNA) in the appropriate buffer at 37°C for 1 h.

### **Ligation**

Ligation was carried out using a 1:1 up to 3:1 molar ratio of insert DNA to vector DNA. 1-2 U T4 DNA Ligase were used in the appropriate buffer and supplemented with PEG 4000 solution if necessary (for blunt end ligation). The mixture was incubated in a waterbath overnight at 16°C.

### **Cloning of the pIRESM25CHA and pIRESM25NHA vectors**

The pIRESM25CHA vector was constructed by PCR amplification of the full length M25 ORF using primers M25CHA-EcoRI and M25CHA-PstI and wild type BAC DNA as template. Primer M25CHA-EcoRI contains an EcoRI restriction site and primer M25CHA-PstI contains the sequence of the hemagglutinin (HA) tag and a PstI restriction site. The HA-tag was added to the M25 C-terminus for later M25 protein detection with an HA-specific antibody. The product was then digested with EcoRI and PstI and ligated into EcoRI/PstI digested pIRES2AcGFP1 between the HCMV major immediately early promoter (MIEP) and the IRES giving rise to pIRESM25CHA. The M25-HA construct was ligated via EcoRI/PstI downstream of the HCMV major immediate early promoter (MIEP) and upstream of the IRES in order to produce the pIRESM25-tagged constructs.

The M25CHA vector construct contains 51 nt spanning the region between the transcript start and M25 translation start codon ATG. This sequence represents the 5' untranslated region (UTR) or leader sequence and should ensure proper recognition of the ATG by ribosomes [Kozak, 1987]. The C-terminal HA-tag could theoretically have a negative influence on M25 protein function by altering the folding of the protein.

Considering this possibility, a second plasmid was constructed in which an HA-tag was added to the M25 N-terminus. The M25 ORF contains more than 10 ATGs in frame. Translation initiation is to some extent determined by the nucleotide context around the ATG [Kozak, 1999]. For adding an HA-tag to the N-terminus, the 5th ATG was chosen since this particular ATG was claimed to be the initiation codon according to Dallas et al., possibly because it is surrounded by a strong context [Dallas et al., 1994]. Primers HANM25-EcoRI and HANM25-PstI were used to amplify the ORF M25 providing 48 nt spanning the 5' UTR. Here, the sequence for the HA-tag is provided with the primer HANM25-EcoRI. The integrity of the M25 sequence and the HA-tag was confirmed by sequencing.

## Quick Mutagenesis of Plasmids by PCR

This protocol is based on the method for the site-directed mutagenesis of double-stranded DNA by PCR [Weiner et al., 1994]. It relies on amplification of full-length plasmid using primers facing opposite directions. The method allows easy and quick introduction of point-mutations, deletions and insertions into plasmids. The plasmid pIRESM25CHA containing the complete predicted M25 ORF [Rawlinson et al., 1996] was used as a template to shorten the M25 ORF by PCR. 60 ng of template DNA were used in a 50  $\mu$ l reaction and 200  $\mu$ M of each forward primer ATG N° 2 to ATG N° 10 were used with the reverse primer HMIEP N°1. Forward and reverse primers were ordered with phosphorylated 5'ends for subsequent circularization of the linear PCR fragments by ligation. The Phusion polymerase (0.5 U/50  $\mu$ l reaction) was used for amplification according to the manufacturers protocol with the following PCR conditions: Initial denaturation, 98°C, 1 min; 35 cycles of (Denaturation, 98°C, 10 sec; Annealing, 62°C, 30 sec; Extension, 72°C, 3 min); Final extension, 72°C, 10 min; hold, 4°C.

The size of the PCR products was analysed by separating 5  $\mu$ l of each reaction on a 1% agarose gel. The remaining 45  $\mu$ l of the PCR reaction were separated on a 1 % agarose gel and DNA fragments with the correct size were excised and purified from agarose using the UltraClean<sup>TM</sup>15 kit and eluted in 30  $\mu$ l ddH<sub>2</sub>O. For removal of methylated template DNA, DpnI was added to the eluted PCR products and was incubated at 37°C for 1 h. The PCR products were purified using the Quick PCR purification kit and the DNA concentration was determined by measuring the OD<sub>260</sub>. An OD<sub>260</sub>=1 is equivalent to 50  $\mu$ g/ml of DNA. The linear plasmids were circularized using T4 ligase in the appropriate buffer overnight at 16 °C

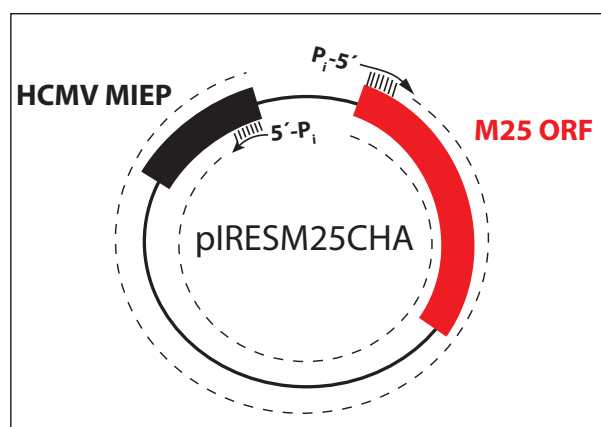


Figure 4.1: **Quick mutagenesis of Plasmids by PCR** A standard reverse primer (HMIEP.rev) was used in all reactions and annealed downstream of the major IE promoter sequence amplifying the promoter sequence and the following vector sequence in the negative orientation. The individual forward primers amplified the plasmid in positive orientation. Primer annealing took place in front of the individual ATG ensuring approximately 50 nt between transcription start and initiation of translation. A 5'-leader sequence of at least 20 nt is required for efficient translation of the 1st ATG in vertebrates [Kozak, 1987]. The scheme is not drawn to scale.

and electroporated in DH10B bacteria for the generation of new plasmids. The presence of the correct DNA fragments was controlled by restriction enzyme digest of plasmid DNA. The integrity of the M25 sequence was checked by sequencing.

## Generation of the M25R virus

For the construction of the M25R virus, the kanamycin resistance gene was excised from the  $\Delta$ M24-m25.2 BAC by Flp-mediated recombination. A 4.3 kbp fragment of the plasmid pOriM25 consisting of the M25 ORF and containing 840 bp of the sequences upstream of the M25 start codon and 748 bp downstream of the M25 stop codon, predicted to provide suitable promoter elements and the polyadenylation signal was excised with *Stu*I/*Pst*I from the pACYC177 vector containing the complete *Hind*III A fragment of the pSM3fr BAC. The fragment was ligated to *Hpa*I/*Pst*I digested pOri6klinker vector giving rise to the pOriM25. The pOri6klinker vector contains of a kanamycin resistance cassette with a single FRT-site. The complete 5.9 kb pOri6M25 construct integrated into the  $\Delta$ M24-m25.2  $\Delta$ KnR BAC using FLP-mediated recombination, giving rise to the M25R BAC. Infectious virus was reconstituted in MEF.

## Sequencing

Plasmids and PCR fragments were sequenced on ABI 3730XL 96-Capillary Sequencers at EUROFINs MWG Operon, Ebersberg. BAC-DNA and products from the 5'/3' RACE were sent to Sequiserve, Vaterstetten and were sequenced on ABI Prism 3730 48-Capillary Sequencers.

## 4.6 RNA Methods

### RNA Preparation

3T3 cells were seeded at a density of  $5 \times 10^5$  cells/well in a 6-well plate the day before the experiment. A total of  $1.5 \times 10^6$  cells was infected with purified virus stock at a MOI of 0.3 with centrifugal enhancement at  $300 \times g$  for 20 min. Total RNA was extracted using the RNeasy kit according to the manufacturers protocol. Cells were directly lysed in the wells using the  $\beta$ -mercaptoethanol - containing lysis buffer RLT. Lysates were homogenized using QIAshredder homogenizers according to the manufacturers instructions.

The quality of the RNA was determined by measuring the OD<sub>260</sub> and OD<sub>280</sub> and calculating the 260/280 ratio. Pure RNA is determined by a ratio between 1.8 - 2.0. An OD<sub>260</sub> of 1 is equivalent to 40  $\mu\text{g}/\text{ml}$  of RNA.

### Northern Blotting

10  $\mu\text{g}$  of purified total RNA were denatured in 20  $\mu\text{l}$  deionised formamide/ 6  $\mu\text{l}$  formaldehyde/ 2  $\mu\text{l}$  20x MOPS for 10 min at 65°C and separated by size at 125 V in a 1% agarose gel (1% agarose, 11.35% (v/v) formaldehyde in DEPC-treated ddH<sub>2</sub>O) in running buffer (1x MOPS/ 7.5 % formaldehyde in DEPC-treated ddH<sub>2</sub>O). The gel was washed 3  $\times$  10 min in DEPC-treated ddH<sub>2</sub>O and was equilibrated together with the nylon transfer membrane for 20 min in 20x SSC. Subsequently, RNAs were transferred onto a nylon membrane in 20x SSC overnight using capillary transfer and were immobilised with 1200 Joules in a UV-light cross-linker. Gene-specific probes were raised by PCR on MCMV wild-type BAC DNA using gene-specific primers. Probes (25 ng) were radiolabeled with <sup>32</sup>P-dCTP (2 MBq/probe) using the DecaLabel DNA labeling kit and were separated from unincorporated nucleotides using MoBiTec spin columns. The membrane was pre-hybridised for 2 h at 42°C in hybridisation buffer (6 x SSC/ 5 x Denhard's solution/ 50% (v/v) deionised formamide/ 1% (w/v) SDS/ 0.5 mg salmon sperm DNA) before the labelled probes were added. Hybridisation of the membrane was carried out overnight at 42°C. The membrane was rinsed once and washed for 15 min in pre-warmed 2x SSC followed by three additional washing steps for 15 min each in pre-warmed washing buffers containing lowered concentrations of SSC (2x SSC/ 0.1% SDS; 1x SSC/ 0.1% SDS; 0.1x

SSC/ 0.1% SDS) and were sealed and exposed to X-ray films.

20x MOPS: 400 mM MOPS, 200 mM sodium acetate, 20 mM EDTA in ddH<sub>2</sub>O

20x SSC: 3 M NaCl pH 7.2, 0.3 M sodium citrate in ddH<sub>2</sub>O

50x Denhard's solution: 1% Ficoll, 1% polyvinylpyrrolidone, 1% bovine serum albumin.

### **Transcript Mapping using Rapid Amplification of cDNA Ends**

For mapping of viral transcripts, infected cells were harvested at different time points and RNA was prepared as described in this section, RNA Preparation. To avoid the binding of the primer to remaining DNA, purified RNA samples were treated with the DNA-free kit. The sample was adjusted to 100  $\mu$ g RNA/ml and the contaminating DNA was degraded using DNase I in the presence of RNase inhibitors. Mapping of the transcription start site (5'-end) and 3'-end of the M25 transcript was carried out with the 5'-/3'-RACE kit according to the manufacturers instructions. (See Fig. 4.2)

In brief, for determination of the 5'-end, first strand cDNA was synthesized from 1  $\mu$ g total RNA using a gene-specific primer 5'-SP1. The mRNA template was degraded by the RNase H activity of the Reverse Transcriptase. The cDNA was purified from unincorporated nucleotides and primers and was then used for addition of a homopolymeric A-tail to the 3'-end of the cDNA. Tailed cDNA was then amplified by PCR using a gene-specific primer 5'-SP2 and an Oligo(dT)-anchor primer. First-strand cDNA synthesis for the determination of the 3'-end of the transcript was initiated at the poly(A)-tail of the mRNA using the Oligo(dT)-anchor primer. The mRNA template was degraded by the RNase H activity of the Reverse Transcriptase. Amplification of the resulting cDNA was then performed using the PCR anchor primer that binds to the Oligo(dT)-anchor primer sequence and a gene-specific primer 5'-SP3. The PCR conditions were optimised by raising the annealing temperature from standard 55 °C to 65 °C to avoid unspecific primer binding. PCR products were separated by agarose-gel electrophoresis. A fraction of the PCR sample was sent for sequencing. When DNA fragments were excised from the agarose-gel, they were purified from agarose using the UltraClean<sup>TM</sup>15 DNA purification kit according to the manufacturers instructions and were sequenced.

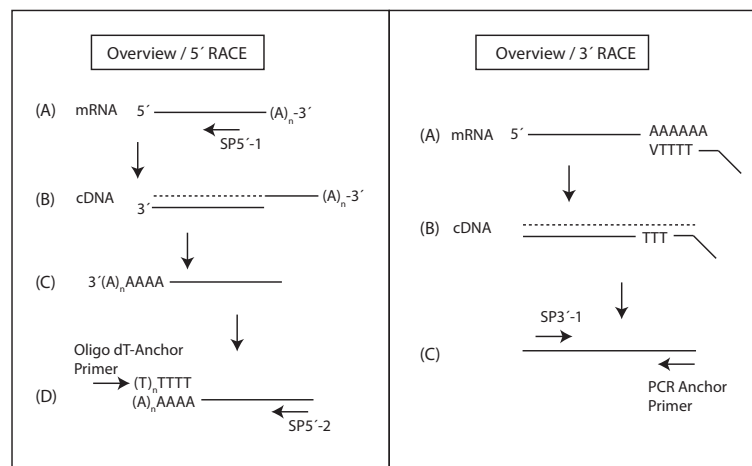


Figure 4.2: **5'/3' Rapid amplification of cDNA ends.** Overview of the 5' RACE. (A) Synthesis of the first strand cDNA with the gene specific primer SP5'-1. (B) Degradation of the mRNA template by the RNase H activity of Transcriptor Reverse Transcriptase. (C) Tailing of the purified cDNA. (D) Amplification of the tailed cDNA by PCR using the Oligo (dT)-anchor primer and a second gene specific primer SP5'-2. Overview of the 3'RACE. (A) cDNA synthesis using the Oligo (dT)-anchor primer. (B) Degradation of the mRNA by the RNase H activity of Transcriptor Reverse Transcriptase. (C) Amplification of the cDNA by PCR using a gene specific primer SP3'-1 and the PCR anchor primer. Scheme is modified from Roche Applied Science.

## 4.7 Protein Methods

### Immunoblotting

#### Preparation of Cell Lysates

For the kinetics of M25 protein expression  $1 \times 10^6$  cells NIH 3T3 cells were infected in 6-well plates ( $5 \times 10^5$  cells/well) for every investigated time point. A MOI of 0.5 was used followed by centrifugation of the plates for 20 min at  $300 \times g$  leading to an approximately 10-fold increase of infection. Cells were scraped and transferred together with the supernatant into 15 ml centrifugation tubes. Cells were pelleted at  $300 \times g$  for 3 min and resuspended in 1 ml ice-cold PBS to determine the number of cells. The cell suspension was transferred into 1 ml centrifuge tubes. Cells were pelleted again and  $1 \times 10^6$  cells were lysed in 100  $\mu$ l lysis buffer (125 mM NaCl, 20 mM Tris/Cl pH 7.4, 1% NP-40) containing 1% protease inhibitors per  $1 \times 10^6$  cells followed by 5 min incubation on ice. Cellular DNA was sheared using needles and cellular debris was pelleted at 14,000 rpm for 5 min using the 5417R Eppendorf table centrifuge. Cell lysates were frozen at  $-20^\circ\text{C}$  or directly used for immunoblotting.

### SDS-PAGE

Proteins were separated by size in either small (8 cm wide) 10% or large (18 cm wide) 7.5% polyacrylamide gels. For the 10% resolving gel, 2.5 ml 40% acrylamide mix, 2.5 ml 1.5 M Tris/Cl pH 8.8, 100  $\mu$ l 10% SDS and 4.8 ml H<sub>2</sub>O were mixed. The polymerisation was started by adding 4  $\mu$ l TEMED and 100  $\mu$ l 10% ammonium persulfate. For the 7.5% resolving gel, 4.7 ml 40% acrylamide mix, 6.3 ml 1.5 M Tris/Cl pH 8.8, 250  $\mu$ l 10% SDS and 13.5 ml H<sub>2</sub>O were mixed. The polymerisation was started by adding 25  $\mu$ l TEMED and 250  $\mu$ l 10% ammonium persulfate. The solutions were casted into vertical electrophoresis units and were overlaid with 2-isopropanol and allowed to polymerise. The Mini-Protean Electrophoresis system was used for the small gels and the Hoefer SE 600 Ruby electrophoresis system was used for the large gels. For the 5% stacking gel a solution was prepared of 0.4 ml 40% acrylamide mix, 0.38 ml 1.5 M Tris/Cl pH 6.8, 30  $\mu$ l 10% SDS, 2.2 ml H<sub>2</sub>O, 3  $\mu$ l TEMED and 30  $\mu$ l 10% ammonium persulfate for small gels and 1.25 ml 40% acrylamide mix, 1.25 ml 1.5 M Tris/Cl pH 6.8, 100  $\mu$ l 10% SDS, 7.3 ml H<sub>2</sub>O, 15  $\mu$ l TEMED and 100  $\mu$ l 10% ammonium persulfate for the large gels and casted onto the polymerised resolving gel.

Cell lysates were diluted 1:1 in protein loading buffer (500  $\mu$ l protein sample buffer, (2%)  $\beta$ -Mercaptoethanol) and were boiled for 5 min at 99°C and loaded onto polyacrylamide gels. The protein samples were loaded onto a polyacrylamide gel and separated by size using a Mini-Protean Electrophoresis system in running buffer A (25 mM Tris base, 250 mM Glycine, 0.1% SDS) at 50-100 V or a Hoefer SE 600 Ruby electrophoresis system in running buffer B (25 mM Tris base, 192 mM Glycine, 0.1 % SDS) at 100 mA.

Protein sample buffer: 100 mM Tris/Cl pH 6.8, 4% SDS (w/v), 0.2% (w/v) Bromphenolblue, 20% (v/v) glycerol

### Western Blotting

Proteins were transferred from the polyacrylamide gels onto nitrocellulose membranes in transfer buffer A (20% methanol, 40 mM Tris base, 119 mM Glycine) using a Mini Trans-Blot Cell apparatus at 0.35 mA for 1 h or in case of the 7.5 % gels in transfer buffer B (10% Methanol, 48 mM Tris base, 380 mM Glycine, 0.1% (w/v) SDS) using a water-cooled TE 62 transfer unit at 100 mA for 16 h.

### Immunostaining

Unspecific binding sites were blocked by incubating the membrane for 1 h in blocking buffer (2% milk powder in PBS/ 0.1% Tween) at RT. The membrane was incubated for 1.5 h with the first antibody diluted in 2% milk powder in PBS/ 0.1% Tween under weak agitation. Excess antibody was removed by rinsing the membrane with PBS/ 0.1% Tween followed by 1 x 15



min and 3 × 5 min washing before incubation for 1.5 h with the horseradish peroxidase-linked second antibody diluted in PBS/Tween 0.1%. After the incubation period the membrane was rinsed once with PBS/ 0.1% Tween and washed 1 × 15 min and 3 × 5 min, treated with ECL Western Blotting detection reagent and developed using a LAS-3000 imager.

### Stripping

Primary and secondary antibodies were removed from the membranes by incubation in stripping buffer (100 mM  $\beta$ -Mercaptoethanol, 2 % SDS, 62.5 mM Tris/Cl pH 6.7) for 30 min at 50°C. The membranes were washed twice for 10 min with large volumes of wash buffer ( PBS/ 1% Tween) at RT followed by repeating the immunostaining protocol.

### Immunofluorescence

Cells were seeded on coverslips ( $\varnothing$  10 mm) at a density of  $1 \times 10^4$  -  $1 \times 10^5$  cells/well in a 24-well plate one day before infection. A MOI of 0.1 was used, followed by centrifugation of the plates for 20 min at 300 × g thereby increasing the infection approximately 10-fold. Cells were briefly washed in PBS and fixed with PBS/ 3% paraformaldehyde (PFA) for 20 minutes at different time points after infection. Remaining PFA was inactivated by incubating the cells in PBS/ 50 mM  $\text{NH}_4\text{Cl}$  for at least 10 min. Incubation with PBS/ 0.2% Triton-X 100 for exactly 5 min was used to permeabilize the plasma membrane. To minimize background staining free binding sites were blocked with PBS/ 0.5% (w/v) BSA at RT for 30 min. Cells were then incubated with the appropriate dilution of the primary antibody, washed 3 × 5 min in PBS, and then incubated with secondary antibody directly coupled to a fluorescent dye. First and second antibodies were diluted in PBS/ 0.5% (w/v) BSA. After incubation with the second antibody cells were washed 3 × 5 min with PBS. Cells were dipped in ddH<sub>2</sub>O to eliminate excess BSA and PBS before they were mounted with Aqua Poly Mount and analyzed using a Zeiss Axio Observer laser scanning microscope. Images were further processed using Adobe Photoshop CS 3. Filamentous actin was labelled using TRITC-Phalloidin. This is a toxin of the mushroom *Amantia phalloides* that binds to and stabilises actin filaments. Fluorophore-coupled Phalloidin is commonly used to visualise actin filaments by fluorescence microscopy.

## 4.8 Cell Tropism Assay

MEF and C127I were seeded in 6-well plates at a density of  $1 \times 10^5$  cells/well 16-20 h before the experiment. Each virus was tested in triplicate cultures. MEF and C127I were infected at a MOI of 0.01. For the initial screening of the growth properties of the MCMV mutants

supernatants of infected cultures were used for infection. Virus stocks or supernatants were quickly thawed in a 37°C water bath and kept on ice. Virus was diluted in pre-warmed complete growth medium and 1 ml/ well was used for inoculation. Virus was allowed to bind to the cells by incubation of the plates for 2 h at 37°C, 5% CO<sub>2</sub> before the virus inoculum was replaced by 2 ml of new growth medium. Cells were then further incubated at 37°C, 5% CO<sub>2</sub>. On day six after infection 200 µl supernatants were harvested from each well. Cells were pelleted at 6000 rpm in a 5417R Eppendorf table centrifuge for 5 min at RT and the supernatants were transferred into fresh tubes, frozen in liquid nitrogen and stored at - 80°C until all samples were obtained. Viral titers were determined by plaque assay on MEF. Virus spread was documented on day two and day six after infection using fluorescence microscopy.

### **4.9 Infection of Cells for the Screening of the Cellular Morphology**

Cells were infected in 6-well plates at a MOI of 0.3 with centrifugal enhancement for 20 min at 300 x g leading to an approximately 10-fold increase of infection. For this, virus was diluted in 1 ml of complete growth medium. The growth medium was removed from the cells and the virus inoculum was pipetted onto the cells. After centrifugation, the cells were incubated for 2 h in a humid atmosphere in an incubator at 37°C and 5% CO<sub>2</sub>. 1 ml of complete growth medium was added after the 2 h incubation. Cellular morphology was analysed at 48 h after infection using fluorescence microscopy.

### **4.10 Analysis of the Cellular Morphology after Transfection of the pIRES vectors**

NIH 3T3 fibroblasts were transfected with the pIRESM25CHA, pIRESM25NHA or the empty pIREsAcGFP1 plasmids as described above. At 48 hours after infection the number of transfected outstretched or round cells was determined in four to five random fields of view from one well of cells transfected with an individual plasmid using a fluorescence microscope. The percentage of round cells of total counted cells from a single field of view was calculated. The value of the mean percentage and its standard deviation was determined from all analysed frames of one plasmid.

## 4.11 Bioinformatic Tools

The following prediction programs were used. For the alignment of two protein sequences and the similarity searches of a protein or a nucleotide sequence, the Basic Local Alignment Tool (BLAST) (<http://blast.ncbi.nlm.nih.gov/Blast.cgi>) was used [Altschul et al., 1990, Tatusova and Madden, 1999]. PSORT II predicts subcellular localization sites of proteins from their amino acid sequence [Nakai and Horton, 1999]. SOSUI discriminates between soluble and membrane proteins by analysing helices hydrophobicity and protein length based on known soluble and membrane proteins [Mitaku and Hirokawa, 1999]. NetPhos, predicts serine, threonine and tyrosine phosphorylation sites in a given protein sequence [Blom et al., 1999]. The molecular weight of a protein was predicted using Compute pI/MW (<http://expasy.org/tools/>).



## 5 Results

The productive infection of epithelial cells and the induction of cell rounding are hallmarks of cytomegalovirus infection. A library of mouse cytomegalovirus mutants was generated, in order to study viral gene function required for the productive infection of epithelial cells and the induction of cell rounding.

### 5.1 Generation of a Library of Mouse Cytomegalovirus

#### Mutants

The MCMV deletion mutants were generated using the BAC mutagenesis technique. The MCMV Smith strain was previously cloned as a bacterial artificial chromosome (BAC) in *E. coli* thereby making it accessible for manipulation using the methods of bacterial genetics [Messerle et al., 1997]. This method uses homologous recombination between linear DNA fragments obtained by PCR and the BAC-cloned MCMV genome employing the recombination enzymes of bacteriophage  $\lambda$ . As an example, a scheme of the construction of the  $\Delta$ M24-m25.2 mutant is shown in Fig.5.1.

In principle, a selection marker, e.g. the kanamycin resistance gene, is amplified by PCR using primers with a 20 bp homology to the kanamycin resistance cassette and a 50 bp homology at either end of the target gene. The amplified linear DNA fragment is electroporated into the bacteria which contain the MCMV BAC and a plasmid expressing the recombination enzymes *exo*, *bet* and *gam*. The recombination enzymes mediate the homologous recombination between the linear DNA fragment and the MCMV BAC. The bacteria containing the mutant BAC are then identified by antibiotic selection. The mutant BAC is isolated and the integrity of the BAC DNA is analysed by restriction enzyme analysis.

All mutants that were generated in this study were analysed for genome integrity by cutting BAC DNA with at least two restriction enzymes. In addition, viral DNA was prepared from infected fibroblasts and the correct DNA pattern was assured by restriction analysis of the DNA.

The restriction patterns of the wild type MCMV BAC and three BAC mutants,  $\Delta$ M24-m25.2,  $\Delta$ m139-m141 and  $\Delta$ m42-M43, after treatment with *EcoRI*, are shown in Fig.5.2.

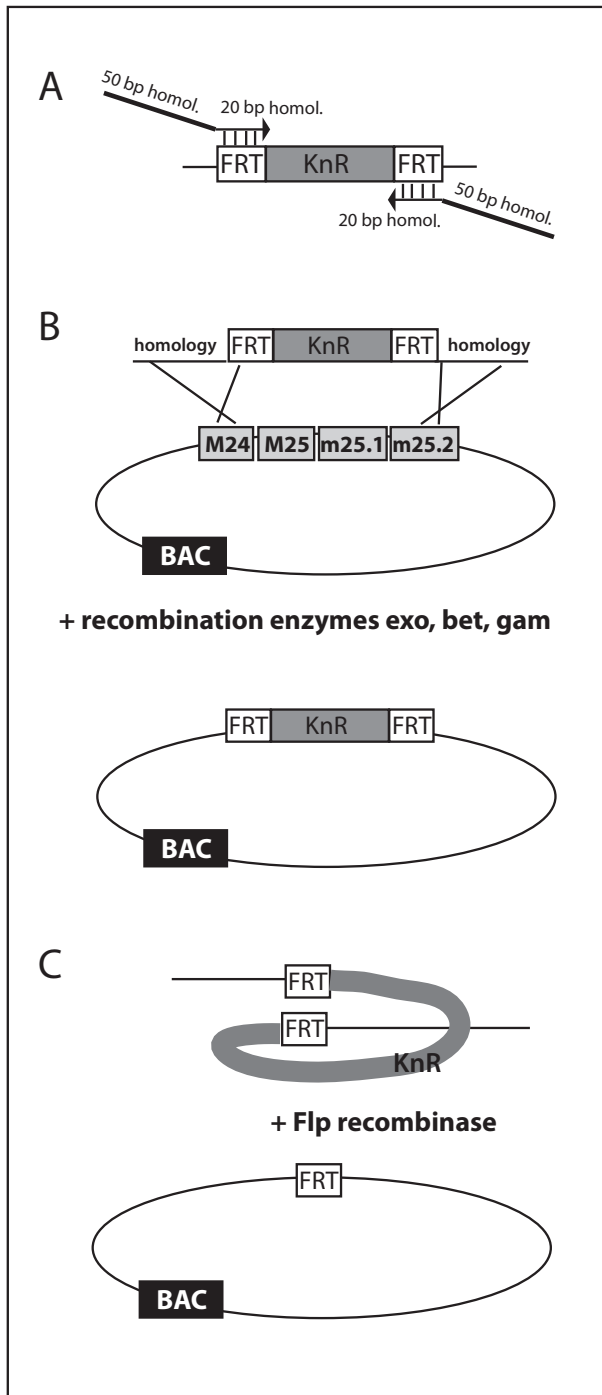


Figure 5.1: **BAC mutagenesis using linear DNA fragments** (A) The kanamycin resistance gene, flanked by FRT-sites was amplified by PCR using primers with a 20 bp homology to the template DNA and a 50 bp homology to the sequence within the ORF M24 or to the sequence within the ORF m25.2 on the MCMV BAC. (B) In the presence of the recombination enzymes *exo*, *bet* and *gam* the linear PCR fragment recombines with the homologous regions of the BAC to replace the sequence between the ORFs M24 to m25.2. (C) In some mutants the kanamycin resistance cassette was excised. The Flp recombinase was expressed and mediates DNA excision between the two directly orientated FRT-sites, leaving only a single FRT-site in the mutant BAC.

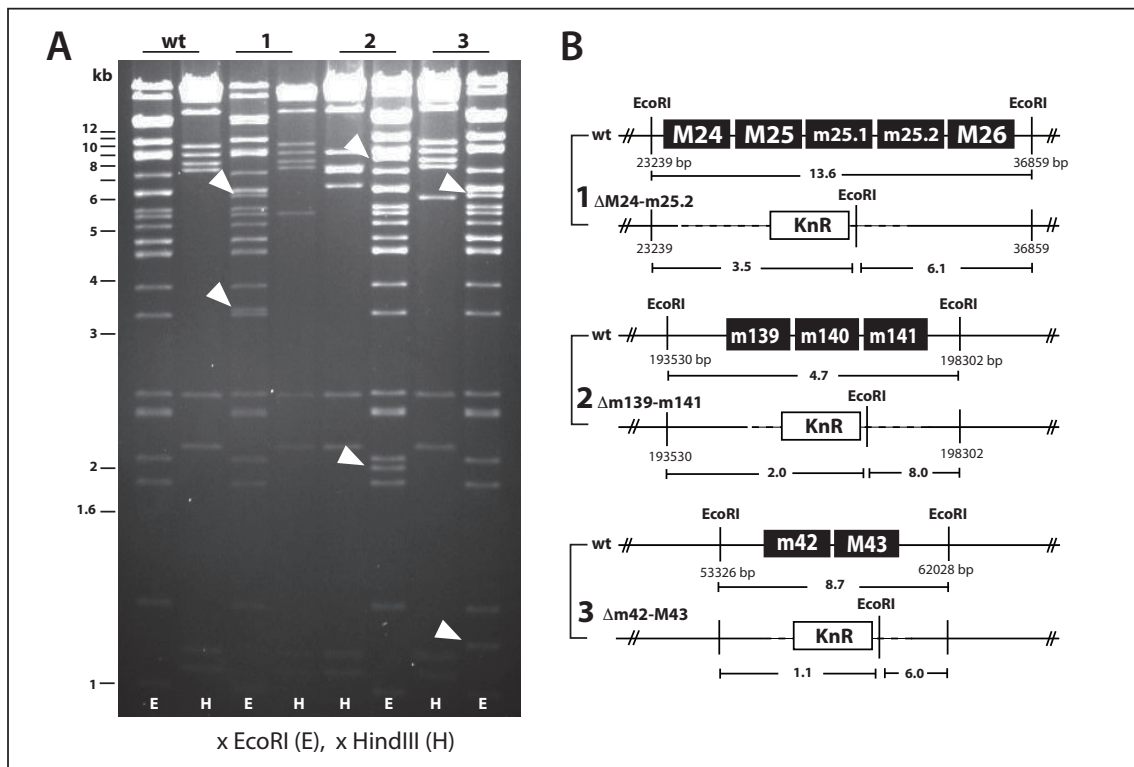


Figure 5.2: **Analysis of MCMV BAC mutants.** (A) BAC DNA from wild type MCMV or MCMV mutants was cut with EcoRI or HindIII restriction enzymes and DNA fragments were separated on an 0.6 % agarose gel. Arrows point to the new fragments generated in the mutant BAC genomes that are not present in the wild type BAC DNA (wt). Size markers are indicated to the left. (B) Schematic illustration of selected DNA fragments after cutting the wild type MCMV BAC (wt), the  $\Delta$ M24-m25.2 BAC (1), the  $\Delta$ m139-m141 BAC (2) and the  $\Delta$ m42-M43 mutant BAC (3) with EcoRI. Genomic positions of the EcoRI sites are indicated in bp and the sizes of the DNA fragments are given in kb. The dashed lines indicate the insertion of the kanamycin resistance cassette. The scheme is not drawn to scale.

The wild type MCMV BAC contains two EcoRI restriction sites upstream of the M24 and downstream of the M26 genes (Fig.5.2B, panel 1, upper line). The intervening fragment has a size of 13.6 kb and was replaced to produce the  $\Delta$ M24-m25.2 BAC. This gave rise to two new fragments of 3.5 and 6.1 kb (Fig.5.2B, panel 1, lower line). The genes m139 to m141 of the wild type MCMV BAC are flanked by two EcoRI sites leading to a 4.7 kb fragment (Fig.5.2B, panel 2, upper line). The  $\Delta$ m139-m141 virus mutant was generated by partially deleting this region thereby disrupting the 4.7 kb fragment. The insertion of the kanamycin resistance cassette produced two new fragments of 2.0 and 8.0 kb (Fig.5.2B, panel 2, lower line). Treatment of the wild type MCMV BAC with EcoRI generates a 8.7 kb fragment containing the m42 and M43 genes. Deletion of the m42 and M43 genes and insertion of the kanamycin resistance cassette disrupted the 8.7 kb fragment and produced two fragments of 1.1 and 6.0 kb (Fig.5.2B, panel 3). Taken together, the fragments produced after cutting with

EcoRI indicated that the mutant genomes had the expected integrity.

The electroporation of BAC DNA of each mutant genome into NIH 3T3 cells led to the reconstitution of infectious virus that was able to produce plaques in fibroblasts.

The BAC mutagenesis technique allowed the manipulation of MCMV genomes and was used for the generation of a library of 18 MCMV mutants. The individual deletions from the MCMV genome encompassed between 1 and 19 genes. In total, 105 genes were covered, referring to the published genomic sequence of the MCMV Smith strain [Rawlinson et al., 1996]. For the generation of the mutant viruses sequences of ranging from 1 to 14 kb were deleted from the wild type MCMV BAC. Genes that are MCMV-specific as well as genes that are common among all CMV were targeted for deletion (Fig.5.3). Most of the targeted genes have previously been shown to be non-essential for viral replication in fibroblasts [Brune et al., 2006]. Genes that are located in the region that is conserved among all herpesviruses and thought to comprise the essential genes for the replication in cell culture e.g. in fibroblasts were not targeted for deletion. The function of the proteins encoded by the majority of the genes targeted for deletion is not known or has not been studied in detail. Manipulating the MCMV genome allows the study of viral gene functions in the context of the viral life cycle. In summary, a library of mouse cytomegalovirus mutants was constructed, which then served as a basis to study viral gene function. In particular, the aim was to identify viral factors of MCMV that are critical for the productive infection of epithelial cells and for virus-induced cell rounding.

## 5.2 Searching for Viral Factors determining the Epithelial Cell Tropism of MCMV

Cytomegaloviruses infect cells of various origin and with various functions such as monocytes and macrophages, smooth muscle cells, fibroblasts, endothelial and epithelial cells. Epithelial cells are of particular interest, firstly because they are among the first cells to become infected by CMV in the oral epithelium of the mucosa and therefore may influence the course of an infection. Secondly, epithelial cells of the salivary gland are major producers of infectious virus and therefore play an important role for the transmission of the virus in the population. To identify viral factors that permit viral growth in epithelial cells, a cell tropism assay was established that allows to investigate the growth of CMV mutants in epithelial cells.



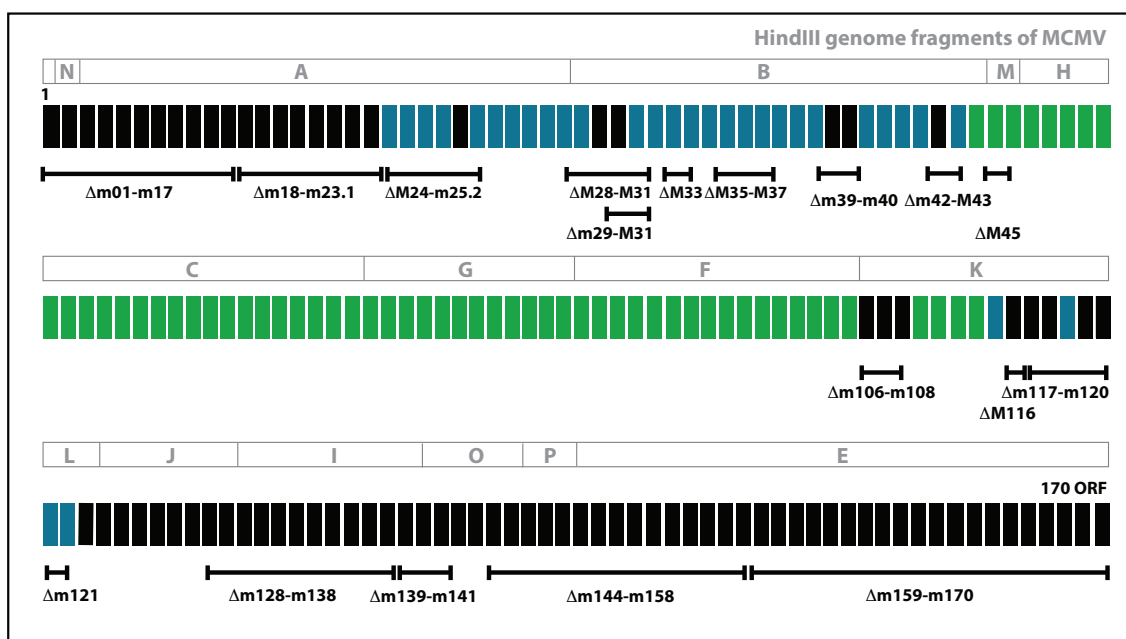


Figure 5.3: **Overview of the constructed MCMV deletion viruses.** The vertical bars represent the ORFs in the genome of the Smith strain [Rawlinson et al., 1996]. Black bars indicate the ORFs which are specific for MCMV. The blue bars indicate ORFs which are common for CMVs and the green bars represent ORFs located in the region that is conserved throughout all herpesviruses. MCMV ORFs with homologs in HCMV are indicated by uppercase prefixes (M45), whereas ORFs without sequence similarity with HCMV ORFs are indicated by lowercase prefixes (m01). The horizontal black lines show the deletions that were introduced and the names of the corresponding virus mutants are mentioned underneath. For an orientation, the HindIII fragments of the MCMV genome are annotated in grey. The scheme is not drawn to scale.

### 5.2.1 Establishment of a Cell Tropism Assay and Screening of a Library of MCMV Mutants

The cell tropism assay was designed in such a way that the growth of a virus in fibroblasts could be compared with the growth of the same virus in epithelial cells. For this, primary mouse embryonic fibroblasts (MEF) and epithelial cells (C127I) were infected with wild type MCMV or mutant viruses. C127I cells are derived from a mouse mammary gland epithelial tumor and both MEF and C127I are permissive for MCMV infection [Kim and Carp, 1971, Smees et al., 1989]. MCMV can infect and replicate in these cells, leading to typical plaque formation, and produces progeny virus. The wild type MCMV represents the standard for viral growth in fibroblasts or epithelial cells and viral growth of the mutants was therefore analysed and compared with regard to the growth properties of the wild type MCMV. The titres of sets of virus mutants and of the wild type MCMV were determined in parallel before the viruses were used in the cell tropism assay (Fig.5.6, diagrams 1-4). In this way, it was assured that

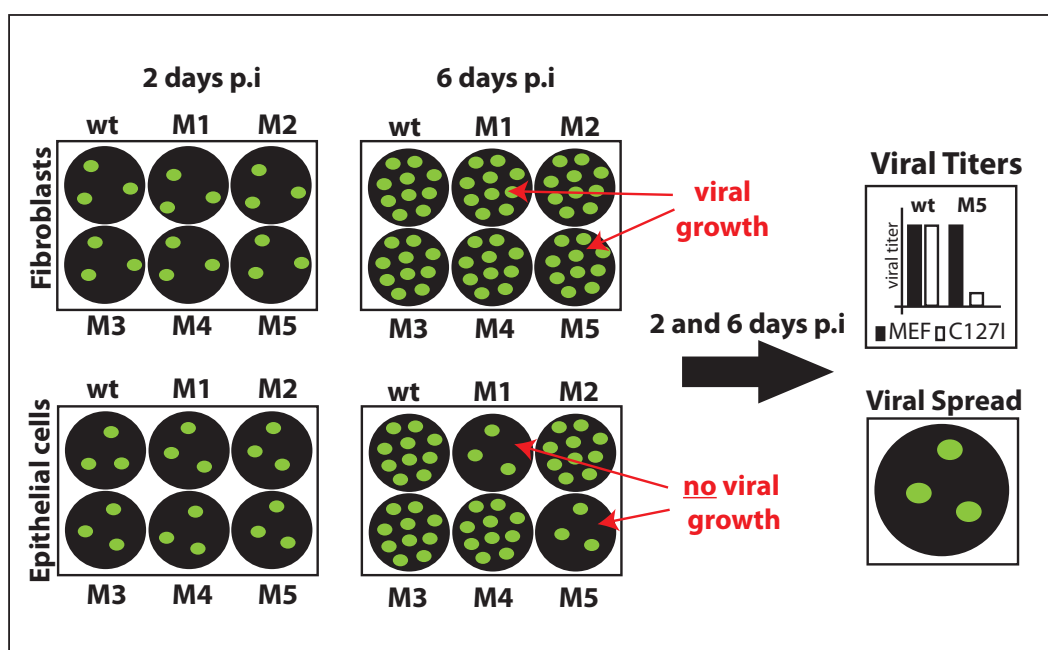


Figure 5.4: **Outline of the Cell Tropism Assay.** Fibroblasts (MEF) and epithelial cells (C127I) were infected using a MOI of 0.01 with wild type MCMV (wt) or various MCMV mutants (M1-5). All viruses express the green fluorescent protein, allowing the identification of infected cells. Wild type MCMV productively infects both, fibroblasts and epithelial cells. Two days post infection (p.i) only a few cells are infected but at day 6 p.i. the virus has spread to most cells. Infection with the mutant viruses leads to a similar number of infected cells at day 2 p.i. All virus mutants are expected to grow in fibroblasts and most virus mutants will grow in epithelial cells. However, if a viral gene is deleted that expresses an epithelial cell tropism factor, the respective virus mutant will not grow in epithelial cells (e.g. M1, M5). Viral growth is analysed by determination of the viral titres and cell-to-cell spread by fluorescence microscopy on day 6 p.i.

the inoculation doses of the viruses were as similar as possible.

A low multiplicity of infection (MOI) of 0.01 was used. A low MOI enables the virus to replicate and to infect neighbouring cells in such a way that the spread of the virus could be monitored. All mutant viruses and the wild type MCMV expressed the enhanced green fluorescent protein EGFP. EGFP emits bright green light when exposed to UV-light, making it possible to identify infected cells by fluorescence microscopy.

Viral titres were determined from supernatants of infected cells harvested at day six after infection. In general, MCMV titres in fibroblasts increase from day 2 to 4 exponentially and reach the stationary phase on day 5 to 6. MCMV growth in epithelial cells in general is slower. Thus, six days after infection represents a suitable time point for the comparison of viral titres of the wild type MCMV with those of different virus mutants. In addition, cell-to-cell spread was documented by taking images from the infected cells with a fluorescence microscope at two and six days after infection. The cell tropism assay is outlined in Fig.5.4.

The cell tropism assay was employed to investigate the viral cell-to-cell spread and growth of all the generated virus mutants. Fibroblasts and epithelial cells were infected in parallel with wild type MCMV or the virus mutants at an MOI of 0.01. Viral spread was documented two days and six days after infection by fluorescence microscopy.

Infected cells could be identified at two days after infection. As an example the viral spread of two selected virus mutants and of the wild type MCMV is shown in Fig.5.5. Single MCMV-infected GFP-positive fibroblasts or epithelial cells infected with either wild type MCMV, the  $\Delta m39-m40$  or the  $\Delta m106-m108$  virus mutants were found. Six days after infection GFP expression was not only visible in single cells but also in neighbouring fibroblasts (Fig.5.5A). This and the formation of plaques indicated that all viruses were able to productively infect fibroblasts.

Infection of neighbouring epithelial cells and plaque formation was observed in wild type MCMV infected cultures (Fig.5.5B) and for most virus mutants. However, the  $\Delta m106-m108$  mutant as well as five additional virus mutants,  $\Delta m29-M31$ ,  $\Delta M28-M31$ ,  $\Delta M35-M37$  and  $\Delta M45$  failed to spread in epithelial cells. The presence of single infected cells and small plaques in epithelial cells indicated that these virus mutants infected epithelial cells but did not spread efficiently in these cells.

At six days after infection the viral titres were analysed. To this end, supernatants from infected fibroblasts or epithelial cells were harvested and the viral titres were determined (Fig.5.6). In fibroblasts, five virus mutants  $\Delta M33$ ,  $\Delta m39-m40$ ,  $\Delta m128-m138$ ,  $\Delta m139-m141$  and  $\Delta m01-m17$  yielded similar titres compared to those of the wild type MCMV. Thirteen virus mutants ( $\Delta m18-m23.1$ ,  $\Delta M116$ ,  $\Delta m106-m108$ ,  $\Delta m159-m170$ ,  $\Delta m29-M31$ ,  $\Delta m42-M32$ ,  $\Delta m117-m120$ ,  $\Delta M28-M31$ ,  $\Delta M24-m25.2$ ,  $\Delta M35-M37$ ,  $\Delta M45$ ,  $\Delta m121$  and  $\Delta m144-m158$ ) yielded maximally two orders of magnitude lower titres compared to the titre of the wild type MCMV. This indicated that the deletion of genes from the virus genome or possibly the insertion of non-viral DNA, i.e. the kanamycin resistance cassette, influenced already the viral growth in fibroblasts.

In epithelial cells, the  $\Delta m42-M43$ ,  $\Delta m139-m141$  and the  $\Delta m01-m17$  virus mutants yielded similar or even higher titres compared to those of the wild type MCMV and 15 virus mutants grew to lower titres than wild type MCMV. The titres of 10 virus mutants,  $\Delta m18-m23.1$ ,  $\Delta M116$ ,  $\Delta m39-m40$ ,  $\Delta M33$ ,  $\Delta m121$ ,  $\Delta m128-m138$ ,  $\Delta m144-m158$ ,  $\Delta M24-m25.2$ , were slightly lower compared to the titre determined for wild type MCMV in epithelial cells (maximally one order of magnitude). Two virus mutants,  $\Delta m29-M31$  and  $\Delta m106-m108$ , grew to titres that were up to three orders of magnitude lower compared to the titre from wild type MCMV infected epithelial cells. The titres of three virus mutants,  $\Delta M28-M31$ ,  $\Delta M35-M37$ ,  $\Delta M45$ , remained below the detection limit. The data obtained from the analysis of the viral titres were consistent with the results obtained from viral spread. Whenever lower titres were

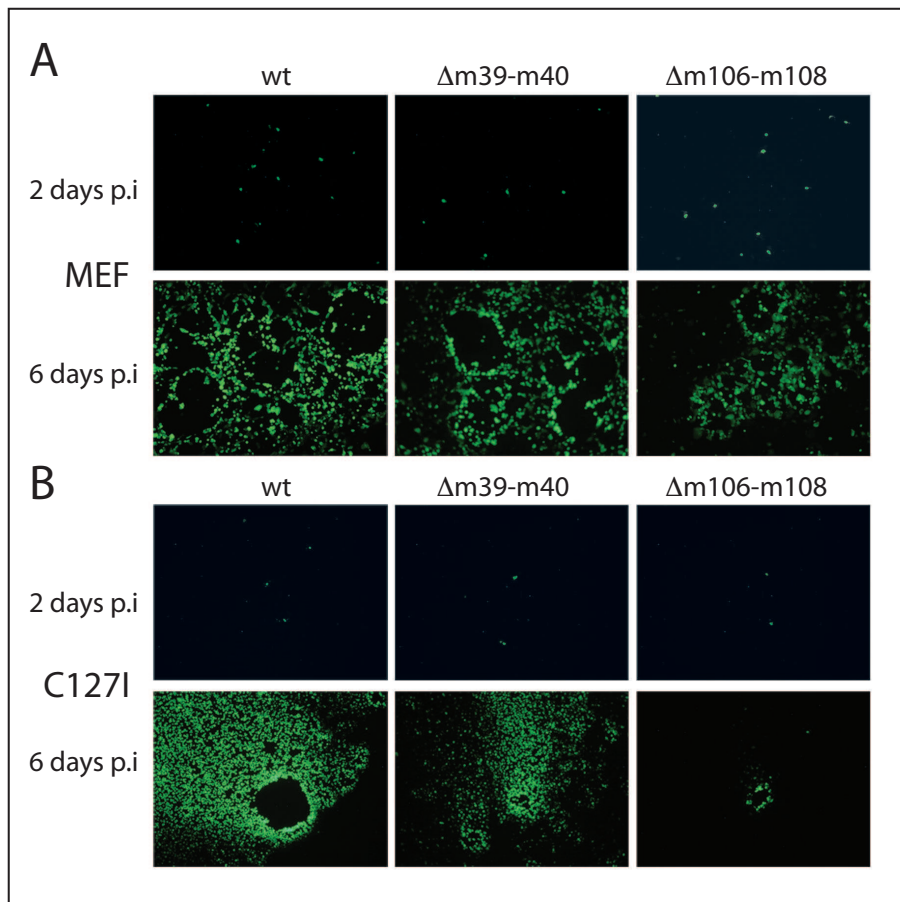


Figure 5.5: **Viral spread of MCMV mutants in fibroblasts and epithelial cells.** MEF (A) and C127I (B) were infected in parallel using a MOI of 0.01 with wild type MCMV (wt) or the virus mutants  $\Delta m39-m40$  or  $\Delta m106-m108$ . MCMV infected cells expressing GFP were monitored at 2 days and 6 days after infection by fluorescence microscopy.

determined, the respective virus did not spread in epithelial cells as efficient as the wild type MCMV. The overall lower titres determined from infected epithelial cells suggest that MCMV grows more slowly on the epithelial cell line C127I as in primary fibroblasts.

In order to identify a virus mutant that is impaired to grow in epithelial cells, the titres of individual virus mutants obtained from epithelial cells were compared to the respective titre of the wild type MCMV. Virus mutants that did not grow at all in epithelial cells or that grew to at least 1.5 orders of magnitude lower titres compared to those of the wild type MCMV were selected. Five virus mutants were identified. Infection of epithelial cells with the  $\Delta m29-M31$  virus yielded 1.5 orders of magnitude lower titres or with the  $\Delta m106-m108$  viruses three orders of magnitude lower titres (Fig.5.6, D2, see arrow), respectively, compared to those of the wild type MCMV. The titres of the  $\Delta M35-M37$ ,  $\Delta M45$  or  $\Delta M28-M31$  viruses in epithelial cells remained below the detection limit. However, the virus mutants  $\Delta M28-M31$ ,  $\Delta m29-M31$ ,

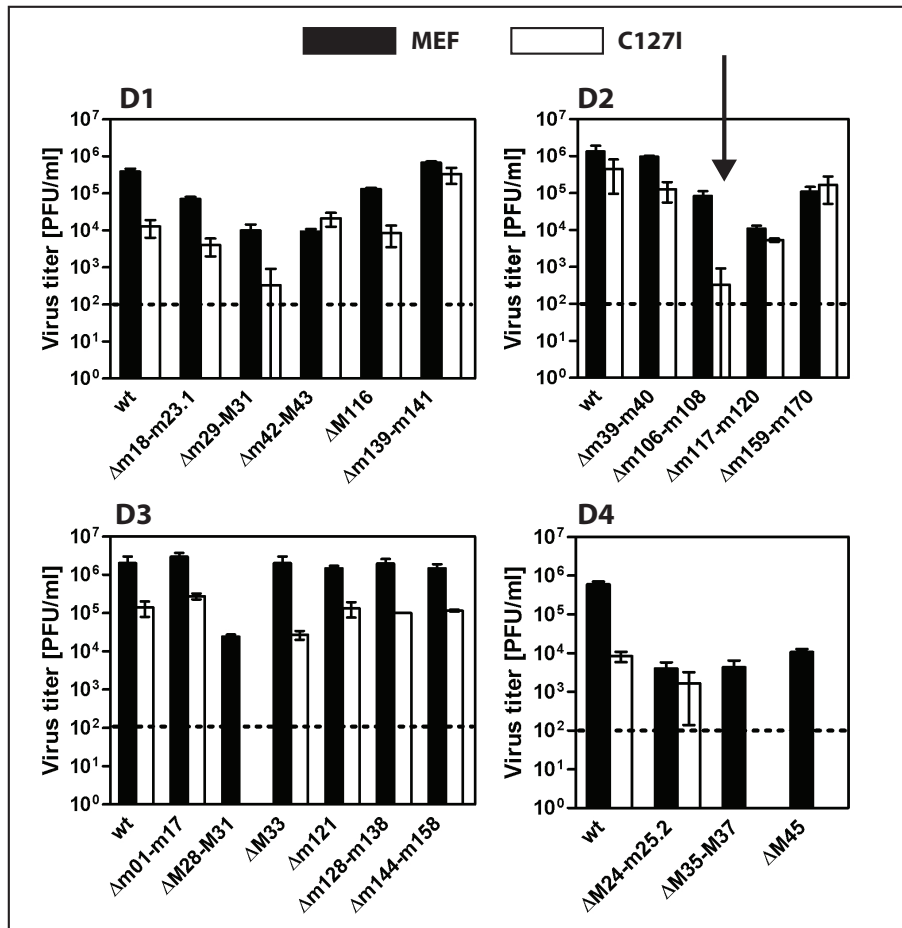


Figure 5.6: **Viral growth of MCMV mutants in fibroblasts or epithelial cells.** MEF and C1271 were infected with wild type (wt) or MCMV mutants using a MOI of 0.01 in triplicate. Supernatants were harvested on day six and viral titres (PFU/ml) were determined by plaque assay on MEF. Data show the results of one representative experiment out of three independent experiments. The dashed line shows the detection limit of the virus plaque assay. Error bars indicate standard deviation of the mean value. Virus mutants were investigated independently as sets of viruses indicated in diagrams D1-D4.

$\Delta$ M35-M37 and  $\Delta$ M45 already failed to grow to high titres in fibroblasts. The titres of these viruses in fibroblasts were at least 1.5 orders of magnitude lower compared to those of the wild type MCMV. This is possibly due to an overall impaired growth caused by the deleted genes and was thus not considered to be unique for the growth in epithelial cells. In contrast, the  $\Delta$ m106-m108 mutant yielded only slightly lower titres in fibroblasts compared to the titre of the wild type MCMV (maximally one order of magnitude). Therefore, this mutant was considered to lack a viral factor required primarily for the growth in epithelial cells and thus the following work focused on the analysis of the m106 to m108 region of the MCMV genome.

### 5.2.2 Analysis of the $\Delta$ m106-m108 Virus Mutant

In order to define the reason for the lack of growth of the  $\Delta$ m106-m108 virus mutant in epithelial cells, additional virus mutants were generated. Three ORFs, m106, m107 and m108, are predicted in the targeted region [Rawlinson et al., 1996]. Additional smaller ORFs m106.1, m106.2, m106.3, m106.4, m106.5, m107.1, m107.2 and m107.3 have also been predicted [Brocchieri et al., 2005]. The m106 gene overlaps with the newly annotated ORFs m106.1 and m106.2 whereas the ORFs m107 and the m108 show a >60 % overlap due to the localisation of the ORF m108 on the complementary strand (Fig.5.7). The newly annotated ORFs m107.1, m107.2 and m107.3 overlap with the ORFs m107 and m108. The ORFs m106.3, m106.4 and m106.5 are located in the region between the ORFs m106 and m107. In addition, a 7.2 kb stable, non-coding intron RNA was reported to be produced from the region between the ORFs m106 and m107 [Kulesza and Shenk, 2006]. The expression of RNA from the predicted ORFs m106, m107 and m108 was also examined using microarray-based oligonucleotide-cDNA hybridisation [Tang et al., 2006]. RNA expression could be confirmed for the ORFs m106 and m108, but the array analysis provided no evidence for the presence of a m107 transcript. The functions of the transcripts mentioned above, have not been elucidated and no proteins encoded from these ORFs have yet been found.

To investigate the role of the ORFs m106, m107 and m108 additional virus mutants were generated using the BAC mutagenesis technique. The generated virus mutants are illustrated in Fig.5.7. Potential expression of the ORFs m106, m107 and m108 was abolished with the deletion of these ORFs giving rise to the  $\Delta$ m106 and  $\Delta$ m107-m108 virus mutants. The deletion of the ORFs m106, m107 and m108 included also the ORFs m106.1, m106.2, m107.1, m107.2 and m107.3. To investigate a potential role of the stable intron RNA in epithelial cell tropism, 3.3 kb were deleted of the DNA sequence including the ORF m106.4, in the mutant denoted  $\Delta$ intron. To exclude possible influences on viral growth, the kanamycin resistance cassette was removed by Flp-mediated recombination from the genomes of the mutant viruses. Infectious virus was reconstituted from the mutant BACs. MEF and C1271 were infected in

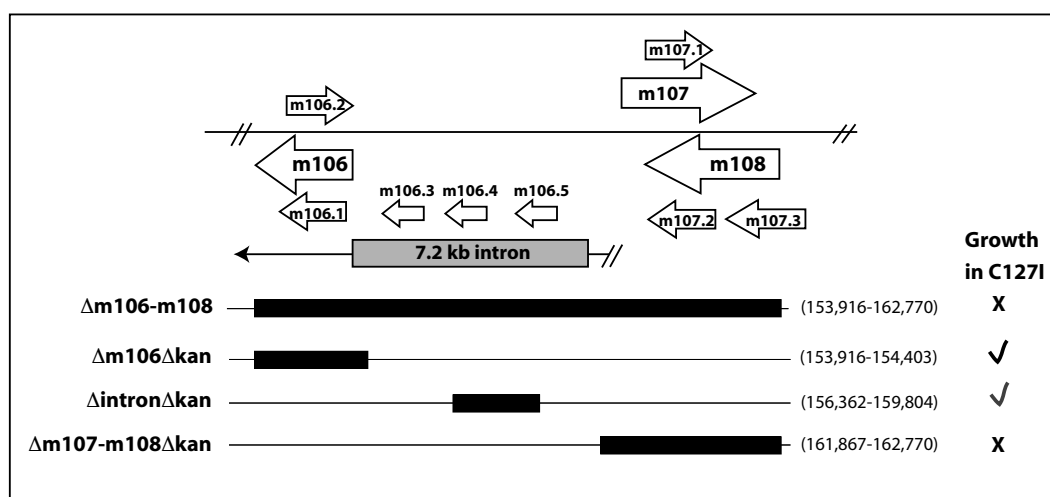


Figure 5.7: **Schematic illustration of the m106-m108 region and the generated deletion viruses.** Black bars indicate the deletions in the virus mutants according to the annotated ORFs. The nucleotide position (bp) of the deletions in the genome is given in parenthesis. Virus mutants that could grow in C127I epithelial cells are marked with a tick, virus mutants that were impaired to grow in C127I cells are marked with a cross. The illustration is not drawn to scale.

parallel with  $\Delta m106\Delta kan$ ,  $\Delta intron\Delta kan$  or  $\Delta m107-m108\Delta kan$  using a MOI of 0.01. Wild type MCMV and the  $\Delta m106-m108$  virus mutant were used as controls. Supernatants from three independent experiments were harvested six days after infection and viral titres were determined by plaque assay.

The titres that were determined for MEF or C127I infected with the virus mutants  $\Delta m106\Delta kan$  or  $\Delta intron\Delta kan$  were comparable to the titres determined for the wild type MCMV (Fig.5.8A). Given that the shorter intron RNA lacking almost half of its sequence is non-functional and no m106 protein can be expressed from the deleted m106 ORF, the results indicate that these factors do not determine viral growth in epithelial cells. Viral growth of the  $\Delta m106-m108$  mutant was reduced in MEF and C127I compared to the growth of the wild type MCMV. Although the titre obtained for MEF was approximately 1.5 orders of magnitude lower compared to those of the wild type MCMV, the titre obtained for the C127I was approximately three orders of magnitude reduced compared to the titre of the wild type MCMV (Fig.5.8A). The titre obtained from  $\Delta m107-m108\Delta kan$ -infected MEF was two orders of magnitude lower compared to those of the wild type MCMV. In contrast, the  $\Delta m107-m108\Delta kan$  virus did not produce detectable amounts of infectious virus. In a second experiment the  $\Delta m107-m108\Delta kan$  virus did grow to detectable titers and yielded more than three orders of magnitude lower titers in C127I compared to those of the wild type MCMV (data not shown).

Viral spread in the infected cultures was investigated after six days of infection (data not shown). Here, small plaques were observed for C127I infected with the  $\Delta m107-m108\Delta kan$

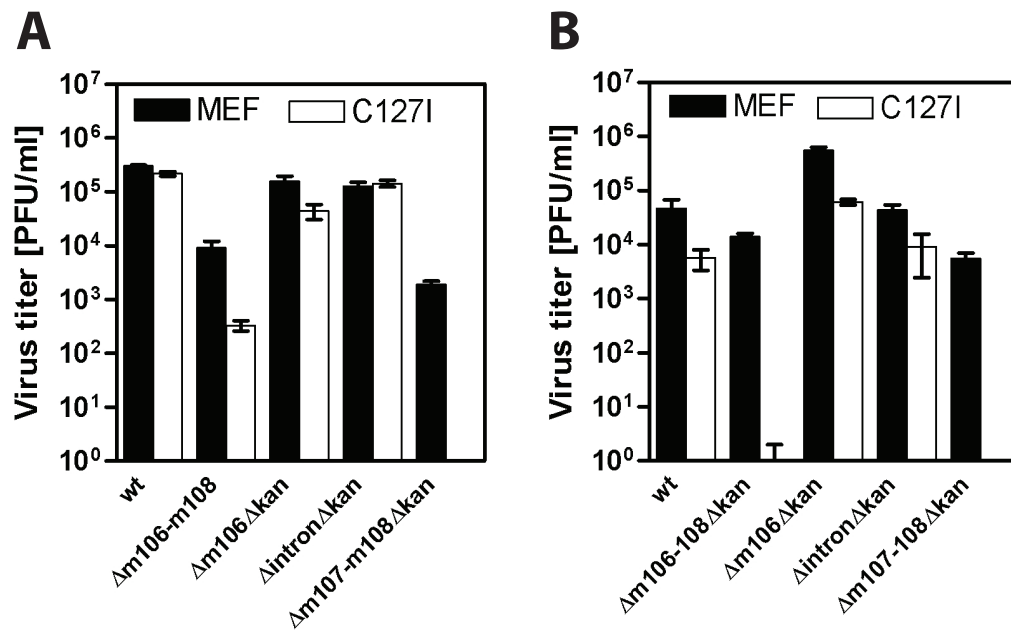


Figure 5.8: **Viral growth of mutants with deletions in the m107-m108 region of the MCMV genome.**

MEF and C127I were infected using a MOI of 0.01 in triplicate with wild type (wt) or MCMV mutants. Supernatants were harvested six days after infection and viral titres (PFU/ml) were determined by plaque assay on MEF. (A) The growth of the  $\Delta m106\Delta kan$ ,  $\Delta intron\Delta kan$  and  $\Delta m107-m108\Delta kan$  viruses was analysed. The  $\Delta m106-m108$  virus genome still contains the kanamycin resistance cassette. Data show the results of one experiment out of two independent experiments. (B) The kanamycin resistance cassette was excised from the  $\Delta m106-m108$  BAC and the growth of the  $\Delta m106-m108\Delta kan$  virus was analysed. Error bars indicate standard deviation of the mean value.

or  $\Delta m106-m108$  viruses, whereas in MEF viral spread was comparable to wild type MCMV,  $\Delta m106\Delta kan$  or  $\Delta intron\Delta kan$  infected cultures. The latter also showed similar viral spread in C127I. Thus, viral spread was consistent with the data obtained for the viral titres in the respective cultures.

In order to compare virus mutants that only differ in the deleted genes the kanamycin resistance cassette was also excised from the  $\Delta m106-m108$  BAC. Virus was reconstituted from the  $\Delta m106-m108\Delta kan$  BAC and viral growth on epithelial cells was investigated together with the  $\Delta m106\Delta kan$ ,  $\Delta intron\Delta kan$  and  $\Delta m107-m108\Delta kan$  viruses (Fig.5.8B) In contrast to the  $\Delta m106-m108$  virus, the  $\Delta m106-m108\Delta kan$  virus grew similarly to the wild type MCMV in fibroblasts but was impaired to grow in C127I. The  $\Delta m107-m108\Delta kan$  virus produced infectious progeny in MEF but failed to do so in C127I.

To conclude, the reduced growth of the  $\Delta m107-m108\Delta kan$  virus mutant in epithelial cells pointed to the presence of factors encoded in the m107-m108 region that are required for viral growth in epithelial cells. In the following, the virus mutants are designated without  $\Delta kan$ .



### 5.2.3 Does the 7.2 kb Stable Intron RNA Function as a Tropism Factor for Epithelial Cells?

The aim of the following experiments was to pinpoint the cause of the impaired growth of the  $\Delta$ m107-m108 virus in epithelial cells. The 7.2 kb stable intron RNA was considered as a potential epithelial cell tropism factor for the following reason: the *in vivo* growth analysis of a virus mutant lacking the intron RNA sequence by another group revealed an impaired growth in the salivary glands [Kulesza and Shenk, 2006]. Since MCMV replication in the salivary gland is restricted to a specialised epithelial cell [Jonjic et al., 1989] it was speculated that the 7.2 kb stable intron limits viral growth in these cells. The shortening of the intron RNA sequence to half of its size did not inhibit viral growth in epithelial cells (Fig.5.8A, B). Although changes of the secondary structure of the intron RNA are expected in this mutant, it could theoretically retain its function as a potential epithelial tropism factor. According to the published coordinates for the primary transcript, from which the intron is spliced, the  $\Delta$ m107-m108 virus lacks at least 66 bp from the 5'- end for the primary transcript including the potential 5'-transcription start site (Fig.5.9.A). Thus, the generation of the intron RNA might be prevented during infection from the  $\Delta$ m107-m108 virus thereby being a limiting factor for viral growth in epithelial cells. In order to investigate this possibility, the 5'-end of the primary transcript was re-analysed first.

#### Mapping the 5'-end of the Primary Transcript that Produces the 7.2 kb Intron RNA

Total RNA was isolated from uninfected or wild type MCMV-infected MEF at 24 hours after infection. This time point was considered as suitable since the 7.2 kb stable intron RNA was shown to accumulate at late times of infection [Kulesza and Shenk, 2004]. For the determination of the ends of the primary transcript rapid amplification of either 5'- or 3'-cDNA ends (RACE) was performed.

To map the 5'-end of the primary transcript of the spliced 7.2 kb intron RNA, cDNA was synthesised and amplified using first and second primers that were located within the m106 ORF. A major band of approximately 550 bp and a slightly lower migrating band of approximately 450 bp were detected as well as a higher molecular weight (MW) smear (Fig.5.9B). Sequence analysis of the major PCR product using the second gene specific primer identified a 473 bp sequence. The first 163 bp of the sequence completely mapped to the region between the primer 106-2 and the predicted splice acceptor site (Fig.5.9C). The remaining sequence mapped to the region starting at the predicted splice donor site and identified the 5'-end of the m106 transcript at position 161,932. A poly(A) signal (AAUAAA) was identified at nt position 153,899, downstream of the mapped m106 transcript. No TATA box was found in

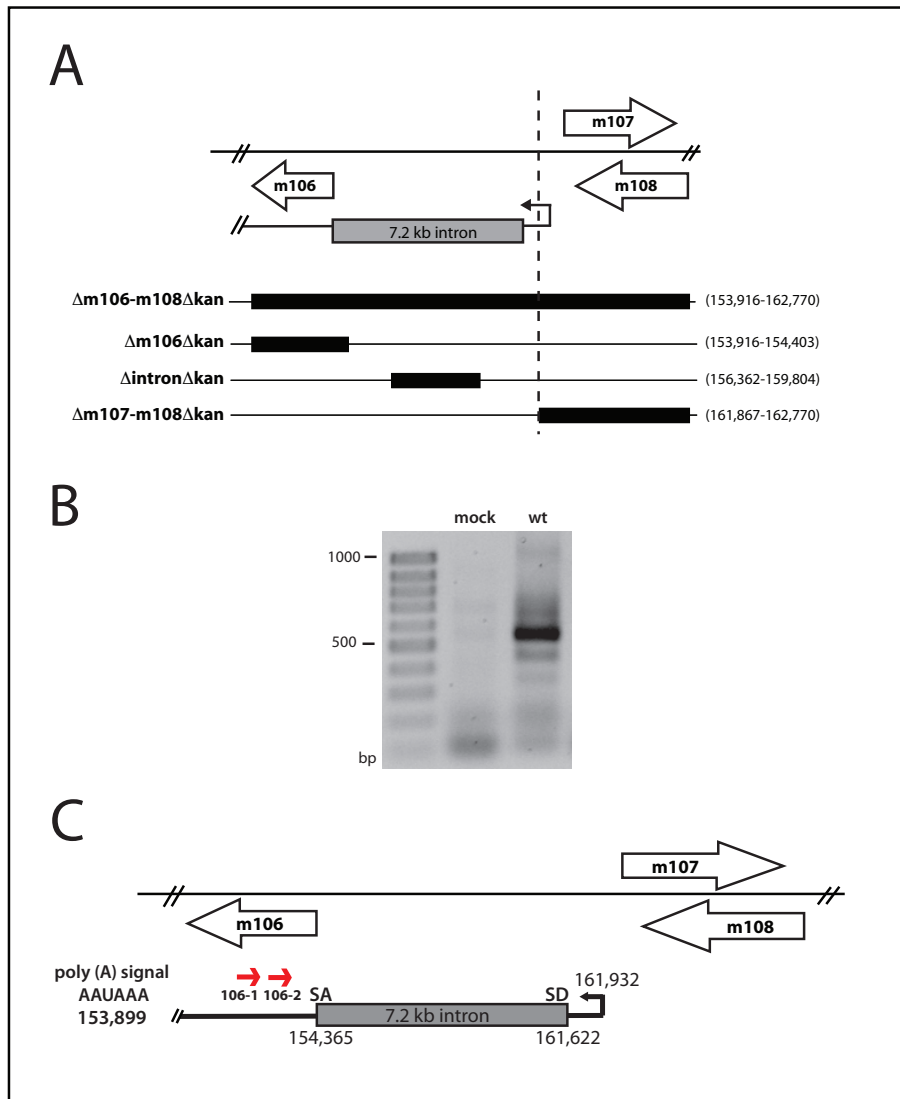


Figure 5.9: **Mapping of the transcription start for the 7.2 kb stable RNA.** (A) Position of the stable intron RNA in relation of the deletions (black bars) of the virus mutants. The ORFs are indicated with open arrows. The dashed line marks one end of the deletion in the  $\Delta$ m107-m108 virus mutant, indicating the lack of the 5'-end of the 7.2 kb intron RNA in this mutant. The nucleotide positions (bp) of the deletions are given in parentheses. (B) Mapping the m106 transcription start by 5'-RACE. Total RNA was prepared from uninfected (mock) or wild type MCMV-infected (wt) MEF at 24 h p.i. First, cDNA was synthesised from total RNA using the gene specific primer 106-1. The cDNA was then PCR amplified with the second gene specific primer 106-2 and an oligo dT anchor primer. PCR products were analysed by agarose gel electrophoresis. Size markers are indicated to the left. (C) The MCMV m106 to m108 region. The location of the primers used for the 5'-RACE experiment is shown. The genomic positions of the splice acceptor (SA), splice donor (SD) and the and the 5'-end of the stable intron RNA are indicated. The illustration is not drawn to scale.

close proximity to the mapped m106 transcription start site. Instead a GC-rich sequence was identified within 85 nt upstream of the m106 5'-end.

These results support the prediction that the generation of the 7.2 kb intron RNA from the  $\Delta$ m107-m108 genome is not possible, as 66 bp of the sequence of the primary transcript including the apparent transcription start site are missing.

### **Analysing the Presence of the 7.2 kb Intron RNA in $\Delta$ m107-m108 Infected Cells**

It was considered possible that an alternative transcription start site, that is present in the  $\Delta$ m107-m108 virus, permits the production of a primary RNA and retains the splicing of the 7.2 kb stable intron RNA.

In order to investigate if the 7.2 kb intron RNA is produced in  $\Delta$ m107-m108 infected cells, Northern blot analysis was performed. MEF were infected with the  $\Delta$ m107-m108,  $\Delta$ m106 and  $\Delta$ intron virus mutants. In addition, cells were infected with wild type MCMV and a  $\Delta$ 7.2kbSD virus mutant in which the splice donor of the 7.2 kb intron RNA was deleted. Total RNA was prepared from infected cultures 24 hours after infection and was processed for Northern blotting. Radiolabeled DNA probes were used for the detection of the 7.2 kb intron RNA. An additional probe, located within the ORF m106, was applied to detect the primary transcript producing the 7.2 kb intron RNA and a GFP-specific probe was used in order to estimate the total amount of viral RNA present in the samples.

The GFP probe detected similar amounts of GFP-specific RNA in all samples except for the  $\Delta$ m107-m108 infected cells, indicating that fewer cells were infected compared to the number of cells infected with wild type MCMV or the other virus mutants (Fig.5.10C, compare lanes 2-4, 6 with lane 5). An approximately 7 kb RNA was detected with the intron probe in cells infected with the wild type MCMV that apparently corresponds to the spliced 7.2 kb intron RNA (Fig.5.10A, lane 2). The same probe also detected an approximately 8 kb RNA that possibly represents the 8 kb intron RNA which is produced from the m106-m108 locus in addition to the 7.2 kb intron RNA but does not accumulate to a much lower level [Kulesza and Shenk, 2006]. In addition, an approximately 5 kb RNA species was detected which is of unknown origin (Fig.5.10A, lane 2). The strong intensity of the signal indicates, that it is not due to unspecific binding of the intron probe, thus, it possibly represents an additional smaller RNA produced from the same locus as the 7.2 kb intron RNA. Consistent with the detection of the 7.2 kb intron RNA, the m106 specific probe detected a RNA that migrated to a size of about 1 kb, which is suggested to represent the spliced transcript, in wild type infected cells (Fig.5.10B, lane 2) [Kulesza and Shenk, 2006]. The calculated length of the mature RNA is 1 kb based on the presence of the sequences from the m106 transcription start site up to the identified poly(A) signal plus a poly (A) tail of about 200 nt. In  $\Delta$ m106 infected cells, no RNA corresponding to the 7.2 kb intron RNA was detected (Fig.5.10A, lane 3). The

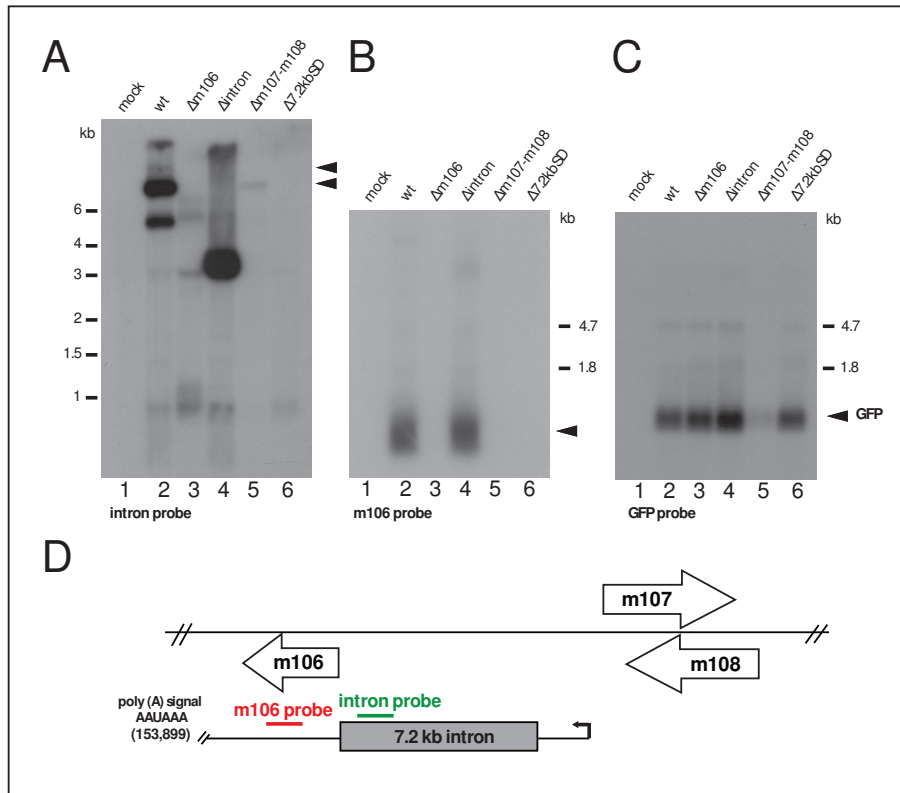


Figure 5.10: **Analysis of MCMV-specific RNAs indicating the presence of a 7.2 kb intron RNA.** (A) MEF were infected with wild type MCMV (wt) or the indicated deletion mutants and total RNA was prepared at 24 hours after infection. Northern blot hybridisation was performed on three different blots with radiolabeled DNA probes. (A) Detection of the intron RNA with a specific probe. The arrows point to the 7.2 and 8 kb intron RNAs. Size markers are indicated to the left. (B) Detection of the approximately 1 kb splice product (arrow) that is generated when the 7.2 kb intron is excised from the primary transcript. (C) The GFP probe detects an approximately 1.4 kb RNA (black arrow). The sizes of the detected RNAs in B and C were estimated relative to the position of the 18s rRNA (1,874 bases) and 28s rRNA (4,718 bases). (D) Location of the probes (red or green bars) within the m106 to m108 region. The genomic position of the potential poly (A) signal of the primary transcript is indicated in parentheses. The ORFs m106, m107 and m108 are illustrated as open arrows. The illustration is not drawn to scale.

absence of the 7.2 kb RNA from  $\Delta m106$  infected cells indicated that splicing of the intron RNA is not possible without the splice acceptor that is deleted in the  $\Delta m106$  BAC. This was also confirmed with the absence of the 1 kb spliced transcript RNA (Fig.5.10B, lane 3). In contrast, an approximately 3.8 kb RNA was detected with the intron probe in  $\Delta intron$  infected cells (Fig.5.10A, lane 4). Further, an approximately 1 kb RNA was detected with the m106 probe (Fig.5.10B, lane 4). This indicated that the deletion of 3.4 kb from 7.2 kb of the intron sequence did not inhibit the splicing event but that a shorter 3.8 kb intron RNA is produced instead that retains its stability at late times of infection.

An approximately 7 kb RNA was the only RNA species detected in  $\Delta m107$ -m108 infected cells (Fig.5.10A, lane 5). The weak signal detected from this RNA could be explained with the low amounts of viral RNA isolated from  $\Delta m107$ -m108 infected cells. The presence of the 7 kb RNA, migrating with the same kinetics as the spliced 7.2 kb intron RNA, suggested splicing of the primary transcript producing the 7.2 kb intron RNA although the transcription start was deleted in this mutant (Fig.5.10A, lane 5). This is possibly due to the presence of an alternative transcription start. If the 7.2 kb intron is produced, the spliced 1 kb transcript should be detectable with the m106 probe. However, this RNA was not detected in RNA isolated from  $\Delta m107$ -m108 infected cells (Fig.5.10B, lane 5). Neither the intron probe nor the m106 probe detected RNA that was prepared from cells infected with the  $\Delta 7.2kbSD$  virus mutant, indicating that the 7.2 kb intron RNA could not be generated in this mutant (Fig.5.10A, lane 6 and Fig.5.10B, lane 6).

To conclude, Northern blot analysis using a probe that hybridises to the 7.2 intron sequence identified a RNA species in  $\Delta m107$ -m108 infected cells that migrated with the same kinetics as the RNA identified as the 7.2 kb intron RNA in wild type MCMV-infected cells. However, no RNA corresponding to the spliced transcript was detected.

### **Analysis of the Growth Properties of the $\Delta 7.2kbSD$ Virus in Epithelial Cells**

To rule out any effects of the 7.2 kb RNA for the epithelial cell tropism of MCMV, the growth of the  $\Delta 7.2kbSD$  virus in epithelial cells was investigated. In the corresponding BAC the splice donor for the generation of the 7.2 kb intron RNA was deleted. In fibroblasts infected with the reconstituted virus no 7.2 kb intron RNA was detected by Northern blotting indicating that generation of the large intron RNA does not occur (Fig.5.10A, lane 6). The investigation of the viral growth of the  $\Delta 7.2kbSD$  virus mutant in epithelial cells should clarify the role of the 7.2 kb RNA for the epithelial cell tropism of MCMV. Cells were infected with the  $\Delta 7.2kbSD$  virus mutant as described for the cell tropism assay. Viral supernatants were harvested and analysed by plaque assay.

In three independent experiments the  $\Delta 7.2kbSD$  virus grew to comparable titres in fibroblasts or epithelial cells (Fig.5.11). Analysis of the viral cell-to-cell spread showed comparable

numbers of infected fibroblasts and epithelial cells (data not shown). This indicated that the 7.2 kb stable intron RNA is not essential for the growth in either cell type and thus a role in epithelial cell tropism of MCMV can be excluded.

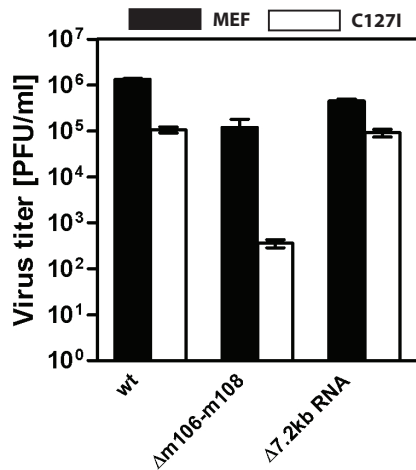


Figure 5.11: **Growth of the  $\Delta 7.2\text{kbSD}$  virus mutant.** MEF and C127I were infected using a MOI of 0.01 in triplicate with wild type (wt) or MCMV mutants. Supernatants were harvested on day 6 and viral titres (PFU/ml) were determined by plaque assay on MEF. Data show the results of one representative experiment out of three independent experiments. Error bars indicate standard deviation of the mean value.

## 5.2.4 Analysis of the m107 and m108 Genes as Viral Factors

### Determining the Epithelial Cell Tropism of MCMV

Next, it was investigated whether the m107 or m108 genes play a role for the epithelial cell tropism of MCMV. For this, the synthesis of RNAs and proteins from the ORFs m107 and m108 were analysed.

Total RNA was isolated from uninfected or wild type MCMV infected MEF at 24 hours after infection. This time point was considered as suitable for the investigation of a m108 transcript since it was shown previously that a m108 RNA is expressed at that time point [Tang et al., 2006]. The 5'- and/or 3'-ends of the potential m107 or m108 transcripts were determined using 5'- or 3'-RACE.

The primer 108-2 binds to the sequence that is predicted to comprise the ORF m108. Using this primer in the m108 5'-RACE, a fragment of about 300 bp was amplified (Fig.5.12A, lane 1). Analysis of this PCR product revealed a sequence of 275 bp that mapped exactly to the m108 ORF. The m108 transcription start site was mapped five nucleotides upstream of the predicted ATG of the m108 ORF to nucleotide position 162,775. For the detection of the 3'-end of the m108 transcript the primer 108-3 was used. Using this primer two fragments of approximately 550 and 650 bp were amplified (Fig.5.12A, lane 2). Analysis of the PCR products revealed that both sequences were identical except for 108 bp that were present in the 620 bp sequence and absent from the 512 bp sequence.

## 5.2 Searching for Viral Factors determining the Epithelial Cell Tropism of MCMV

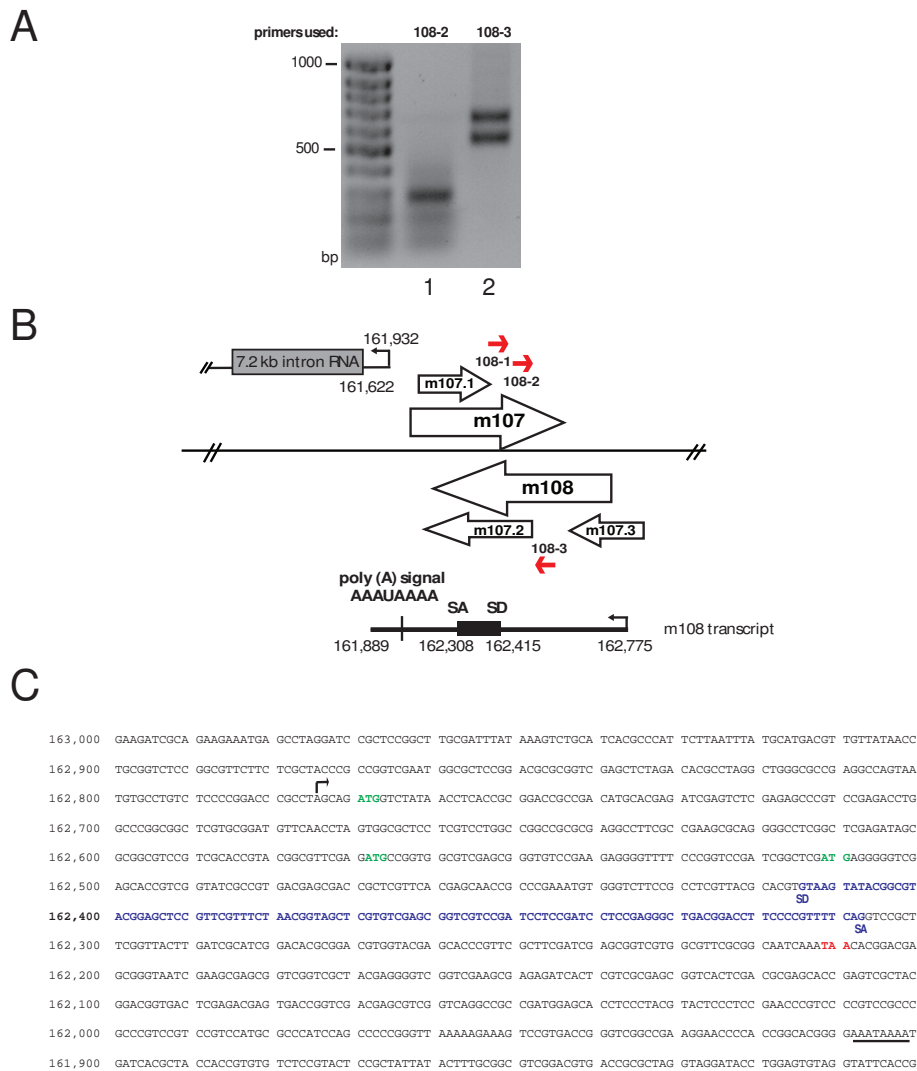


Figure 5.12: **Detection of a m108 transcript.** (A) 5'-/3'- RACE. Total RNA was prepared from wild type MCMV infected MEF. First, cDNA was synthesised from total RNA using the gene specific primer 108-1. The cDNA was then PCR amplified with the second gene specific primer 108-2 and an oligo dT anchor primer (lane 1). For mapping of the 3'-end of a m108 transcript, cDNA was synthesised using the oligo dT anchor primer. The cDNA was amplified with the 108-3 primer and the PCR anchor primer (lane 2). PCR products were analysed by agarose gel electrophoresis. Size markers are indicated to the left. (B) Illustration of the MCMV m107- m108 region. Predicted ORFs are illustrated with open arrows. The genomic position of the 7.2 kb stable intron RNA and the location of the primers used for the RACE experiments are shown. The genomic positions of the primers 108-2, 108-3, the splice acceptor (SA) and splice donor (SD) of the identified 108 bp intron as well as the mapped transcription start site and the 3'-end are indicated. (C) Genomic sequence of the m108 transcript. The putative translation start codons ATG and the stop codon TAA are indicated in green and red, respectively. The mapped start site of the transcript is marked with an arrow. The putative poly (A) signal is underlined. The 108 bp intron RNA sequence is indicated in blue letters with the splice donor (SD) and splice acceptor (SA). The illustration is not drawn to scale.

This result indicated the presence of an 108 bp intron which is spliced from a primary transcript. Sequence analysis of the 108 bp intron splice donor site (exon-**gcacgt/gtaagt**-intron) and splice acceptor site (intron-**cag/gtccgct**-exon) revealed the presence of consensus splice donor or splice acceptor sequences [Proudfoot et al., 2002]. A conserved splicing signal (CUAAC) required for branching of the intron RNA during the splicing process was identified 75 nt upstream of the splice acceptor within the intron sequence. The 3'-end of the transcripts was mapped to the nucleotide position 161,889 and a poly (A) signal (AAUAAAA) was found 21 nt upstream of the 3'-end.

The synthesis of a m107 transcript was analysed by mapping the 5'- and 3'-end using the primers 107-1, 107-2 and 107-3. A PCR product, indicative of a m107 transcript, was not found even when different PCR conditions were applied (data not shown). This suggests that no m107 transcript is synthesised.

To summarise the data, a m108 transcript could be identified by mapping the m108 transcription start site and the 3'-end. Further there is evidence for a 108 bp intron that is excised from a m108 primary transcript. The existence of a m107 transcript was not evident.

### **Is the m108 Gene an Epithelial Cell Tropism Factor?**

Since m108 gene expression could be demonstrated by identifying a m108 transcript, the next aim was to investigate m108 protein expression. For this a virus was generated encoding a HA-tagged m108 protein. The sequence coding for the hemagglutinin(HA)-epitope (YPYDVPDYA) was inserted at the 3'-end of the predicted m108 ORF upstream of the stop codon. The integrity of the DNA sequence for the HA-tag in the BAC was checked by sequencing.

Lysates from cells infected with the m108HA virus for 24 hours were used for immunoblotting with a HA-specific antibody. In addition, lysates from uninfected or wild type MCMV infected cells were included as negative controls and a lysate from cells expressing a HA-protein of a known molecular weight of 72 kDa was used as a positive control. Computer-based analysis predicted a molecular mass of the putative m108 protein of approximately 20 kDa. No protein of this size nor any other specific signals were detected by immunoblotting (data not shown). Thus, by using this approach, the expression of a m108 protein could not be demonstrated.

To further investigate the role of a putative m108 protein for the epithelial cell tropism of MCMV, additional virus mutants were constructed.

The m108mutATG virus was constructed to prevent translation of the m108 transcript (Fig.5.13A, panel 1). Here, the first ATG of the m108 ORF was replaced by a stop codon (TGA) using site-directed BAC mutagenesis. The integrity of the nucleotide exchange was checked by sequencing of the BAC. Virus was reconstituted and the growth of the m108mutATG virus in MEF and C127I cells was investigated as described in the cell tropism



assay. Comparing the titres of the m108mutATG virus and of the wild type MCMV obtained from infected MEF or C127I revealed a similar growth capacity of both viruses in these cell types (Fig.5.13B, upper panel). Similar to the results obtained from previous experiments, the  $\Delta$ m106-m108 and  $\Delta$ m107-m108 viruses yielded at least two orders of magnitude lower titres in C127I compared to those of the wild type MCMV or did not produce detectable amounts of virus in this cell type (Fig.5.13B, upper panel). From this, it was concluded that the m108 protein is not required for viral growth in epithelial cells.

The first ATG of the m108 ORF is located 5 nt downstream of the mapped transcription start site (Fig.5.12C). This indicated a very short 5'-untranslated region within the m108 RNA sequence. The analysis of the length of 5'-untranslated regions of mRNAs derived from distinct taxonomic classes revealed an average length of 100 to 200 nt upstream of the start codon [Pesole et al., 2000]. Further, it is assumed that the start codon is not recognized by the ribosome when it is located only 10 nt or less downstream of the 5'-end of a transcript [Kozak, 1978]. In frame with the first ATG a second ATG is present 198 nt further downstream (nt 162,569) and a third ATG is located 255 nt downstream of the first ATG (nt 162,512) (Fig.5.12C). It is possible that the second ATG in the m108 ORF, which is not mutated in the m108mutATG virus, represents the start codon for translation and therefore a m108 protein could still be expressed.

Therefore a second virus mutant,  $\Delta$ m108, was generated in which the ORF m108 was disrupted (Fig.5.13A, panel 2). The deletion covered 20 bp within the m108 sequence between the third ATG codon and the splice donor of the m108 bp intron thereby deleting six amino acids and introducing a frame shift. Infectious virus was reconstituted and growth of the  $\Delta$ m108 virus was tested as described in the cell tropism assay.

In three independent experiments the wild type MCMV yielded titres in C127I that were similar to those in MEF in three experiments (slightly higher or maximally one order of magnitude lower) (Fig.5.13B, lower panel). The  $\Delta$ m107-m108 virus was used as a control virus. The titres of the  $\Delta$ m107-m108 virus in MEF were somewhat lower compared to those of the wild type MCMV in three independent experiments (maximally two orders of magnitude). In C127I, the  $\Delta$ m107-m108 virus yielded lower, but variable titres compared to the respective titre of the wild type MCMV (Fig.5.13B, lower panel), ranging from at least one order of magnitude lower to below the detection limit. In three independent experiments the  $\Delta$ m108 virus mutant yielded similar titres in MEF compared to those of the wild type MCMV (maximally one order of magnitude lower) (Fig.5.13B, lower panel). In C127I, the virus mutant yielded lower, but variable titres compared to those of the wild type MCMV (in two independent experiments maximally one order of magnitude lower and in one experiment maximally two orders of magnitude lower titres, respectively).

These data, together with the previous data obtained from the m108 RACE, strongly

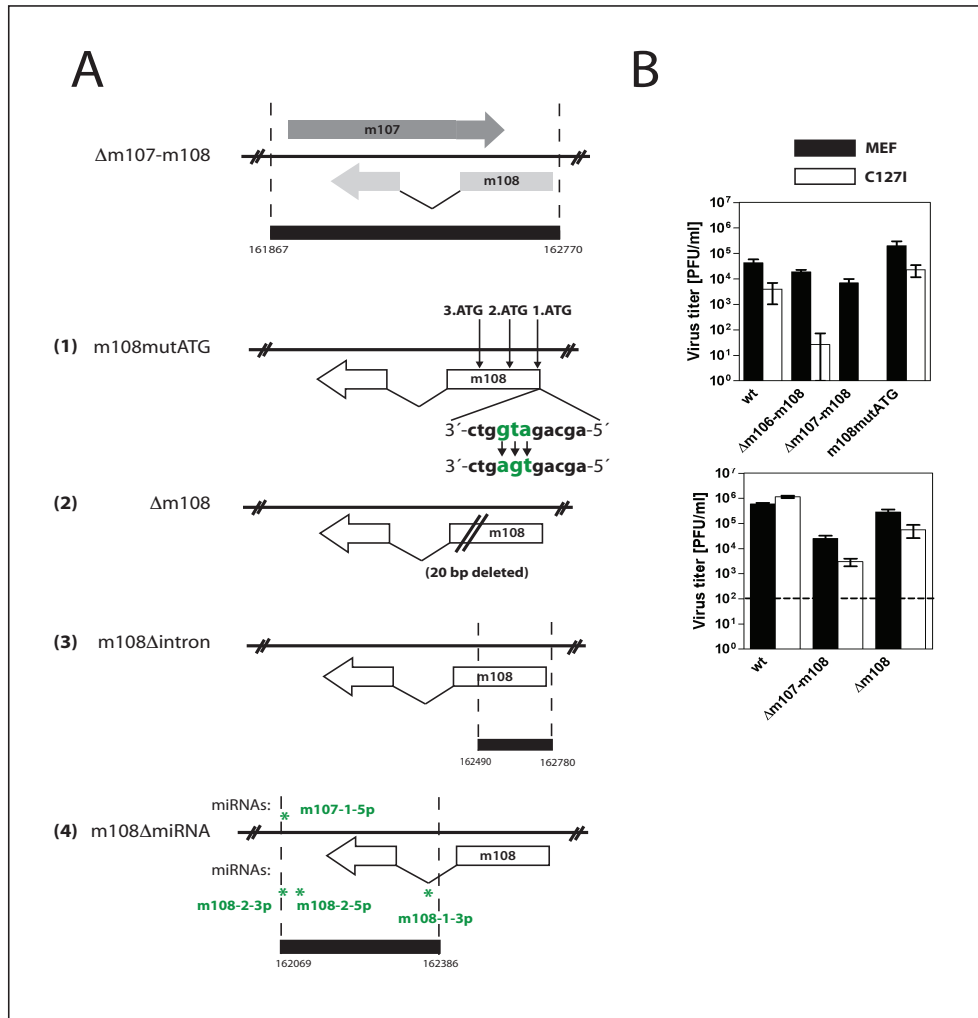


Figure 5.13: **Analysis of the ORF m108 for MCMV growth in epithelial cells.** (A) Analysis of MCMV mutants. (1) The ATG start codon is replaced by the stop codon TGA in the m108mutATG virus genome. (2) The  $\Delta m108$  virus genome lacks 20 bp of the m108 ORF. (3) The 5'-region, including the transcription start site is deleted in the 108 $\Delta$ intron virus mutant. A primary transcript and thus the 108 bp intron RNA is not expected to be generated. (4) The 3'-region of the m108 gene is deleted in the m108 $\Delta$ miRNA virus genome indicated as a black bar. The nucleotide positions in the genomes are given. Three miRNAs are encoded from the m108 transcript and a single miRNA is encoded from the opposite strand. miRNAs are indicated as asterisks [Dölken et al., 2007, Buck et al., 2007]. 5p and 3p describe the 5' or 3' hairpin precursor sequences of the miRNAs. The illustration is not drawn to scale. (B) Viral growth of the deletion mutants. MEF or C127I were infected with a MOI of 0.01 in triplicate with wild type (wt) or MCMV mutants. Supernatants were harvested on day 6 and viral titres (PFU/ml) were determined by plaque assay on MEF. Data show one experiment of two independent experiments (upper panel) or one experiment of three independent experiments (lower panel). Error bars indicate standard deviation of the mean value. The dashed line represents the detection limit of the virus plaque assay.

suggest that if a m108 protein is produced it is dispensable for the growth of MCMV in epithelial cells. Further, the  $\Delta$ m107-m108 virus was impaired to grow in epithelial cells but the growth in this cell type was variable.

### **Is the 108 bp Intron RNA a Limiting Factor for Viral Growth in Epithelial Cells?**

Next, it was investigated whether the 108 bp intron RNA is required for the growth of MCMV in epithelial cells. The deletion in the previously generated  $\Delta$ m108 virus mutant led to changes in the coding sequence but the splicing of the primary transcript should not be affected since the DNA sequence was only changed upstream of the splice donor. Similar to the 7.2 kb stable intron RNA the 108 bp intron RNA, which is produced from the m108 primary transcript, could be stable and play a role as a factor determining the epithelial cell tropism of MCMV. To investigate if the 108 bp intron RNA might be a tropism factor for epithelial cells, and thus account for the impaired growth of the  $\Delta$ m107-m108 virus mutant in epithelial cells, the m108 $\Delta$ intron virus was constructed (Fig.5.13A, panel 3). In this virus mutant, the generation of an intron RNA is expected to be prevented by the deletion of the 5'-region of the m108 ORF including the m108 5'- transcription start site. Thus, the m108 primary transcript would be absent, and no intron RNA can be generated. Investigation of the viral titers in the cell tropism assay showed that infection of C127I and MEF with this virus mutant yielded titers that were comparable to those of the wild type MCMV (data not shown).

From these experiments it was concluded that the 108 bp intron RNA does not account for the impaired growth of the  $\Delta$ m107-m108 virus in epithelial cells and does not determine the epithelial tropism of the MCMV.

As an alternative to investigate the role of a putative stable 108 bp intron RNA as a factor determining epithelial cell tropism, a second virus mutant was constructed in which the splicing of the 108 bp intron is prevented by the deletion of the 3'-region of the m108 ORF including the splice acceptor for the generation of the 108 bp intron RNA, termed m108 $\Delta$ miRNA virus (Corinna Benkartek, personal communication) (Fig.5.13A, panel 4). To investigate the viral growth of this virus, MEF and C127I were infected as described in the cell tropism assay. In this experiment infection with the m108 $\Delta$ miRNA virus was analysed by Fluorescence Activated Cell Sorting (FACS) making use of the GFP expression of the viruses.

To investigate viral infection, the numbers of MEF and C127I infected with the m108 $\Delta$ miRNA virus were determined. As controls, cells were infected with wild type MCMV or the  $\Delta$ m107-m108 virus mutant. The numbers of infected cells were analysed at day two after infection to ensure comparable numbers of infected cells within the viruses in C127I or MEF. The numbers of infected cells were again analysed at six days after infection to analyse the spread of the viral infection of the viruses. Less MEF and C127I were infected with the  $\Delta$ m107-m108 compared to the number of infected MEF and C127I with the wild type MCMV.

In contrast, for the m108 $\Delta$ miRNA virus the number of infected MEF and C127I was similar to the number of MEF and C127I infected with the wild type MCMV (C.Benkartek, personal communication).

To conclude, first, the results obtained from determining numbers of cells infected with the  $\Delta$ m107-m108 virus by FACS were comparable to the results obtained from determining the viral titres of the  $\Delta$ m107-m108 virus. This highlights the FACS method as a suitable alternative for the investigation of viral infection in cell culture. Second, the growth of the  $\Delta$ m108intron and the m108 $\Delta$ miRNA viruses, obtained from measuring viral titres or the number of infected cells, was similar to those of the wild type MCMV. This indicated that a putative stable 108 bp intron RNA is not a limiting factor for virus production in epithelial cells.

### **Investigation of the miRNAs Expressed from the ORFs m107/m108 as Possible Tropism Factors**

In order to explain the lack of growth of the  $\Delta$ m107- m108 virus in epithelial cells, other possible factors were considered. It was experimentally shown that 18 micro RNAs (miRNAs) are expressed from the MCMV genome [Dölken et al., 2007, Buck et al., 2007] in cultured fibroblasts. Four miRNAs are encoded from the m107-m108 region (Fig.5.13A, panel 4). This led to the speculation that these miRNAs might be required for viral growth in epithelial cells. Three miRNAs potentially originate from the m108 primary transcript (Fig.5.13A, panel 4). The deletion in the m108 $\Delta$ miRNA virus mutant described above also comprise the sequences of all the four miRNAs. As mentioned before the m108 $\Delta$ miRNA mutant was able to grow in epithelial cells to a similar extent as in fibroblasts indicating that the miRNAs expressed from the m107-m108 locus do not account for the limited virus production of the  $\Delta$ m107-m108 virus in epithelial cells.

## 5.3 Identification of a Viral Gene Involved in MCMV-Induced Cell Rounding

Cells infected with CMV show cytopathic effects. Cell rounding is one of these cytopathic effects. Cell rounding induced by HCMV has been analysed, whereas this effect caused by MCMV has not yet been studied. However, neither the mechanism leading to the round cell shape caused by CMV nor the benefit for the virus, if any, has been determined.

### 5.3.1 MCMV M25 plays a Major Role in Changing Cellular Morphology after CMV Infection

The aim of this study was to identify the viral gene products that cause changes of cellular morphology during MCMV infection. To this end, MEF were infected with the MCMV mutants described in chapter 5.1 and were screened for conspicuous phenotypes. The infection of MEF with a virus mutant that carried a deletion spanning the ORFs M24 to m25.2 did not lead to typical cell rounding (Fig.5.14C, upper right panel). Cells infected with the mutant virus were still outstretched, forming protrusions at 48 hours after infection. In contrast, most cells infected with wild type MCMV showed a round cell shape (Fig.5.14C, upper left panel).

The large deletion comprised four predicted ORFs (Fig.5.14A). The ORFs M24, M25, m25.1 and m25.2 have been predicted for the MCMV Smith strain [Rawlinson et al., 1996]. To identify the responsible gene for cell rounding, individual virus mutants were generated in which the single ORFs M24, M25, m25.1 were deleted using the BAC mutagenesis method (Fig.5.14A, (lane 4-6)).

The kanamycin resistance cassette was excised from the  $\Delta$ M25 BAC by Flp-mediated recombination to keep the possibility of using the same selection marker to target a second gene for deletion in the same genome or for later in vivo application (Fig.5.14A (lane 6)).

Since the m25.2 ORF is partially overlapping with both the m25.1 ORF and the M26 ORF, the importance of the m25.2 ORF for the induction of cell rounding was investigated by deleting sequences of the M24 ORF to the m25.1 ORF (Fig.5.14A, (lane 3)). The m25.2 ORF was not targeted in this virus. A restoration of function to induce cell rounding in this virus would then be linked to the m25.2 ORF. Sequences in the middle of each ORF, rather than the complete ORF were deleted to avoid the disruption of adjacent poly (A) signals or promoter sequences necessary for the expression of neighbouring ORFs. The correct integrity of the mutant BACs was confirmed by restriction enzyme analysis (Fig.5.14A,B). Exploiting viral GFP expression as means to detect infected cells, the induction of cell rounding was observed in cells infected either with wild type MCMV or mutants still expressing

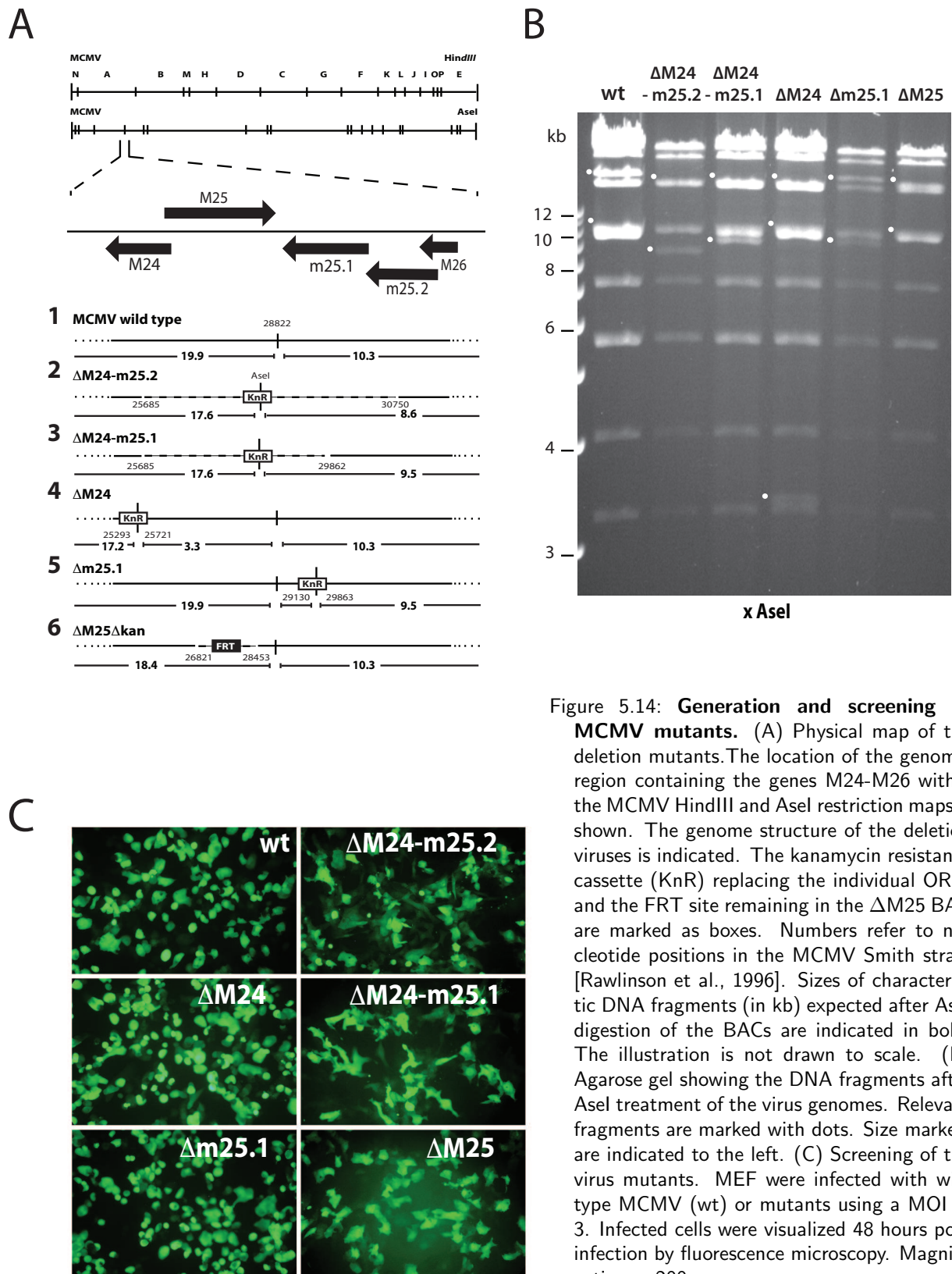


Figure 5.14: **Generation and screening of MCMV mutants.** (A) Physical map of the deletion mutants. The location of the genomic region containing the genes M24-M26 within the MCMV HindIII and AseI restriction maps is shown. The genome structure of the deletion viruses is indicated. The kanamycin resistance cassette (KnR) replacing the individual ORFs and the FRT site remaining in the  $\Delta$ M25 BAC are marked as boxes. Numbers refer to nucleotide positions in the MCMV Smith strain [Rawlinson et al., 1996]. Sizes of characteristic DNA fragments (in kb) expected after AseI digestion of the BACs are indicated in bold. The illustration is not drawn to scale. (B) Agarose gel showing the DNA fragments after AseI treatment of the virus genomes. Relevant fragments are marked with dots. Size markers are indicated to the left. (C) Screening of the virus mutants. MEF were infected with wild type MCMV (wt) or mutants using a MOI of 3. Infected cells were visualized 48 hours post infection by fluorescence microscopy. Magnification,  $\times$  200.

M25 (Fig.5.14C, (left panels)). The majority of cells infected with these viruses displayed a round cell shape and a decreased cell size. In contrast, cells infected with the virus mutants lacking the M25 gene did not change their shape (Fig.5.14C, (right panels)). Here the majority of cells maintained a fibroblast-like morphology. Infected cells remained outstretched and formed protrusions. Thus, for all virus mutants that were tested, those that were lacking the M25 ORF, did not cause cellular rounding in fibroblasts.

In order to analyse if the failure to induce cell rounding is limited to primary cells or is cell type specific, NIH 3T3 fibroblasts or C127I epithelial cells were infected with wild type MCMV or the  $\Delta$ M25 virus. A distinct plaque formation was not only observed in MEF but also in NIH 3T3 and in C127I cells (Fig.5.15, (right panels)). A plaque induced by wild type MCMV consisted of a cluster of infected cells undergoing cell rounding. These cells lost contact to neighbouring cells thereby forming a hole in the cell monolayer (Fig.5.15, (left panels)). In contrast,  $\Delta$ M25 virus infected cells did not change their morphology or interrupted the cell monolayer, but instead remained in contact with neighbouring cells. Thus, the phenotype is also present in a fibroblast cell line, in addition to primary fibroblasts, and in epithelial cells.

The M25 ORF has been investigated in earlier studies [Dallas et al., 1994, Wu et al., 1999]. A transcript was found and protein expression from the M25 transcript has been detected, but the function of the M25 protein remained elusive. Searching the non-redundant protein database for similarity to the M25 amino acid sequence of the Smith strain (Refseq. NC 004065) revealed that the M25 amino acid sequence has a conserved domain at the C-terminus (Fig.5.24). Homology to this domain was found in the HCMV proteins UL25 and UL35 that constitute the UL25 gene family. The alignment of the M25 amino acid sequence and the UL25 amino acid sequence of two HCMV isolates, TB40/E and AD169, revealed 26% homology that mapped to amino acid 494 to 880 at the M25 C-terminus whereas 23% homology was discovered between M25 and UL35.

It is possible that the conserved region of the protein contains domains that are necessary for the interaction with proteins required for the induction of cell rounding. In order to investigate whether the C-terminal conserved region or the non-conserved region at the N-terminus of M25 influence the induction of cell rounding, two additional MCMV mutants were generated.

The M25 protein variant expressed from the M25 $\Delta$ C virus lacks the M25 C-terminus. The amino acids 490 - 932, covering the complete conserved region, were deleted in the genome of this virus (Fig.5.16A and Fig.5.24). The M25 protein variant that would be made from the M25 $\Delta$ N virus lacks the N-terminal amino acids 75-407. DNA sequences were deleted covering the first ATG downstream of the M25 transcription start site that was mapped by Dallas et al. [Dallas et al., 1994] (Fig.5.24). In the M25 $\Delta$ N virus, M25 protein synthesis is possibly initiated at the 10th ATG (aa 421) that is the next start codon downstream of the deletion. Neither the M25 $\Delta$ C nor the M25 $\Delta$ N virus induced cell rounding concluding that both regions

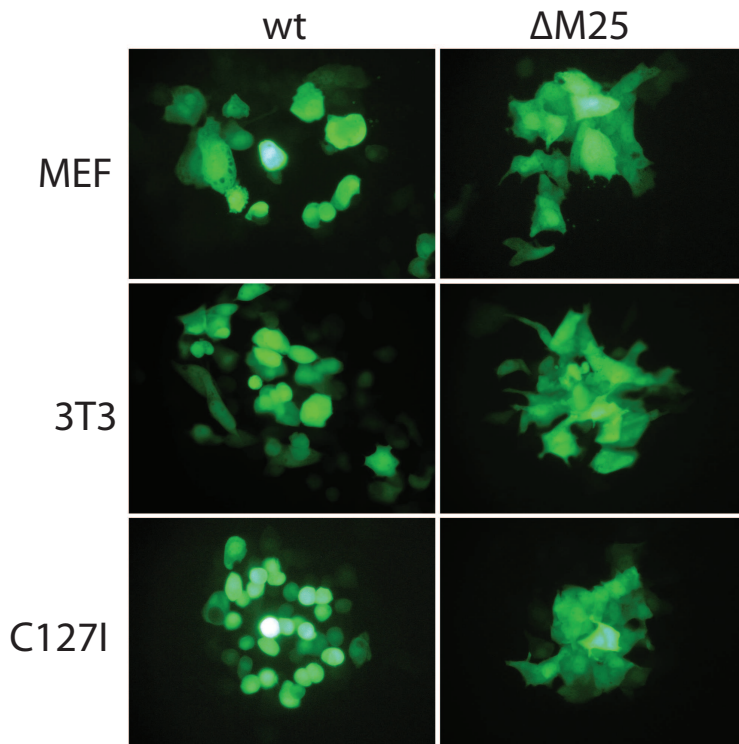


Figure 5.15: **MCMV-induced cytopathic effect.** Mouse embryonic fibroblasts, NIH 3T3 fibroblasts or C1271 epithelial cells were infected with wild type MCMV or the  $\Delta$ M25 virus using a MOI of 1. Images show MCMV infected GFP-positive cells at 72 hours after infection.

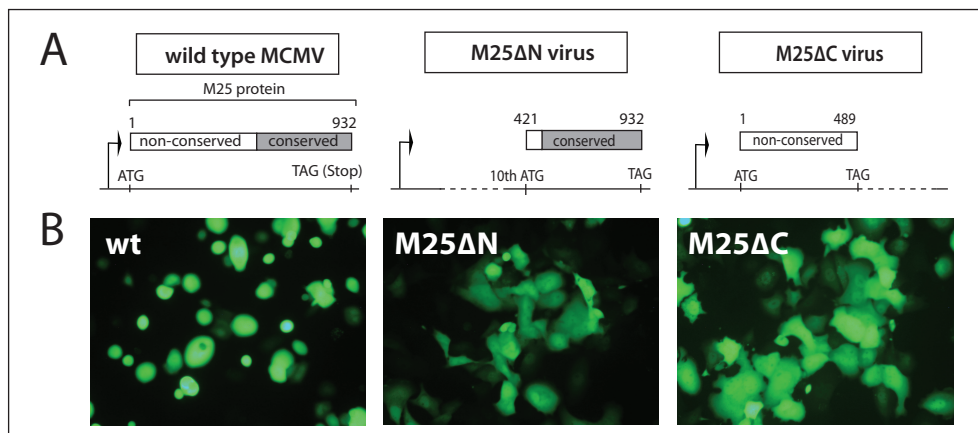


Figure 5.16: **Phenotypic analysis of the M25 $\Delta$ N and M25 $\Delta$ C viruses** (A) Scheme of the amino acid sequence of the M25 variants synthesised from the wild type MCMV, M25 $\Delta$ N or M25 $\Delta$ C virus mutants. The amino acids 75-407 are deleted from the genome of the M25 $\Delta$ N virus and the amino acids 490-932 are deleted from the genome of the M25 $\Delta$ C virus. The dashed line indicates the deletion in the respective mutant BAC. The amino acids present in the M25 variants are given in numbers referring to the M25 ORF predicted by Rawlinson et al. [Rawlinson et al., 1996]. The illustration is not drawn to scale. (B) Mouse embryonic fibroblasts were infected with wild type MCMV or the M25 mutants using a MOI of 3. The morphology of infected cells was examined 48 hours post infection by fluorescence microscopy. Magnification,  $\times$  200.



within the M25 ORF are essential for this process (Fig.5.16B).

Taken together, these results indicate a key role for the M25 protein in altering cellular morphology after CMV infection.

### 5.3.2 Re-Insertion of the M25 Gene

If M25 is a key factor for the induction of cell rounding, the re-insertion of the M25 gene into a  $\Delta$ M25 BAC should enable the corresponding virus to induce morphological changes in cells. To address this hypothesis experimentally, a plasmid containing the M25 gene was inserted into the  $\Delta$ M24-m25.2 BAC resulting in the M25R BAC (Fig.5.17A). For this, the parental  $\Delta$ M24-m25.2 BAC was recombined with the plasmid pOriM25 containing the full length 2.7 kb M25 ORF with additional 840 bp at the 5'-end and 748 bp at the 3'-end predicted to comprise the M25 ORF promoter and poly (A) signal, respectively. The additional nucleotides flanking the M25 ORF also contained sequences of the M24 gene and the m25.1 gene. However, expression of these genes is not possible since the 3'-end of the ORF M24 and the 5'-end of the M25 ORF were missing. The M25R induced morphological changes in infected cells similar to the wild type MCMV (Fig.5.17B). These data reinforce the statement that changes of cellular morphology and plaque formation are dependent on the presence of the M25 gene.

In conclusion, based on the deletion of single ORFs and the generation of a rescuant virus, the ability to induce cell rounding was ascribed to the presence of the M25 gene.

### 5.3.3 Analysis of the Growth Properties of the $\Delta$ M25 Virus

HCMV disrupts the actin cytoskeleton at sites of cell entry [Jones et al., 1986]. Treatment of cells with Cytochalasin B, a toxin that inhibits the formation of actin filaments, before infection with HCMV increases the production of infectious virus particles. Three orders of magnitude higher titers have been measured when cytochalasin B has been added prior to HCMV infection [Jones et al., 1986]. Under these conditions more virus particles are believed to reach the nucleus through the actin meshwork and to initiate viral gene expression resulting in the production of more virus particles. Since morphological changes within the cell are associated with rearrangements of the cytoskeleton the absence of cell rounding in  $\Delta$ M25 virus-infected cells might be due to the failure to interact with the actin cytoskeleton. Consequently, if the above outlined scenario holds also true for MCMV,  $\Delta$ M25 growth should be impaired.

The growth properties of the  $\Delta$ M25 virus were analysed and compared to those of the wild type MCMV by analysing the presence of viral proteins characteristic for the three stages of viral gene expression and by determining the viral titers.

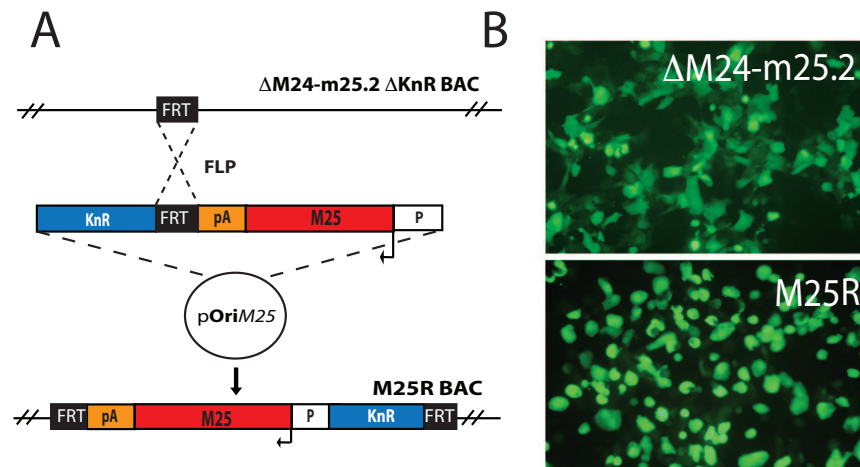


Figure 5.17: **Phenotypic analysis of the M25R virus.** (A) To construct the M25R virus, the kanamycin resistance gene was excised from the  $\Delta$ M24-m25.2 BAC by Flp-mediated recombination. A 4.3 kbp fragment of the plasmid pOriM25 consisting of the M25 ORF and containing 840 bp of the sequences upstream of the M25 start codon and 748 bp downstream of the M25 stop codon, predicted to provide suitable promoter elements and the polyadenylation signal was integrated into the  $\Delta$ M24-m25.2  $\Delta$ KnR BAC using FLP-mediated recombination, giving rise to the M25R BAC. The M25R genome lacks the ORFs M24, m25.1 and m25.2. The direction of the M25 ORF is indicated with a black arrow. (B) Mouse embryonic fibroblasts were infected with the M25R virus or the  $\Delta$ M24-m25.2 virus using a MOI of 3. The morphology of infected cells was examined 48 hours post infection by fluorescence microscopy. Magnification,  $\times$  200.

To identify a difference in the cascade of viral gene expression as a possible consequence of an impaired disruption of the actin cytoskeleton during cell entry, the expression of an immediate early protein (IE1), early protein (E1) or a late protein (20/352/4) was analysed. Cell lysates were prepared from  $\Delta$ M25 virus or wild type MCMV infected NIH 3T3 cells and probed by Western blotting using IE1-, E1 or 20/352/4 -specific antibodies. Proteins of the different kinetic classes were present in lysates from both wild type MCMV and  $\Delta$ M25 virus-infected cells (Fig.5.18A). The abundance of IE1, E1 or 20/352/4 proteins detected in lysates from  $\Delta$ M25 virus-infected cells in this experiment was even slightly higher compared to the abundance of IE1, E1 or 20/352/4 proteins in lysates from cells infected with wild type MCMV. In other experiments, the abundance of the viral proteins was slightly reduced in  $\Delta$ M25 virus-infected cells compared to wild type MCMV-infected cells but the proteins of the different kinetic classes were always present. Hence, the absence of the M25 gene did not alter the kinetic pattern of viral gene expression and although specific classes of proteins were present cell rounding was not induced.

Next, the growth kinetics of the  $\Delta$ M25 virus were analysed in NIH 3T3 and MEF (Fig.5.18B). Infection with a low MOI of 0.1 as well as a high MOI of 3 yielded slightly lower titres of the  $\Delta$ M25 virus compared to those of the wild type MCMV. In this specific

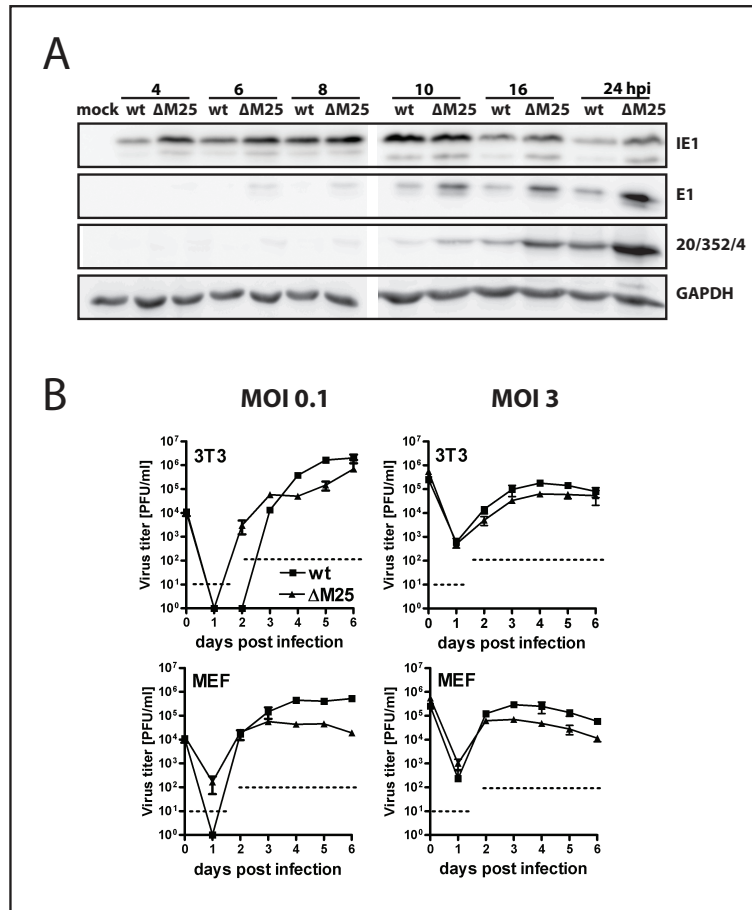


Figure 5.18: **Growth analysis of the  $\Delta$ M25 virus.** (A) Kinetics of viral gene expression in cells infected with the  $\Delta$ M25 virus or wild type MCMV. NIH 3T3 cells were infected with a MOI of 1 with the  $\Delta$ M25 virus or the wild type MCMV (wt). Cells were harvested at the indicated time points and lysates were separated on a 10% SDS-polyacrylamide gel and analysed by immunoblotting using antibodies specific for the immediate-early protein IE1, the early protein E1, and a late protein (mAb 20/352/4). Membranes were re-probed with a GAPDH specific antibody as a control for loading equal amounts of total protein. Mock, lysates from uninfected cells. (B) NIH 3T3 or MEF were infected with wild type or the  $\Delta$ M25 virus using a MOI of 0.1 or 3. Supernatants were harvested at the indicated time points and titers were determined by plaque assay on MEF. The dashed line represents the detection limit of the virus plaque assay. Error bars indicate standard deviations of the mean value of triplicate cultures.

experiment, the  $\Delta$ M25 virus produced progeny virus slightly faster in NIH 3T3 cells compared to the wild type MCMV when a MOI of 0.1 was used for infection. In two additional experiments, the faster growth of the  $\Delta$ M25 virus was not observed but the  $\Delta$ M25 virus yielded similar titres in both cell types compared to those of the wild type MCMV or titres that were about one order of magnitude lower, respectively (data not shown).

These data demonstrate that the absence of M25, and thus cell rounding, did not severely affect viral growth and had no influence on viral gene expression suggesting that the virus does not strictly rely on this process for replication in vitro.

### 5.3.4 Morphological Changes are Induced at Early Stages of Infection and are M25 Dependent

MCMV-induced cell rounding has not yet been described or illustrated in detail. Therefore, the cellular morphology of wild type MCMV-infected cells was recorded by laser scanning microscopy. MEF were fixed at different time points during the course of one replication cycle of 24 hours and at subsequent time points. TRITC-phalloidin was used to label actin filaments and GFP expression of the virus allowed the identification of infected cells.

The onset of alterations in cellular shape in wild type MCMV-infected cells was observed at five hours after infection (Fig.5.19). From this time point on GFP expression was observed allowing the identification of infected cells. Uninfected cells were outstretched with a fibroblast-like morphology. Long actin filaments were visible spanning the cell body (Fig.5.19, 5 h p.i., white arrows). In contrast, at this time point (5 h p.i.) infected GFP-positive cells appeared already more round. These cells were characterised by pronounced cortical actin (Fig.5.19, 5 h p.i., white triangle). Infected cells could clearly be distinguished from uninfected cells by their altered morphology. Two types of cells infected with wild type MCMV were present between 8 to 12 hours after infection: Most cells showed alterations in their shape becoming circular, whereas some cells were already completely round. This may be explained by the different infectious doses per individual cell. Assuming that the kinetics of cell rounding are influenced by the number of infectious virus particles taken up and thus the level of M25 protein expression per cell, different stages of cell rounding can be expected. Alternatively, the cells might be infected asynchronously. At final stages of infection, 24, 48 and 72 hours after infection, tiny and completely round cells were found. All infected cells changed their cell shape from outstretched into spherical. The actin filaments were visible as a spherical ring localised to the cortex of an infected cell (Fig.5.19, 48 h p.i., white triangle).

Next, the cellular morphology of  $\Delta$ M25 infected cells was analysed. To monitor cellular morphology in the absence of the M25 gene, MEF were infected with the  $\Delta$ M25 virus as described for the wild type MCMV. In contrast to the infection with wild type MCMV, drastic

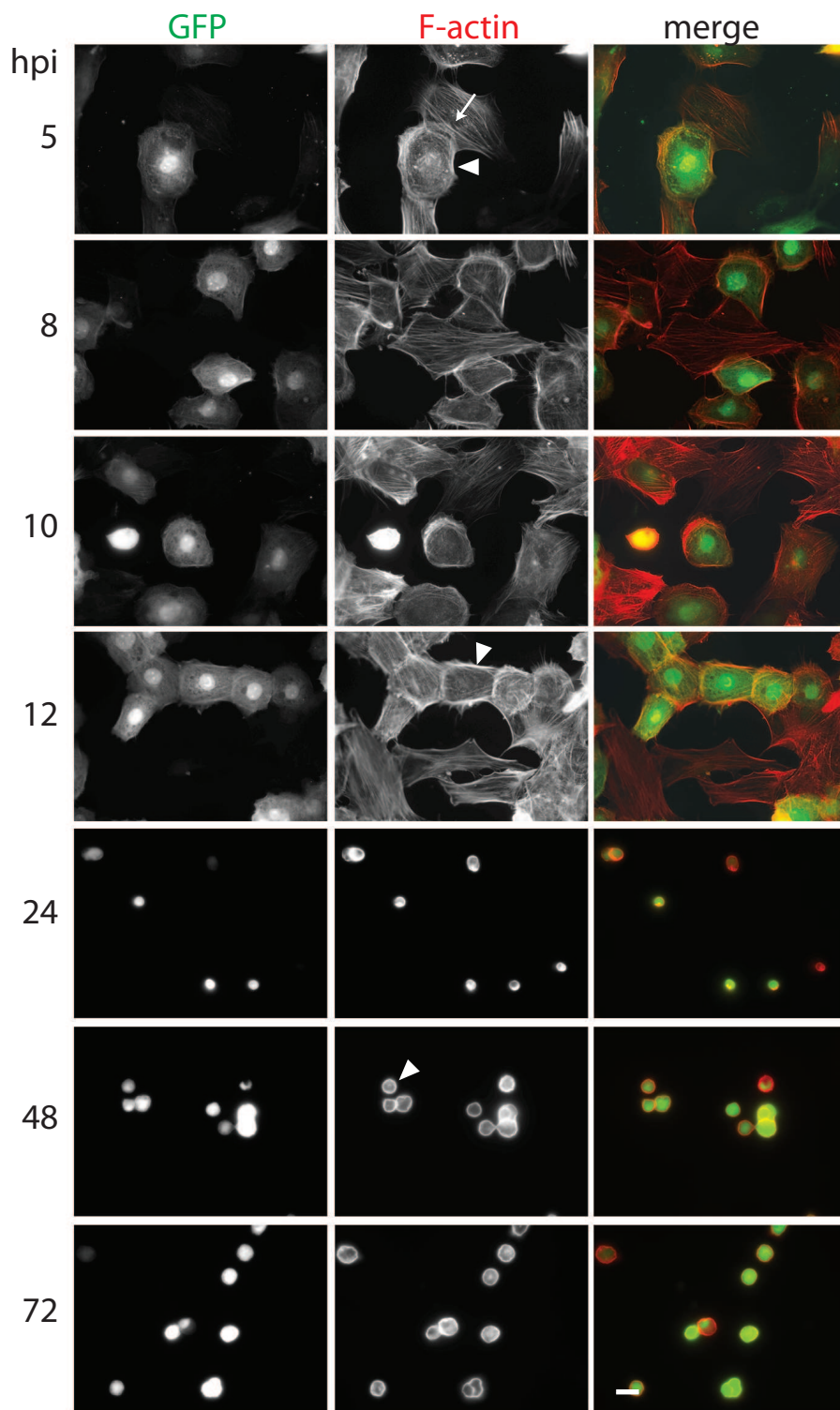


Figure 5.19: **Kinetics of wild type MCMV-induced cell rounding.** MEF were infected with a MOI of 1 with wild type MCMV expressing GFP. Cells were fixed at the indicated time points and actin filaments were visualised by TRITC-Phalloidin. Cellular morphology was analysed by laser scanning fluorescence microscopy. Actin filaments are marked with a white arrow and cortical actin with a white triangle. Bar, 20  $\mu\text{m}$ . Numbers indicate hours post infection.

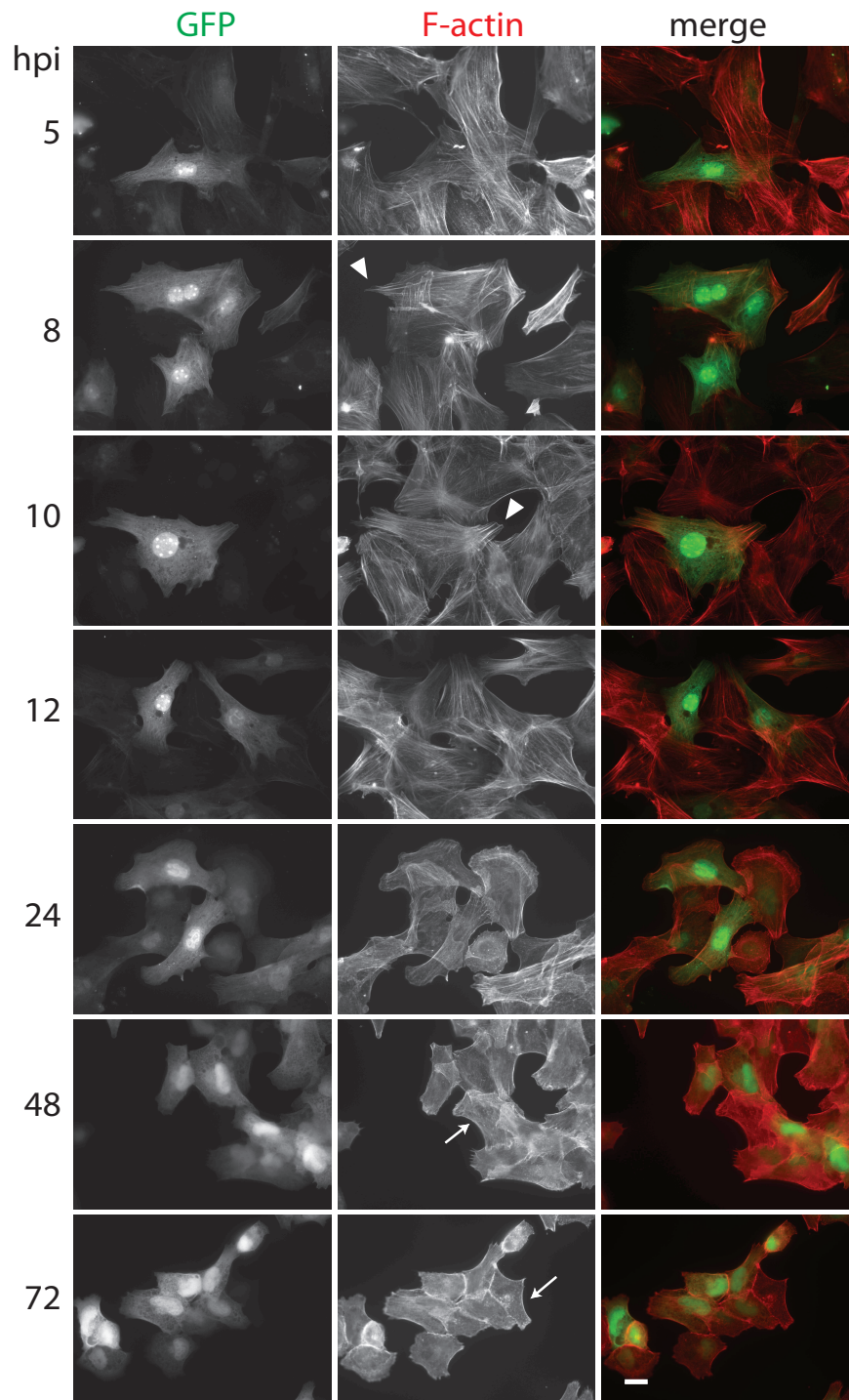


Figure 5.20: **Morphology of  $\Delta$ M25-infected cells at different time points of infection.** MEF were infected with  $\Delta$ M25 virus expressing GFP using a MOI of 1. Cells were fixed and treated as described in Fig.5.19. Cellular protrusions are exemplarily marked with a white triangle. Arrows indicate uninfected cells. Bar, 20  $\mu$ m. Numbers indicate hours post infection.

alterations in the cellular morphology of  $\Delta$ M25-infected cells were not observed. In the time frame of 5 to 12 hours after infection,  $\Delta$ M25 infected cells retained the typical morphology of uninfected fibroblasts with actin filaments and protrusions (Fig.5.20, 8-12 h p.i., white triangles). Cells remained outstretched and could not be distinguished from uninfected cells. In contrast to wild type MCMV-infected cells,  $\Delta$ M25 infected cells still formed protrusions between 24 to 72 h post infection. The morphology of  $\Delta$ M25-infected cells was similar to those of uninfected cells (Fig.5.20, 48-72 h p.i., compare infected and uninfected cells).

Taken together, these data demonstrate that MCMV-induced cell rounding is a process starting at five hours after infection or earlier, finally leading to completely circular and tiny cells. The absence of cell rounding in  $\Delta$ M25 infected cells during a full infection cycle of 24 hours indicated that M25 has a large impact on rearrangements of the cytoskeleton and that M25 function is not substituted by other viral factors during the viral replication cycle.

### 5.3.5 Investigation of M25-Induced Cell Rounding Outside the Context of the Viral Genome

Next, M25-induced cell rounding was investigated in the absence of other viral factors. The presence of M25 during viral infection was found to be essential for changes in cellular morphology. In other words, no other viral protein substituted for M25. However, it was still unclear whether additional viral proteins were required for M25 to exert its function. As a proof of M25 specificity to induce cell rounding, cellular morphology was investigated in M25 transfected cells (Fig.5.21).

For this experiment the M25 ORF was cloned into the pIRES2AcGFP1 vector. The pIRES2AcGFP1 vector contains an internal ribosome entry site (IRES) between the multiple cloning site and the ORF encoding the green fluorescent protein (AcGFP1) (Fig.5.21A). The IRES permitted the synthesis of both the AcGFP1 protein and the protein of interest from a single bicistronic mRNA. Expression of GFP allowed the detection of transfected cells.

The pIRESM25CHA vector was constructed by PCR amplification of the full length M25 ORF and subsequent ligation of the PCR product into the pIRESAcGFP1 vector. An HA-tag was added to the M25 C-terminus to detect the M25 protein with an HA-specific antibody.

The C-terminal HA-tag could theoretically have a negative influence on M25 protein function by altering the folding of the protein. Considering this possibility, a second plasmid was constructed in which an HA-tag was added to the M25 N-terminus directly upstream of the start codon. The M25 ORF contains more than 10 ATGs in frame. Translation initiation is to some extent determined by the nucleotide context around the ATG [Kozak, 1999]. For adding an HA-tag to the N-terminus, the 5th ATG was chosen since this particular ATG was claimed to be the initiation codon according to Dallas et al., possibly because it is surrounded by a

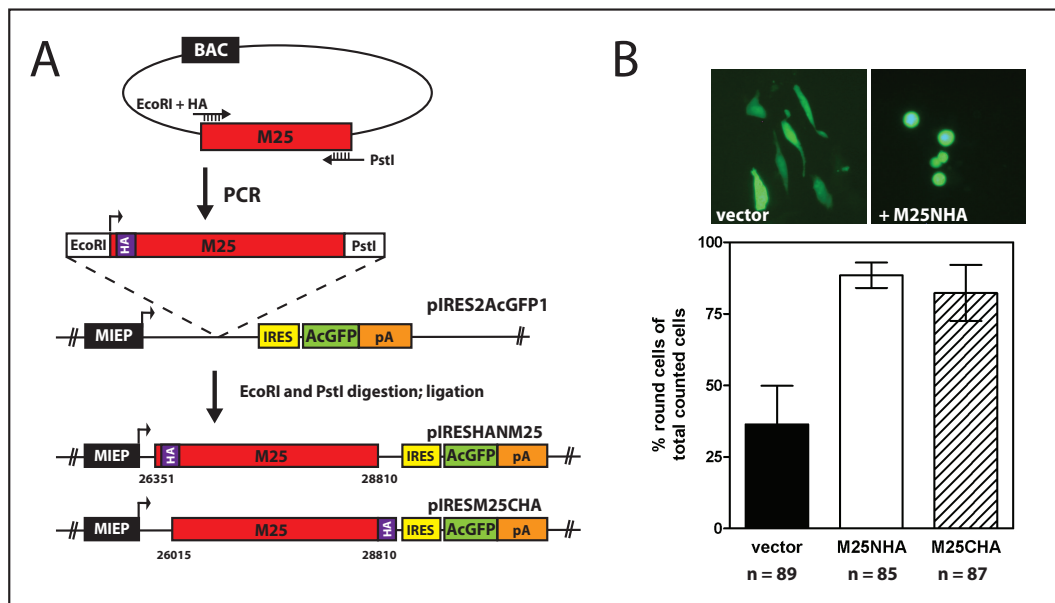


Figure 5.21: **Cloning of the M25 ORF into the pIRES2AcGFP1 vector.** (A) Cloning of the full length M25 ORF into the pIRES2AcGFP1 vector. The full length M25 ORF was amplified by PCR from wild type MCMV BAC DNA with primers containing EcoRI or PstI restriction sites. Either the PstI- or the EcoRI - primer contains the sequence for the Hemagglutinin-tag to be added to the M25 N- or C-terminus. The nucleotide positions of the M25 ORF, refer to the MCMV Smith strain. (B) (Top) Images show NIH 3T3 fibroblasts transfected with either pIRES2AcGFP1 or the pIRESM25NHA construct 48 hours after transfection. (Bottom) 48 hours after transfection the cellular morphology of GFP positive cells was analysed. Error bars indicate standard deviation of the mean value, n= number of total analysed cells

strong context [Dallas et al., 1994].

NIH 3T3 fibroblasts were transfected with each of the M25 constructs or the empty pIRES vector as a control. GFP expression was first observed around 24 hours after transfection. 48 hours after transfection was chosen as a time point for the assessment of cellular morphology. GFP and M25 are translated from the same transcript thus the presence of the M25 protein is expected at the same time GFP is present. At 48 hours after transfection sufficient amounts of intracellular GFP allowed the detection of transfected cells. Further, at this time point the changes of the cellular morphology in M25 expressing cells compared to cells transfected with the empty vector were most obvious. Most fibroblasts transfected with the M25 constructs appeared round whereas most of the fibroblasts that had been transfected with the pIRES vector remained outstretched (Fig.5.21B).

To quantify round cells after transfection, the number of cells transfected with the individual plasmids having a fibroblast morphology and those with a circular shape were counted. The percentage of round cells was at least twice as high for the M25 constructs compared to the vector control (Fig.5.21B). The M25 expression from both vector constructs induced cell



rounding to a similar extent indicating that the presence of the HA-tag and its position did not influence the function of M25. The percentage of round cells transfected with the empty vector could represent cells undergoing stress. It is also possible that the transfection process induced cell death resulting in cell rounding.

M25 expression in the absence of additional viral proteins induced cell rounding in fibroblasts concluding that M25 alone is sufficient to provoke morphological changes.

### **5.3.6 The M25-Derived 105 kDa Protein is the Predominate Species Expressed During Early Stages of MCMV-Infection**

In the following experiment a possible correlation of M25 protein expression with the observed kinetics of virus-induced cell rounding was investigated. M25 protein expression has been previously analysed by immunoblotting cell lysates of MCMV-infected cells using a monoclonal antibody directed against an M25 epitope [Wu et al., 1999]. A 105 kDa protein species is expressed at nine hours after infection followed by the detection of 130 kDa and 95 kDa proteins after 18 hours. Since the M25 dependent onset of morphological changes was observed five hours after infection using fluorescence microscopy, it was hypothesised that the responsible M25 protein is present at this time. To investigate this hypothesis, M25 protein expression was re-analysed. For this, a MCMV virus was constructed that expressed an HA-tagged M25. An antibody directed against the HA-tag could then be used for the detection of the M25 protein. The MCMV M25HA BAC was constructed using BAC mutagenesis with the HA-tag being inserted directly upstream of the M25 stop codon.

NIH 3T3 fibroblasts were infected with the M25HA virus or wild type MCMV. M25 proteins could be already detected after five hours of infection (Fig.5.22, lane 2). The most abundant species at this early stage of infection was a protein migrating with approximately 105 kDa followed by a protein species migrating with approximately 80 kDa. In addition, a protein of approximately 130 kDa and proteins of lower molecular weights were detected in low abundance. The 130 kDa protein species and additional 52- and 48 kDa-M25 proteins have been identified before, in preparations from purified MCMV virions [Wu et al., 1999, Kattenhorn et al., 2004]. Thus, the low abundance of the 130 kDa protein and the lower molecular weight proteins might result from incoming intracellular virus particles since a high MOI of five was used for infection. The appearance of the approximately 105 kDa protein is likely to be newly synthesised from an early viral transcript. Compared to overall GAPDH protein levels the concentration of the three major proteins, 130, 105 and 80 kDa increased at 18 hours after infection possibly caused by the ongoing synthesis of viral proteins (Fig.5.22, lane 7). Similar concentrations of the 130, 105 and 80 kDa proteins were detected in lysates starting from 24 hours after infection (Fig.5.22, lane 9-11). The abundance of the low

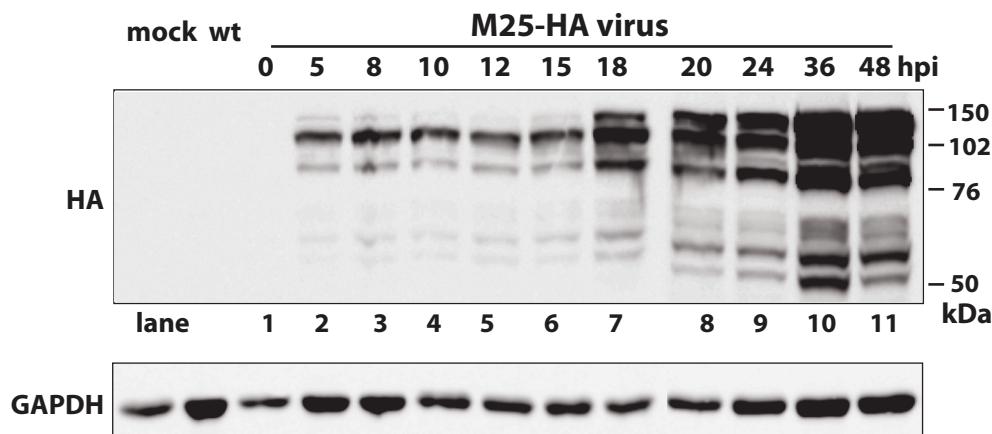


Figure 5.22: **Expression kinetics of M25-encoded proteins.** Expression of HA-tagged M25 proteins at different time points of the MCMV infection cycle. NIH 3T3 fibroblasts were infected with the M25HA virus using a MOI of 5. Cell lysates were harvested at the indicated time points. The time point 0 indicates cells harvested immediately after infection. Proteins were separated in a 10% SDS-polyacrylamide gel and an HA-specific antibody was used to detect M25 proteins by immunoblotting. Membranes were reprobbed with an anti-GAPDH antibody to demonstrate the loaded protein amounts. Lysates from mock infected cells or from wild type MCMV infected cells were harvested 24 hours post infection (p.i) and served as controls. Arrows point to the 130, 105 and 80 kDa protein species. Protein size markers are indicated to the right.

molecular weight proteins also increased with time. These proteins are likely to be M25 protein species since uninfected or wild type MCMV-infected cells, harvested after 24 hours, did not show any background signal.

The expression profile of the M25 revealed that several M25 proteins are synthesised throughout the MCMV infection cycle. Correlation of the M25 protein expression to the induction of morphological changes at early stages of infection reinforces the suggestion of their participation in virus-induced cell rounding.

### 5.3.7 Analysis of M25 Transcripts

The detection of a major 105 kDa M25 protein species at early stages of infection, after 5 hours of infection, by immunoblotting argued for a related transcript. Dallas et al. detected a single approximately 3 kb M25 transcript only at late stages, after 16 hours of infection by Northern blot analysis of total RNA from MCMV infected cells [Dallas et al., 1994]. Considering the possibility that, in the previous publication, an early M25 RNA was not detected due to a low infection dose the presence of an early M25 transcript was re-investigated. Northern blot analysis was performed using total RNA of MEF infected with a high MOI of 3 with wild type MCMV or  $\Delta$ M25 virus as a control. Cells were harvested at 6 or 24 hours after infection

and total RNA was prepared. For hybridisation a radiolabeled M25-specific DNA probe was used (Fig.5.23A). A transcript of approximately 2.8 kb was present at six hours after infection whereas two transcripts of approximately 3.1 kb and 2.8 kb were detected at 24 hours after infection (Fig.5.23B). A high specificity of the probe was ensured since no signal was present in total RNA from  $\Delta$ M25 infected fibroblasts. These data support the assumption that a M25 transcript is present at early times which maybe translated into the 105 kDa M25 protein.

In order to further characterise the identified transcripts, their 5' and 3'-ends were mapped by 5'/3'-rapid amplification of cDNA ends.

For the identification of the 5'-end of the M25 transcript the M25 specific primer (M25-1) was used to synthesise cDNA from the RNA pool. The second M25-specific primer (M25-2) was used for the amplification of cDNA by PCR (Fig.5.23C). A PCR product of approximately 200 bp was amplified from RNA prepared from cells infected for six hours whereas a product of approximately 500 bp was obtained from RNA at 24 hours after infection (Fig.5.23C). Besides the main product of about 500 bp, minor products of about 200 bp and 300 bp were also detected. The 200 bp product possibly originated from the same RNA transcript detected at six hours after infection that was still present at 24 hours after infection. Sequence analysis of the 200 bp product, detected at six hours after infection, mapped the 5'-end to nt position 26504 of the MCMV genome. The 5'-end of the 500 bp transcript was mapped to nt position 26191 (Fig.5.23A and Fig.5.24). For identification of the 3'-end of the M25 transcript cDNA was synthesised from total RNA with the M25 specific primer (M25-3). PCR products of approximately 400 bp were detected at 6 hours and 24 hours after infection (Fig.5.23C). Sequence analysis of the 400 bp products revealed identical 3'-ends at nt position 28956. Both identified transcripts probably share the same poly (A) signal. A TATA box was identified 22 nt upstream of the 5'-end of the longer RNA (nt 26191) (Fig.5.24). Both, the 5'/3'-ends and the TATA box are located within the predicted M25 ORF [Rawlinson et al., 1996]. A single poly (A) signal was identified 18 nt upstream of the 3'-end of the RNAs (Fig.5.23A and Fig.5.24).

Taken together, further analysis of the M25 transcripts confirmed the presence of two M25 transcripts that were identified by Northern blotting. Using the 5'/3' RACE technique, the 5'/3'-ends of two M25 transcripts were mapped that differed in their 5'-ends but shared the same 3'-end.

### 5.3.8 Identification of Proteins Expressed from M25 Transcripts

The expression of multiple M25 protein species and the presence of several potential M25 translation initiation codons raised the question of which ATGs are used for translation. Of particular interest was the origin of the approximately 105 kDa protein since it was the pre-

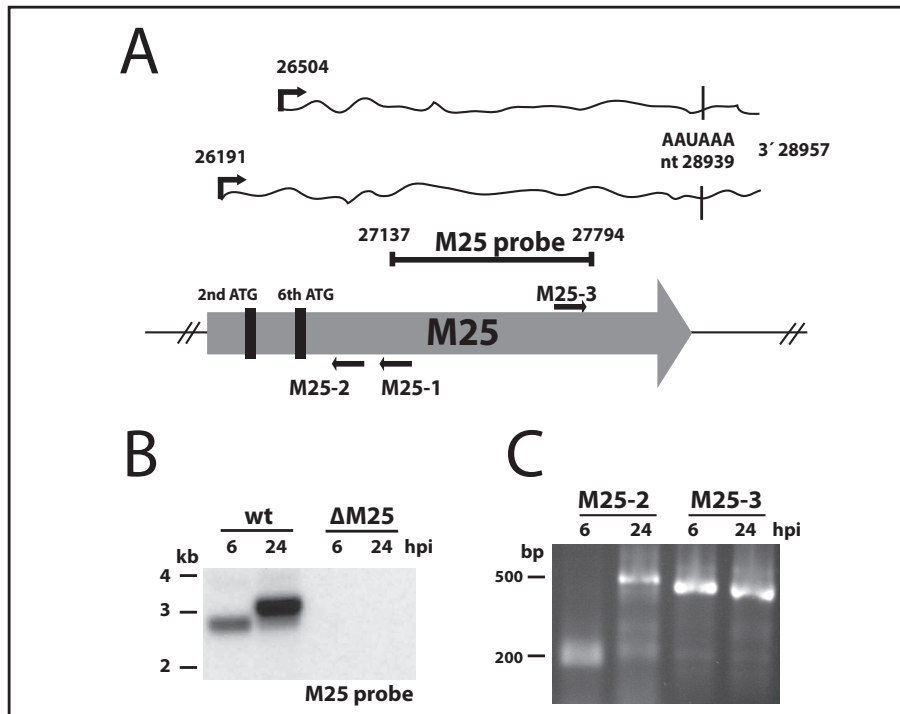


Figure 5.23: **Detection of M25 transcripts.** (A) Location of primers (bold arrows) used in the 5'-RACE or 3'-RACE and of the probe (black bar) used for Northern blotting. The M25 ORF is depicted as a gray arrow. The transcription start/end sites identified in this study and the poly(A) signal are indicated referring to the Smith strain. Potential start codons (ATG) of the transcripts are indicated. The illustration is not drawn to scale. (B) Northern blot analysis. Total RNA was isolated from infected cultures at 6 or 24 h p.i. and subjected to Northern blot hybridization using a radiolabeled M25 specific probe indicated in (A). The positions of RNA marker bands are indicated to the left. (C) 5'/3'-end mapping of the M25 transcripts. Total RNA was harvested from wild type MCMV-infected cultures at 6 or 24 hours post infection. The 5'/3'-ends of the M25 transcript were mapped using the primers indicated in (A). PCR products were separated by agarose gel electrophoresis and visualized by ethidium bromide staining.

### 5.3 Identification of a Viral Gene Involved in MCMV-Induced Cell Rounding

```

*
26001 CCCCGCCGG CGGGATGAGC CAGTTCGTAC AGCAGCTGCG TGACCGTGGC CTCGGCGCTG TCCACCAGCG GTCGCGACGC GGCCTCGAAC CGCGAGCCGA
26101 TTTTCCCCCGT CGAATCCATC TCCGCATCCG AACCCCTGCC AGAGATGGAG ACGTGCACCT ATATAAAATC ACGAGAGCCG GGTCTCGCGT GCCGAGCCGC
26201 CTATTCCCGC TGCCGGGCGG TCCCTTTGCA CCTCGAACGC CTGTCCGAGA ACCCCCACTC ACCCGAACGA TGAACCTCGC ATCCTCCAAG GACCGTCGTA
26301 TGTTCTGTCAC CGACGACTCG TCGGATGATG ACGACGACGA TGTGATGATC ATGGACCCCC CGGAGACGAC GTCGCTGCTG TCATCGGCGC TGCGGACGCG
26401 GCGGGGAGT CGGGGCGTTC CCCATGCCCC GCCTCCAAC TCCGCCACGG CGGGGCGGCG CTCGCGAGAC ACATACAAGC CATTGAGCAT CCGTCTGAG
26501 GAACTAAACG GCGAAGAGGA GGAGAGAGAC GAAGAAGACA TGTCACGCGA CGGACCCCGC CGGCACAGCC AGGACGACGA CTTTACTTAT GCGGACCCGG
26601 CCGATGTGAC ACTCGGGGCG ATGATGGGCA ATAGTACGGC GCGACAGAGT CCGAGTGCGG CGACAGCGGG AGCAGCGTCC CGGAATGATA GTGGAGCCGT
26701 GTCGCCCGTG ACCCTTTTGG ATGAGGACGG ATACCGGATA ATCCCGACCC CACCTACTTC GCGCGACGAT TCGCGACAGC TCGTCTGGGA CGACGACGAC
26801 GACGAGGATG ATGATTCACA CTACGGGCGT ATGACAGTGC CTCCGACGCC ACCCAACTGG CCACCGAAGA GTCGACCTTC GACCAAAAAA TCGGCGGAGG
26901 AAAAGCAATC TTCCACCGCC GGGCGGTCCA GAGGCGGCTC GACCGCACGC CGGACCCCGA AGAAGGCTCA AGAGACCGCT CCGGCGGCGC CGGCGGGCTC
27001 GCAAAACGCG CAAAACACAC GCCAGCAGCA GCAACAACAG CCTCCACGCC GCGAATCTTA CCACCTTCCA CCCGATTATC CTCGCCCAAC TCGGCGGAGG
27101 CAGCGCACTG TGTCCGCTCC TCTCCCCAGG ACCCCGACGC CCAACGACGA CGATGACGAC GATGACAACG ACGAGCCGGG TCCGAGCAAC ACACGCCCGG
27201 GCAAAACGCG CAGCGGCTGT GTCGATCACA CGGAGATAAA TCATCTATAC GAGACCCCGA TATCCGCCAC GGCATATGGT ATCGATATCG AAGATGACGA
27301 GGACGAAGAG ACCGGGCGCG CCGCCGACGA CGCGTCTATC GTCTGCAAG ATGATGATGA AGAAGAGGAG AACGATTGCG AGGAGATCTG CGACGGGGAA
27401 GAAAGCGCGC CAGCAGCAGC AGCAGCAGCG GCGCATCTGT CBTGACTCC TCATCGCACC CAGCCTCTGC GTCGCCACCC GTCGCTCCGC CGATCAGCCG
27501 GCGAGCTCGG GTTCTCGGCC GGTGTAGTGA GCGGTCAGGA CGCCAGATTC ATCGCGCGGT GCCTCCACCA CTCGCGACGC CCGCAGGTGC ACATCATAAA
27601 TCCYPMPPPYTTLDALESEPVLTKKKALRLCAGVLRPVVICACCTGCTATCGTACACCTAGACGCGTCTGAGCCAA GAAGGCGCTG CGTGCAGCGG GGTGCTGCGC GCGGCTATC
27701 KLAILELVNYCYVGIIGRLARARALSKDLMTTPPRIETAGCTAGCCA TCTGTGAA TTACTACTGC GTAGGGATCG GCGTCTGCG CCGTCTGCG GCGCTGTCCA AAGATCTGAT GACCCCGCG CGATCGAGA
27801 CLRRLRLEGLLPQQTSPSPPMCLRLVLRGLNITAAQCGTGGCGCG CCGTCTGAGG GCGTCCCGC CTGAAACATCA CCGCGCGCA
27901 HKASCDTIDQLMKPMQERERERRRQKTQCAQLFRSGACAAGSCAGTCTCGATA CGATCGACCA ACTGATGAAA CCGATGACAG AACGCGAGCG CCGCCGACAG AAGACGAGT GCGCACAGTT GTTCCGACG
28001 KNL L F S P P R F T R E G A K T L Y M R N I K I L N S D E E D T T A G A A C C T G T A C T C G G A A C A G A C A T C A G A T C T G A A C A G G A C G A G A T A C G A
28101 LNLVMTL L N P H P T R E D V L N D A I F C L S L G N F V Y N F C G T G A A C C T A G T G A C C T G A A T C C G A T C C C A C G A G G A A G A T G T G L A A C G A C G A T C T T T T G C C T G C G T G G A A C A T T T G T G A C A C T T
28201 S R A L E E L R G M I R C Q F E D L T E T L Y A A Y Y Q C P I M R C T C G C G C G C T C G T A G A A A C T G C G G A A T G A T C A G A T G C A G T T C G A G G A C T G A C C C A G A C C A G C C T G T A C T A T C A G T G T C C A T A T A G A
28301 D D Y R V L C S E V A N E I T S P R E D G Q G L S A L C R R S S L A F G A C G A C T A C C G C G T G T G T C C C G A G T G C G A A C G A G A G C A C G A C A G G C C G T T G T C C G C G C T A G C C T G C G T
28401 A R R C Y N E G V F F S P S Y V K Y L I K C A A M E E A G F E G Y T C G C G C G C G C T G T A C A A C G A A G C G T G T T T T C T C A C G T C T A C T C A A G T A T C T G A T C A A G T G C G G C C A T G G A A G A G C A G C T G A A G G C T A
28501 S L E S A A R S L A N P D I F R P L P D E S S A R R M L R R T I H C T C G T C G A G C G G C G G A G A T C T G C G C G A A C C C G C C G A T C T C C G C C G T A C G A G A T A G C G C C C C G C A T G T C G C G C G C A C A G A T A C A C
28601 F V R V D G T P S S S R Q I P T T H I P T H A N Y E L F L Q A S R M T T C G T G C G C G T C G A C G G G A C C C C T C G T C T C C A G A C A G A C C C A T C C C A A C A C A C G C C A C T A C G A G T G T C T C T G A A G C G T C T C G A
28701 I V P Q Q Q Q S R R S S T P P P S S S P P P P A A G G P K Y S K R T G A T C G T T C C G C A A C A G C A G T C A C G A G A C C C C C A C G A T C A T C T C T C T C T C C C C G C C G C G A G G C C A A A G T A C T C C A A G C T
28801 T F L * T A C C T T T C G T A A T C T T A G T T A A T C A G C A G A T A C C A A A A A A G C A C T T A G C A C T T A G C C A C A G A A T C G A G T A A G T A A G T T A C A A T C T A T A C
28901 A C C C C C C C A T G T A C T T C T T C T T C A T A A T T T C A C T G A A T A A A A A A G A T C A C N S C A A A A A A G A C A A G A G A C A T C G T G T G T G T A A T T C A G T T A

```

Figure 5.24: Nucleotide sequence of the MCMV M25 gene. The potential TATA box and the polyadenylation signal as well as the aa sequence that is conserved between MCMV M25 (aa 494-893) and HCMV UL25 are underlined. Methionines in the M25 aa sequence are marked in bold. The 2nd and the 6th Methionine are encircled. The identified transcription start sites are indicated with arrows and the mapped 3'-end is framed. A bold asterisk indicates the start of the predicted M25 ORF in the Smith strain (accession number NC 004065) [Rawlinson et al., 1996]. A nuclear localisation signal was predicted consisting of the amino acids PRKSRPS (aa 283-289) shown in parentheses. The M25 protein is predicted to be soluble.

dominant species identified at early stages of infection at the same time as cell rounding was induced.

The M25 ORF contains several potential start codons for translation. Translation of each of the identified transcripts might be initiated at different ATGs generating proteins of different molecular weights with different N-termini. A potential ATG for translation initiation of the 3.1 kb transcript is the 2nd ATG referred to the predicted M25 ORF in the Smith strain since it represents the first ATG downstream of the 5'-end of the 3.1 kb transcript whereas the 6th ATG is the first ATG downstream of the 5'-end of the 2.8 kb transcript and hence a potential start codon.

First, a computational analysis, predicting the molecular weights of the potential proteins initiated from the different translation initiation start sites was done. Molecular weights ranging of 103 kDa for the longest possible M25 ORF, initiated at the 1st ATG, to 57 kDa for the protein initiated at the 10th ATG were predicted. The predicted molecular weights did not match with the size of the identified proteins, thus making it necessary to analyse individual protein expression.

It was proposed that M25 protein synthesis is either initiated at the first or the 5th ATG of the M25 ORF [Rawlinson et al., 1996, Dallas et al., 1994]. Therefore a transfection-based approach was used to determine the size of the proteins expressed from the previously cloned M25 plasmids pIRESM25NHA and pIRESM25CHA (Fig.5.21A ). The plasmid pIRESM25CHA contains the full length M25 ORF and the HA-tag is fused to the C-terminus of the M25 sequence whereas in the pIRESM25NHA plasmid an HA-tag is fused to the N-terminus upstream of the 5th ATG (Fig.5.25 (a-b)). Immunoblotting using an HA-specific antibody identified a protein species in pIRESM25NHA transfected 293T cells that migrated with a lower molecular weight than the 130 kDa protein species, detected in lysates from M25HA virus infected 3T3 cells (Fig.5.26A). A protein species migrating at >130 kDa was identified in lysates prepared from pIRESM25CHA transfected cells. The lower abundance of this protein in the pIRESM25CHA lysate may result from a low transfection efficiency. Besides these two proteins, no additional protein species were identified in the respective lysates. None of the M25 expressed proteins correlated in size to the previously detected 130, 105, 80 kDa or low molecular weight-M25 proteins in M25HA virus infected cells concluding that neither the 1st ATG nor the 5th ATG of the M25 ORF represents the initiation codon for M25 protein synthesis during viral infection.

To identify the start codon for the production of the 105 kDa protein, additional M25 constructs were generated. The PCR-based quick mutagenesis protocol was used in order to shorten the M25 ORF using the pIRESM25CHA vector as the template. Expression plasmids starting with the 2nd ATG, 4th ATG, 6th ATG, 7th ATG, 9th ATG or 10th ATG of the M25 ORF were constructed. The 3rd ATG was excluded since it is only separated by 27 nt from the 2nd ATG and no detectable difference in protein size was expected. The 5th ATG and

### 5.3 Identification of a Viral Gene Involved in MCMV-Induced Cell Rounding

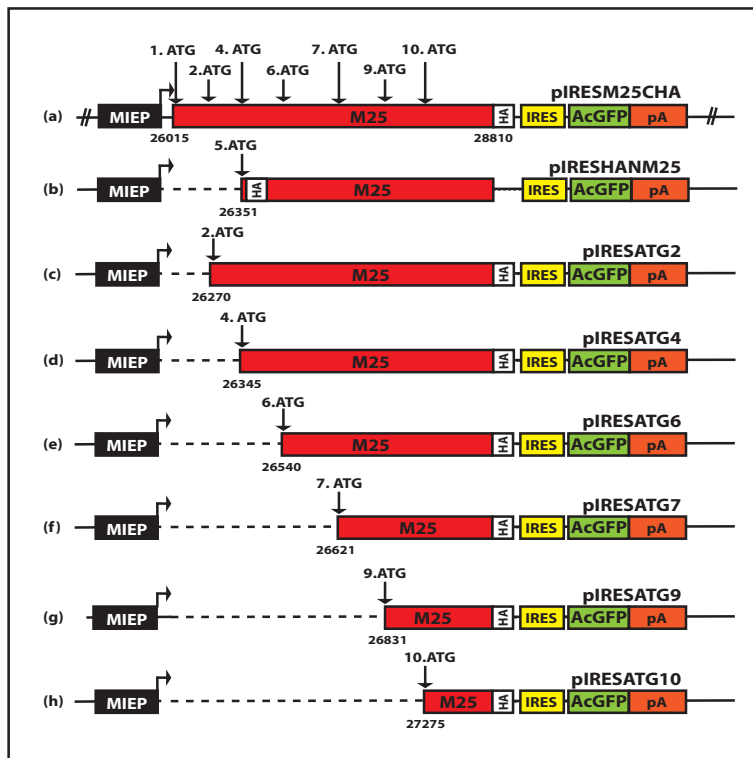


Figure 5.25: **Structure of the M25 expression plasmids.** The pIRESATG vectors were constructed by means of the PCR-based quick mutagenesis protocol using pIRESM25CHA as the template. Amplification with M25 specific primers and a standard primer binding to the major IE promoter led to vectors with shortened M25 ORFs (c-h) downstream of the HCMV major immediate early promoter (MIEP) and upstream of an internal ribosome entry side (IRES), the ORF AcGFP and the SV40 early poly (A) signal. Nucleotide positions of the ATGs are indicated referring to the Smith strain. The illustration is not drawn to scale.

the 8th ATG are located three nucleotides downstream or in direct proximity to another ATG, respectively and were not investigated separately for the aforementioned reasons. Figure 6.25 illustrates the M25 constructs.

Immunoblotting of lysates from transfected 293T cells revealed a single major protein species expressed from each of the shortened M25 ORFs (Fig.5.26A). Protein synthesis starting at the 2nd ATG of the M25 ORF resulted in a protein species migrating with the same molecular weight as the 130 kDa protein synthesised from the M25HA virus. Protein expression starting at the 6th ATG of the M25 ORF revealed a protein species correlating in the molecular weight with the 105 kDa protein made from the M25HA virus. The protein that was synthesised starting at the 4th ATG of the M25 ORF migrated to approximately 120 kDa similar to the protein made from the pIRESM25NHA plasmid. Protein synthesis from the pIRESM25NHA plasmid was initiated at the 5th ATG of the M25 ORF which is only 6 nt downstream of the 4th ATG. An approximately 95 kDa protein was produced when protein synthesis started at the 7th ATG of the M25 ORF, an approximately 85 kDa protein species from the 9th ATG and an approximately 60 kDa protein was detected in lysates from pIRESATG10 transfected cells. Besides the main proteins originating from the different M25 ORFs, additional M25 specific protein species migrating to approximately 80, 50 and 48 kDa were detected in all lysates of transfected cells except from pIRESM25NHA and pIRESM25CHA transfected cells. The 80 kDa protein species was absent when translation started at the 10th ATG and no further

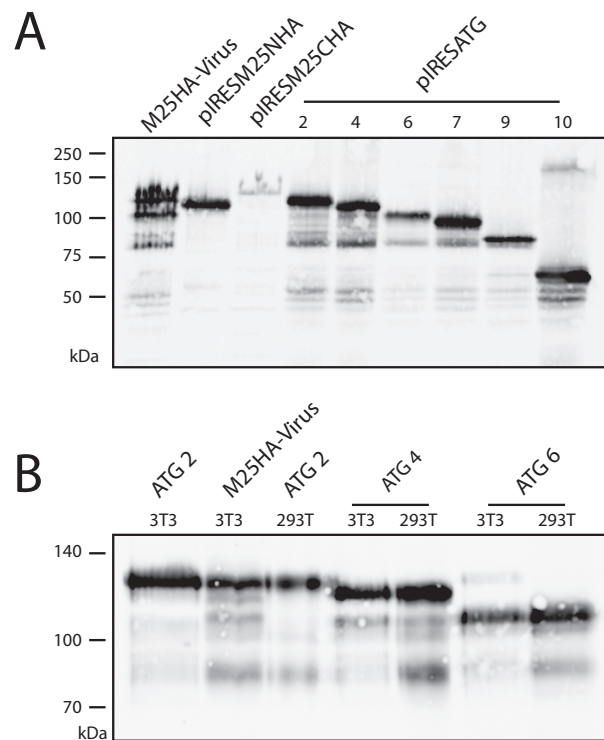


Figure 5.26: **M25 proteins expressed from M25 plasmids.** (A) Lysates of 293T cells transfected with the M25 constructs shown in Fig.5.25 were prepared 48 hours after transfection and separated on a 7.5%-18% SDS-polyacrylamide gradient gel followed by immunoblotting with an anti-HA antibody. Lysate prepared from 3T3 fibroblasts infected for 24 hours with the M25HA virus was used to compare the molecular weight of the proteins. (B) Lysates used in (A) and lysates from transfected NIH 3T3 fibroblasts were separated on a 8% SDS-polyacrylamide gel followed by immunoblotting with an anti-HA antibody. Protein markers are indicated to the left.

ATG is present between the 9th ATG and the 10th ATG of the M25 ORF that could initiate translation of the 80 kDa protein.

Whereas the major protein species seem likely to originate from the individual M25 ORFs, the origin of the shorter M25 protein species remains elusive. Notably, M25-derived proteins of lower molecular weight have also been identified from purified MCMV virions including M25 proteins migrating with 52 and 48 kDa [Kattenhorn et al., 2004]. These protein species might have resulted from translation initiation at downstream ATGs. Alternatively, the additional M25 proteins present in the lysates from cells transfected with the shortened pIRESM25 constructs may have resulted from protein degradation. It is striking that the abundance of the 80 kDa protein is higher compared to the other small proteins which may indicate that this protein is a major degradation product.

A single M25 transcript is expected to originate from the plasmids since viral co-factors that potentially regulate the expression of the two M25 transcripts, detected during virus



infection, are missing. Unlike the transcription of viral genes that is a highly regulated process dependent on viral proteins, translation of viral mRNAs is restricted to the host cell machinery [Mocarski et al., 2007]. An unfavourable ATG-context, meaning that the first ATG on the transcript is not surrounded by a strong context sequence, i.e. the classical Kozak sequence GCCRCCAUGG (R= A or G), leads to translation re-initiation at downstream ATG codons by means of leaky scanning [Kozak, 1991, 2002]. This enables the production of separately initiated proteins from a single mRNA. Thus, the first ATGs in the shorter constructs may be surrounded by a weaker context as the ATGs in the pIRESM25NHA or pIRESM25CHA constructs. Consequently, M25 proteins possibly originate from the downstream ATG codons.

In order to have a direct comparison of the M25 proteins expressed from pIRESATG2, pIRESATG4 and pIRESATG6, lysates obtained from transfected NIH 3T3 cells and 293T cells were separated by SDS-polyacrylamide electrophoresis side-by-side with the lysates from M25HA virus infected NIH 3T3 cells (Fig 6.26B). M25 protein synthesis in NIH 3T3 as well as 293T cells, initiated at the 2nd ATG of the M25 ORF, generated a protein comigrating with the 130 kDa protein expressed from the M25HA virus and a protein comigrating with the 105 kDa protein was detected when M25 protein synthesis started at the 6th ATG. Protein synthesis initiating at the 4th ATG yielded a protein with a molecular weight of approximately 120 kDa. The 50 and 48 kDa protein species could only be seen when the blot was overexposed but were present in all lysates.

A comparison of proteins expressed from the M25 constructs to those expressed by the M25HA virus revealed that synthesis of the 105 kDa protein is initiated at the 6th ATG of the M25 ORF. The synthesis of the 130 kDa protein is initiated at the 2nd ATG whereas the origin of the 80 kDa M25 protein could not be linked to a specific ATG of the M25 ORF. These data provide experimental evidence for the potential initiation codons on the two M25 transcripts.

### 5.3.9 Subcellular Localisation of M25 Proteins

CMV induced cell rounding involves morphological alterations and cellular shrinkage. During this process, the cytoskeleton must be triggered to disassemble or to rearrange its components, e.g. filamentous actin. The MCMV M25 that was identified as a key factor for MCMV-induced cell rounding could exert its function in two possible ways. A direct interaction of the M25 proteins with actin filaments or other cytoskeletal components in the cytoplasm could influence cellular morphology. On the other hand, M25 proteins may indirectly regulate the rearrangement of the cytoskeleton. This could occur by interacting with adaptor proteins in the cytoplasm which regulate the cytoskeleton or by protein-DNA interactions in the nucleus.

Determining the subcellular localization of a protein is an important first step toward

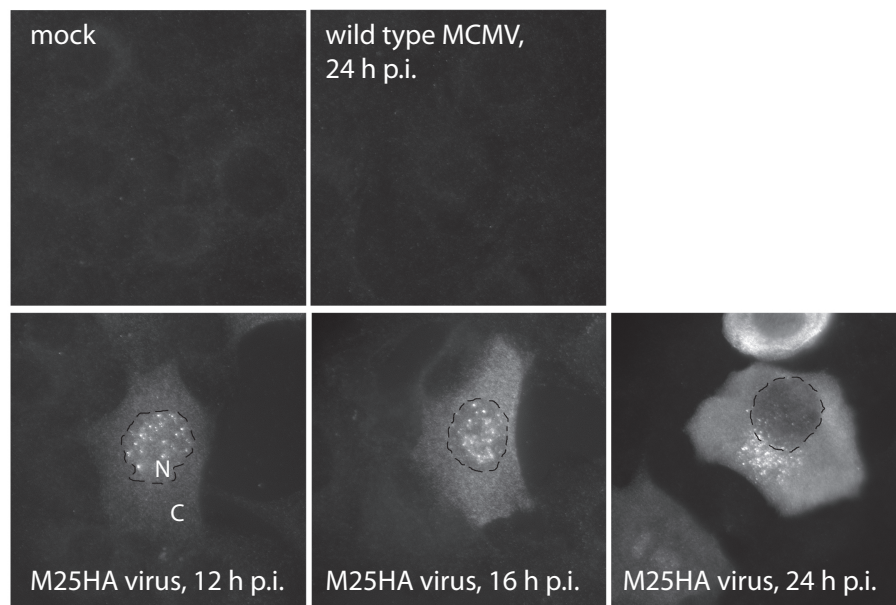


Figure 5.27: **Subcellular localization of M25 proteins.** C127I epithelial cells were infected with the GFP-negative M25HA-tagged virus using a MOI of 1. Cells were fixed at the indicated time points. An antibody directed against the HA-tag was used to locate the M25 proteins within the cell. Uninfected (mock) and wild type MCMV infected cells served as controls. The dashed line marks the nucleus. N = nucleus, C = cytoplasm

understanding its function. To investigate in which cellular compartment M25 potentially exerts its function, the subcellular localisation of M25 was analysed by immunofluorescence. C127I epithelial cells were infected with the M25HA-tagged virus and an antibody directed against the HA-tag was used to visualise M25 within the cell at different time points after infection (Fig.5.27). After 12 h of infection the HA-signal was observed as a punctate pattern that was localised to the nucleus. In addition, a diffuse signal in the cytoplasm was observed. Both M25-specific signals are likely to originate from newly synthesised M25 proteins and not from incoming particles for the following reasons. First, a low infection dose of one plaque forming unit per cell was used and second at 12 h after infection incoming viruses will have undergone uncoating and will have disassembled. The HA-signal was still associated with the nucleus at 16 hours after infection. A localisation clearly outside of the nucleus was detected at late stages of infection, after 24 hours. Here, the HA-signal was concentrated to one side of the nucleus in addition to a dispersed signal in the cytoplasm (Fig.5.27).

The HA-signal detected in M25-HA infected cells could result from several proteins expressed from the two M25 transcripts. The signal detected at 12 hours after infection probably results from the 105 kDa protein that is the most abundant species at early stages of infection (Fig.5.22) whereas several other M25 protein species are present in the same abun-

dance like the 105 kDa protein at late stages of infection. The 130 kDa protein is the only protein identified in purified virus particles by Wu et al. and is suggested to be incorporated as a tegument protein [Wu et al., 1999]. The tegumentation of virus capsids takes place at the Trans-Golgi-Network (TGN) by budding into transport vesicles constricted from the TGN-cisternae [Eickmann et al., 2006]. The cytoplasmic signal detected at 24 hours after infection possibly reflects the situation when the 130 kDa protein is present in the cisternae during the ongoing tegumentation process. No HA-specific signal was detected in uninfected or wild type MCMV infected cells.

These experiments showed that the subcellular localisation of M25 is linked to the different stages of MCMV infection: at early stages of infection M25 is made in the cytoplasm and is then translocated into the nucleus, whereas at late stages of infection, M25 localisation is primarily found in the cytoplasm. This suggested that, for the induction of cell rounding, protein-protein interactions of M25 in the cytoplasm as well as interactions of M25 proteins with the DNA in the nucleus are possible.



## 6 Discussion

### 6.1 Generation of a Library of Mouse Cytomegalovirus Mutants

For the productive infection of endothelial cells and macrophages, MCMV requires specific tropism factors that are dispensable for virus growth in fibroblasts. This suggests that also the growth of MCMV in epithelial cells is dependent on specific tropism factors.

The fact that cell rounding occurs during CMV infection indicates that viral factors account for this effect. The aim of this thesis was to identify viral factors that determine the epithelial cell tropism of MCMV and the viral factors that induce cell rounding during MCMV infection. Viral factors can be proteins, like the already identified tropism factors, but could potentially also be non-protein factors like miRNAs, non-coding RNAs, intron RNAs or cis-active binding sites for transcription factors.

To identify the factors of MCMV, responsible for the productive infection of epithelial cells and induced cell rounding, a forward genetic procedure was used. To this end, a library of MCMV mutants was generated employing site-directed mutagenesis of the MCMV genome that was previously cloned as a BAC. Cells infected with these mutants were then screened for the appearance of specific phenotypes followed by the identification of the responsible region on the viral genome. In this way, the M25 gene could be identified to induce cell rounding in fibroblasts and epithelial cells and the m107-m108 region to contain factors that influence the productive infection of epithelial cells.

The forward genetic procedure has been successively used in the past to associate the appearance of a phenotype with the deletion of a specific gene [Brune et al., 2001, Ménard et al., 2003, Dunn et al., 2003, Loewendorf et al., 2004, Zimmermann et al., 2005, Lilja et al., 2008]. Whereas the work in some of these publications was based on random, transposon insertion mutagenesis of the MCMV genome creating a large library of mutants, the present study used the site-directed BAC mutagenesis technique [Messerle et al., 1997]. An advantage of site-directed mutagenesis over the transposon-mediated mutagenesis is the deletion of large areas of the viral genome in one step, accelerating the screening process of the corresponding mutants. A region of interest can then be identified and narrowed down by the production of

mutants containing smaller deletions. A limitation of the generation of a mutated library by introducing large deletions is that genes, whose deletion might cause a phenotype, would not be revealed if they hide within the core region of essential genes.

The BAC mutagenesis technique exploits bacterial genetics in that the gene of interest is interrupted by the insertion of a selection marker via homologous recombination between a linear PCR fragment and the BAC-containing viral genome in *E. coli* [Borst et al., 2007]. The identification of expected DNA sequences, by cutting BAC DNA and viral DNA prepared from the individual mutants in this study, indicated a correct integrity of the mutant genomes.

The MCMV genome has been predicted to contain a total of 170 ORF, based on the genome sequence of the Smith strain [Rawlinson et al., 1996]. Recent work confirmed the majority of these ORFs by detecting their transcripts [Tang and Maul, 2006]. However, for most ORFs the potentially expressed protein has not been characterised and thus the function is unknown. All herpesvirus genomes contain a core of conserved genes. In HCMV, the core region encompasses the ORFs UL44 to UL115 [Mocarski et al., 2007]. This includes the essential genes encoding the viral replication machinery e.g. the viral DNA polymerase and proteins necessary for virion maturation such as tegument proteins and glycoproteins. The core functions and the position of the respective genes M44-M115 is retained in MCMV [Rawlinson et al., 1996]. In the regions flanking the herpesvirus core genes, predicted MCMV genes have sequence homology to HCMV genes or are unique to MCMV.

For the selection of the genes to be deleted the region that is conserved among CMV or that is unique for MCMV was chosen since the majority of genes in this region has been found to be non-essential for the infection of fibroblasts *in vitro* [Brune et al., 2006]. This cell type is commonly used as a standard for virus production in cell culture. Further, four out of five cytomegalovirus cell tropism factors that have been previously identified are located outside the core conserved region [Brune et al., 2001, Ménard et al., 2003, Hahn et al., 2004, Wang and Shenk, 2005b]. MCMV M36, M45, m139, m140 and m141 genes promote the production of virus progeny in endothelial cells or macrophages. The HCMV UL131-UL128 genes are necessary for the productive infection of endothelial and epithelial cells. This approach was recently supported by the identification of Rh01, a factor that is essential for the growth of rhesus CMV in epithelial cells [Lilja et al., 2008]. The Rh01 gene is located in the region that is unique for rhesus CMVs.

A library of 18 MCMV deletion mutants was created that lack either a single gene or multiple genes. The deletions targeted a total of 105 predicted viral genes, referring to the published sequence of the Smith strain [Rawlinson et al., 1996]. The reconstitution of infectious virus from all 18 virus mutants in fibroblasts indicated that the deleted genes were not essential for the production of progeny virus in fibroblasts. These results are in agreement with the previous observation of M. Wagner [Brune et al., 2006] and extended the set of genes that are

dispensable for virus productivity in fibroblasts by the region containing the ORFs m106-m108. The growth of individual virus mutants was analysed in fibroblasts and epithelial cells using a cell tropism assay. As revealed by this assay, the titres from the virus mutants in fibroblasts were not uniform. It is possible that genome size negatively influenced the packaging of the genome into the viral capsid possibly affecting infectivity. However, both the virus mutant  $\Delta$ m01-m17 that has the smallest genome and the  $\Delta$ M33 mutant that has the largest genome yielded similar titers in fibroblasts compared to those of wild type MCMV. This indicated that the presence or absence of specific gene functions rather than the genome size determined the productivity of each individual mutant.

An overall genome size of about 230 kb that is conserved between several MCMV isolates suggests that the maximal size of a MCMV genome packaged into a capsid cannot exceed 230 kb to ensure viral fitness [Smith et al., 2008]. The Smith strain that was manipulated in the present study has a size of 230,278 bp. The added BAC vector contains 8396 bp and the marker gene, GFP, 1526 bp (M.Messerle, personal communication). Thus, the complete MCMV-BAC has a size of 240,200 bp. However, due to selection pressure against oversized genomes, it has been observed that only the viral genome is packaged, due to spontaneous excision of the BAC vector sequences in eukaryotic cells by homologous recombination [Wagner et al., 1999]. The size of the mutant BAC genomes generated in the present study were in the range of 224,812 bp ( $\Delta$ m01-m17) to 240,359 bp ( $\Delta$ M33). The analysis of viral DNA prepared from fibroblasts infected with mutants with a genome size exceeding 230,000 bp, revealed that the BAC vector sequences were missing. This confirmed that the BAC vector was excised due to selection pressure against oversized genomes.

## 6.2 Searching for Mouse Cytomegalovirus Epithelial Cell Tropism Factors

Productive infection of epithelial cells is thought to be important for CMV entry into the host and for host-to-host transmission. Infectious virus has been found in body fluids such as saliva, breast milk and urine possibly secreted from secretory epithelial cells [Mocarski et al., 2007]. Virus shedding from salivary gland epithelial cells has been shown during the persistent phase of infection [Jonjic et al., 1989]. Salivary glands, and thus epithelial cells, exhibit a reservoir of latent MCMV genomes, since reactivation of CMV from these organs has been observed [Reddehase et al., 1994]. Thus, epithelial cells may be necessary to enable CMV to replicate at mucosal sites of entry, to influence transmission by releasing virus into the bloodstream or by passing the virus onto traversing leukocytes and to secrete virus for host-to-host transmission.

However, sites of primary CMV infection are not well characterised and the factors that

promote the productive infection of a certain cell type, e.g. epithelial cells, so called tropism factors, were unknown.

The aim of the present study was to investigate whether factors of MCMV exist that are required for the productive infection of epithelial cells. To this end, a library of mouse cytomegalovirus mutants was created and their growth properties on epithelial cells were investigated. Comparative analysis of their titers and their spread in epithelial cells and fibroblasts to those of wild type MCMV identified five mutants that showed a reduced growth in epithelial cells. Specifically, a reduced capacity for production of viral progeny and spread in epithelial cells was ascribed to the deletion of the ORFs M28-M31, m29-M31, M35-M37, M45 and m107-m108.

Evidence that deletion of these genes limited viral productivity in epithelial cells was obtained from comparing the titres of 18 virus mutants to those of the wild type MCMV in a cell tropism assay. Five virus mutants,  $\Delta$ M28-M31,  $\Delta$ m29-M31,  $\Delta$ M35-M37,  $\Delta$ M45 and  $\Delta$ m106-m108, were identified that yielded lower titres in epithelial cells compared to those of wild type MCMV or the titres remained below the detection limit (Fig.5.6). Further, the spread of the mutant viruses in epithelial cells was restricted to single cells surrounding the primary infected cell (Fig.5.5). In contrast, wild type MCMV established a broad infection of surrounding cells. However, the comparison of the titres of the virus mutants and wild type MCMV obtained from fibroblasts revealed that the  $\Delta$ M35-M37,  $\Delta$ M45,  $\Delta$ M28-M31 or  $\Delta$ m29-M31 mutants also yielded lower titres in fibroblasts. The titres were at least 1.5 orders of magnitude lower compared to the titres of wild type MCMV. This indicated that the deletion of these genes affected growth in fibroblasts and in epithelial cells and so these genes were not considered to be specific for the growth in epithelial cells. In contrast, the  $\Delta$ m106-m108 virus yielded three orders of magnitude lower titres in epithelial cells and only one order of magnitude lower titres in fibroblasts compared to those of the wild type MCMV. For this reason, the  $\Delta$ m106-m108 mutant was considered to lack viral factors that are required primarily for the productive infection of epithelial cells and was therefore further characterised. Additional virus mutants in which the m106 ORF, and a DNA sequence giving rise to a stable intron RNA were targeted for deletion, and these viruses yielded similar titres in epithelial cells and fibroblasts, excluding these factors as potential candidates. In contrast, the  $\Delta$ m107-m108 mutant showed reduced productivity in epithelial cells. miRNAs that are expressed from this region in addition to putative proteins expressed from the overlapping m107/m108 ORFs were also shown not to account for the limited virus productivity.

Combining all the deletions that were introduced into the m107-m108 region revealed that sequences of 252 and 103 bp were not targeted for deletion and thus could encode potential epithelial tropism factors. The 252 bp sequence is partly located in the predicted m107 5'-untranslated region and partly inside the m107 ORF whereas the 103 bp sequence



is located inside the predicted m107-m108 ORFs. Since potential m107 and m108 proteins were dispensable for the growth in epithelial cells, this led to the speculation that cis-acting elements within the m107-m108 DNA sequence may determine the epithelial cell tropism of MCMV.

## Screening of a Library of MCMV Mutants

The overall titres obtained from epithelial cells infected with the 18 individual mutants or wild type MCMV were at least 1.5 times lower than those obtained from fibroblasts. A possible explanation for this might be an impaired release of virus particles.

GFP expression, as a marker for immediate early gene expression in epithelial cells infected with the growth deficient  $\Delta$ M28-M31,  $\Delta$ m29-M31,  $\Delta$ M35-M37,  $\Delta$ M45 or  $\Delta$ m107-m108 mutants showed that these mutants had successfully entered epithelial cells. This supported the working hypothesis of the present study that the cell tropism of a virus is not only determined by cellular receptors permitting viral attachment and viral entry but also by viral factors that interact with other cellular factors at the post-entry step. The hypothesis was based on the work of others. Heparan sulphate, integrins and two other unknown proteins have been shown to bind HCMV at the cell surface of various cell types [Compton et al., 1993, Wang et al., 2005, Nowlin et al., 1991]. However, the expression and binding to the attachment receptor did not result in IE protein synthesis in every cell type that was tested, indicating that the virus had also to overcome other cellular barriers to start viral gene expression [Nowlin et al., 1991]. A number of viral genes have been identified from different CMV species that are required at a post-entry step for viral growth in a specific cell type [Brune et al., 2001, Ménard et al., 2003, Lilja et al., 2008]. The corresponding proteins control cellular functions in order to establish a productive infection in the cell [Mack et al., 2008, Cicin-Sain et al., 2008].

Viral entry into the cell is a prerequisite for viral gene expression. A HCMV UL132-UL128 deletion mutant failed to initiate IE1 expression and consequently did not replicate in primary endothelial cells, although IE1 gene expression and wild type virus-like titers had been observed in fibroblasts [Hahn et al., 2004]. A recent study attributed this phenotype to the failure to form a glycoprotein complex, containing the UL128/UL130/UL131 proteins, that is required to enter endothelial cells by fusion in endocytic vesicles. Entry of fibroblasts occurs directly by fusion at the plasma membrane and therefore depends on other viral factors [Ryckman et al., 2008]. The above mentioned study is, up to date, the only report of cell tropism factors of CMVs that are essential for viral entry into a specific cell type prior to viral gene expression.

The impaired growth of the  $\Delta$ M28-M31,  $\Delta$ m29-M31,  $\Delta$ M35-M37,  $\Delta$ M45 or  $\Delta$ m107-m108 mutants in epithelial cells correlated with greatly reduced spread in epithelial cells compared to wild type MCMV. As a read out system, extracellular progeny virus was measured and

cell-to-cell spread was followed until day six after infection. Alternatively to impaired virus entry, the deletion of gene expressing cell tropism factors could also block the release of virus particles. Infectious virus particles could be retained inside the cell due to impaired transport of virions to the plasma membrane. Consequently, this would result in decreased progeny virus in the supernatants.

The analysis of viral gene expression could provide information at which step of the infection cycle a virus mutant is blocked. To find out whether differences in viral gene expression between the virus mutants and wild type MCMV existed, the kinetic expression of viral genes in epithelial cells should be investigated. However, MCMV-infected GFP-positive cells indicated that at least the IE genes were expressed since the GFP gene is inserted in the IE2 locus that is transcribed from the major immediate early promoter at immediate early stages of infection. Thus possibly early or late viral gene expression could be blocked.

## **The Genes Selected for Deletion Encode Already Known Cell**

### **Tropism Factors**

Several genes that have been previously associated with cell- or tissue tropism are among the genes that were targeted for deletion in the present study. The MCMV M45 and M36 genes have been previously identified as determinants of productive infection of endothelial cells and/or macrophages [Brune et al., 2001, Ménard et al., 2003]. Infection of epithelial cells with the  $\Delta$ M45 or  $\Delta$ M35-M37 mutants yielded titres that remained under the detection limit. This indicated that the productive infection of epithelial cells also requires the M45 protein. The M45 protein inhibits TNF $\alpha$ -stimulated caspase-independent cell death by interacting with the regulatory receptor interacting protein (RIP)1 [Mack et al., 2008, Upton et al., 2008]. Different cell type-dependent expression levels of RIP1 are suggested to determine sensitivity to caspase-independent cell death. In this way, endothelial cells might be more sensitive to caspase-independent cell death than fibroblasts. It is conceivable that epithelial cells are sensitive to this RIP1-mediated cell death similar to endothelial cells and are protected by the M45 protein. In case of the  $\Delta$ M35-M37 mutant, the lack of the M36 protein is speculated to cause the phenotype, since the M36 protein is required for MCMV growth in macrophages [Cicin-Sain et al., 2008], but this has to be further investigated.

The deletion of the M43 or the m139-m141 genes has previously been shown to negatively affect virus production in macrophages [Ménard et al., 2003]. However, since the  $\Delta$ m42-M43 or  $\Delta$ m139-m141 mutants did not yield lower titres in epithelial cells compared to those of wild type MCMV indicated that these genes are dispensable for virus productivity in epithelial cells.

Four genes that have positional homologs in MCMV, RhCMV Rh01 and HCMV UL128, UL130, UL131, have been described as epithelial cell tropism factors [Lilja et al., 2008, Wang

and Shenk, 2005b, Ryckman et al., 2008]. The respective viruses only productively infected epithelial cells in the presence of these factors. However, similar titres of the  $\Delta$ m01-m17 and  $\Delta$ m128-m138 MCMV mutants and wild type MCMV obtained from epithelial cells suggested that these genes are only positional homologs and have other functions during MCMV infection. In fact, the chemokine homolog MCK-2 is translated from an mRNA that is expressed by the MCMV m129-m131 genes [Fleming et al., 1999]. An MCK-2 mutant failed to produce high titers in the salivary glands and was cleared more rapidly from spleen and liver during acute infection compared to wild type MCMV [Saederup et al., 2001, Fleming et al., 1999]. The majority of cells in the salivary gland are epithelial cells suggesting that the lower titres are due to an impaired of the virus mutant to grow in epithelial cells. The growth properties of a  $\Delta$ m129-m131 mutant have not been analysed in epithelial cells until now. The present study adds content to the aforementioned findings in that the phenotype of the  $\Delta$ m129-m131 mutant in salivary glands is most likely not due to a failure to productively infect epithelial cells.

A  $\Delta$ m132 mutant has been shown to produce lower titres in salivary glands. Therefore the m132-encoded protein was named salivary gland growth protein sgg1 [Manning et al., 1992]. Consistent with the finding from Lagenaur and co-workers, who observed that the sgg1 mutant was able to enter epithelial cells of the salivary gland [Lagenaur et al., 1994], the  $\Delta$ m128-m138 mutant infected epithelial cells and grew to similar titres in these cells compared to those of wild type MCMV. Therefore it can be excluded that the impaired growth of the  $\Delta$ m132 mutant in the salivary gland is determined by the failure to productively infect epithelial cells.

The present study is the first report that associates the predicted MCMV m106-m108 genes with MCMV epithelial cell tropism. The  $\Delta$ m106-m108 mutant showed the most significant growth defect in epithelial cells of all of the mutants tested, and was therefore further investigated.

## **Analysis of the m106-m108 Region for Epithelial Cell Tropism**

### **Factors**

In order to identify the factor that causes the growth defect of the  $\Delta$ m106-m108 mutant in epithelial cells, additional mutants were generated. Deletions were introduced into the predicted m106 ORF or the overlapping m107/m108 ORFs or into the large non-coding region between the m106 and m107/m108 ORFs. The finding that the  $\Delta$ m106 mutant was not impaired to grow in epithelial cells indicated that the predicted m106 ORF is dispensable for viral growth in epithelial cells.

Kulesza and Shenk identified a 7.2 kb intron RNA that is produced from the large non-coding region between the ORF m106 and m107/m108 [Kulesza and Shenk, 2006]. The

detection of this intron RNA and its appearance throughout the virus life cycle suggested that it is a stable intron RNA. A mutant virus that is unable to produce the intron RNA failed to produce similar titers in the salivary glands during the persistent phase of infection [Kulesza and Shenk, 2006]. The salivary gland phenotype raised the hypothesis that the intron RNA might be an epithelial tropism factor and thus is responsible for the reduced growth of the  $\Delta$ m106-m108 mutant in epithelial cells. However, the observation that the  $\Delta$ intron mutant, in which half of the intron RNA sequence was deleted, yielded similar titres in epithelial cells compared to those of the wild type MCMV suggested either that the intron RNA is not produced and is therefore dispensable for growth in epithelial cells, or that the intron RNA is still produced in this mutant and the deletion did not inhibit its function as an epithelial tropism factor.

The finding that the infection of epithelial cells with the  $\Delta$ m107-m108 mutant, from which the predicted overlapping genes m107 and m108 had been deleted, yielded reduced titers compared to those of the wild type MCMV, suggested that one of these ORF determines the epithelial cell tropism of MCMV.

The synthesis of potential m107 and m108 proteins would require the presence of a transcript. A m108 transcript was detected at 24 hours after infection and its 5'- and 3'-ends could be mapped. In contrast, a m107 transcript could not be detected. This suggested that there is no m107 transcript and no m107 protein. Consistent with these results no mRNA transcribed from the m107 gene could be detected using microarray analysis or reverse transcriptase PCR from total RNA prepared from fibroblasts at 24 hours after infection, whereas a m108 transcript could be detected under the same conditions [Tang et al., 2006]. The potential MCMV m107/m108 ORFs were predicted by analysis of the viral DNA sequence but not by analysing viral gene expression in cells [Rawlinson et al., 1996, Brocchieri et al., 2005]. It is possible that transcription from the m107 gene only occurs at immediate early or early stages of infection and thus a transcript would not be detectable in fibroblasts 24 hours after infection. Alternatively, cell type specific m107 gene expression is conceivable. This possibility has to be investigated by analysing m107 gene expression in epithelial cells.

Possible roles of potential m107 and m108 proteins as limiting factors for growth in epithelial cells were investigated in this study by the generation of several mutants in which the overlapping m107/m108 ORFs were targeted for deletion. These viruses produced infectious virus in epithelial cells similar to the wild type MCMV indicating that potential m107 or m108 proteins are dispensable for the growth in epithelial cells.

Sequences that were deleted in the  $\Delta$ m107-m108 mutant contained not only the ORFs m107/m108 but also parts of the 5'-/3'- non-coding regions of the predicted m107/m108 genes. The 7.2 kb intron RNA was reported to be spliced from a primary transcript whose 5'-end was predicted to be in the region that is deleted in the  $\Delta$ m107-m108 mutant [Kulesza

and Shenk, 2006]. Thus, potentially, the intron RNA is an epithelial tropism factor that retained its function as a shorter RNA in the  $\Delta$ intron mutant but could not be produced in the  $\Delta$ m107-m108 mutant. Mapping the 5'-end of the putative primary transcript confirmed the previously published splice donor and splice acceptor sites of the intron RNA and identified the 5'-end of the primary transcript within the region that was deleted in the  $\Delta$ m107-m108 mutant. In order to investigate if the 7.2 kb intron RNA is an epithelial tropism factor, a mutant was generated in which the sequence of the splice donor was deleted and the absence of the 7.2 kb intron RNA was confirmed by Northern blotting. The finding that the  $\Delta$ 7.2kb intron mutant grew to similar titres in fibroblasts and epithelial cells clarified that the intron RNA is not an epithelial cell tropism factor. This was also supported by the fact that the  $\Delta$ m106 mutant grew to similar titres in epithelial cells and fibroblasts although the splice acceptor of the intron RNA was deleted and thus the intron was not produced, as could be shown by Northern blotting.

In addition to the 7.2 kb intron RNA, Kulesza and Shenk also speculated that a 8 kb intron RNA is produced from the 106-m108 region that shares the splice acceptor but differs in the splice donor site. This 8 kb intron RNA accumulates to a much lower level than the 7.2 kb intron RNA and could possibly be produced from a splicing event of a m108 primary transcript. Consistent with the published data from Kulesza and Shenk, a 8 kb RNA could be detected by Northern blot analysis with the same probe used for the detection of the 7.2 kb intron RNA. Further, the presence of a m108 transcript was confirmed by analysis of its 5'- and 3'-ends. There was no evidence of a splicing event of the m108 transcript producing the 8 kb intron RNA. Instead, a 108 bp intron RNA was identified to be spliced from the m108 transcript. Thus, the present study confirmed the data from Tang and Maul who identified the expression of a 108 transcript and adds content to these data in that the m108 transcript coordinates were determined and post-transcriptional modifications, namely splicing of an 108 bp intron, were identified.

The fact that proteins and the 7.2 kb intron RNA did not account for the reduced growth of the  $\Delta$ m106-m108 mutant in epithelial cells, suggested that other factors than proteins cause the defect. During productive HCMV infection, 14 miRNAs have been identified [Fannin Rider et al., 2008] and 18 miRNAs are expressed during lytic infection of MCMV [Dölken et al., 2007, Buck et al., 2007]. miRNAs are small RNA molecules. They can be transcribed in clusters of miRNAs leading to a polycistronic primary transcript or as individual miRNAs Kim [2005], Sarnow et al. [2006], Scaria et al. [2006]. miRNAs originate often from intron RNAs of protein-coding or from non-protein-coding genes but can also be located in the 5'-/ 3'-untranslated regions of a transcript. The function of miRNAs is to control protein synthesis. The mode of action is achieved by a partial or complete binding to the target mRNA. Only little is known about the targets for viral miRNAs and their function.

The HCMV expressed miRNA miR-UL112-1 was reported to downregulate the ligand MICB for the activating receptor on natural killer cells. The virus benefits from consequential less killing of virus-infected cells by NK cells [Stern-Ginossar et al., 2007]. Whereas most of the herpesvirus miRNAs have been attributed to viral gene expression, immunomodulation or maintenance of latency, their exact mechanisms remain elusive and no viral miRNA has been yet identified that functions as a cell tropism factor [Fannin Rider et al., 2008]. However, since viral gene expression has been found to be species and cell-type specific [Lafemina and Hayward, 1988, Goodrum et al., 2002, Jurak and Brune, 2006], one might also envision a cell type-specific viral miRNA expression.

Dölken and coworkers have detected four MCMV miRNAs that are produced in fibroblasts during the early late phase of gene expression and are localised within the m107/m108 region [Dölken et al., 2007, Buck et al., 2007]. The functional relevance of these miRNAs has not been investigated to date. In the present study, a possible role for the miRNAs as epithelial tropism factors was addressed and a virus mutant was constructed lacking either the 5'-arm or both 5'/ 3'-arms of each miRNA hairpin precursor. No differences were found in the number of infected epithelial cells compared to those infected wild type MCMV. This indicated that the previously detected miRNAs were dispensable for viral growth in epithelial cells and thus are likely to fulfil other functions.

## **Essential vs. Accessory Factors that Promote Cell Type-Specific Viral Growth**

Infection of epithelial cells with the  $\Delta$ m106-108 or  $\Delta$ m107-108 virus yielded reduced titres compared to those of the wild type MCMV. The reduction however was not uniform within different experiments. The difference of the titres from the of  $\Delta$ m106-108 or  $\Delta$ m107-108 virus, obtained from epithelial cells varied between 1 and 3 orders of magnitude compared to those of the wild type MCMV. In some cases the virus mutants did not produce detectable amounts of progeny virus in epithelial cells. The titres of the  $\Delta$ m106-108 or  $\Delta$ m107-108 virus obtained from fibroblasts were uniformly 1.5 to 2-fold lower compared to those of wild type MCMV. Thus, the alterations in the measured titers of the  $\Delta$ m106-108 and  $\Delta$ m107-108 virus mutants indicated that the phenotype displays some variability.

Contrary to the previously published tropism factors, in the present study, no viral protein could be attributed to the observed phenotype. Instead the deletion of regulatory DNA sequences is suggested to account for the observed phenotype. Therefore, and with respect to the last paragraph, it is tempting to conclude that growth in epithelial cells is determined by a yet undetermined viral factor that is not essential but rather accessory for the productive infection and spread of MCMV in epithelial cells.

## **cis-acting Elements as Potential Factors that Determine Viral Productivity in Epithelial Cells**

Proteins, miRNAs and the large intron RNA, expressed from the m107-m108 region were found to be dispensable for the growth of MCMV in epithelial cells. Since infection of epithelial cells with the  $\Delta$ m107-m108 mutant yielded reduced titres compared to those from wild type MCMV, factors other than the aforementioned must account for the impaired growth.

Specific regions within the m107-m108 region were targeted for deletion and the corresponding virus mutants were analysed for their growth properties in epithelial cells. All of these sequences have been shown dispensable for the growth of MCMV in epithelial cells. Sequences of 103 and 252 bp within the m107-m108 region have not yet been targeted and analysed. Thus, they might contain viral factors for the productive infection of MCMV in epithelial cells. It is tempting to speculate that cis-acting elements, located within these sequences, could account for the phenotype. Cis-acting elements are specific DNA sequences that are binding sites for transcription factors thereby regulating the expression of adjacent genes.

The detection of a binding site for a transcription factor does not necessarily identify the regulated gene. Thus, it can only be speculated which of the adjacent genes, upstream or downstream of the putative cis-acting element within the m107-m108 region, are target genes to be regulated. These are for example the essential genes M112/M113 which are located downstream of the ORFs m107-m108.

Comparable analysis of the MCMV genome with the HCMV genome revealed sequence similarity of the MCMV M112/113 ORFs and the HCMV ORFs UL112/113 [Rawlinson et al., 1996]. Further, the M112/113 proteins showed a comparable expression pattern and localisation to those encoded from the HCMV ORFs UL112/113 [Ciocco-Schmitt et al., 2002]. Both, the M112/113 and UL112/113 proteins regulate viral gene expression. A combination of viral proteins, including those expressed from the HCMV UL112/113 locus have been shown to enhance the expression of viral genes required for replication e.g. encoding the DNA polymerase [Iskenderian et al., 1996]. The M112/113 proteins interact with their own transcriptional activator IE3, thereby preventing the repressive effect of IE3 on the major IE promoter and ensuring IE gene expression [Tang et al., 2005].

M112/113 gene expression might be differentially regulated in epithelial cells and fibroblasts. The following scenario is conceivable: In addition to enhancers and repressors that regulate M112/113 gene expression in fibroblasts, expression of the M112/113 genes in epithelial cells could depend on transcription factors that bind to cis-acting sequences located within the m107-m108 region. These cis-acting sequences then represent factors that determine the productive infection of MCMV in epithelial cells.

Taken together, the tropism of MCMV for epithelial cells might be determined by cis-

regulatory elements in the m107/m108 region of the virus genome which bind to epithelial cell-specific transcription factors that are required for the expression of adjacent genes in epithelial cells.

### **6.3 Identification of a Viral Gene Involved in MCMV-Induced Cell Rounding**

Cell rounding is a cytopathic effect of cytomegaloviruses that is induced at early stages of infection [Kim and Carp, 1971, Furukawa et al., 1973, Albrecht et al., 1980, 1983]. The viral factors required for the induction of these morphological changes induced by MCMV remained unknown until now. The present study identified M25 as the first viral gene shown to be a key factor in MCMV-induced cell rounding and showed that M25 transcripts and proteins were present at early stages of infection correlating with the onset of virus-induced cell rounding.

The results of three experimental approaches provided clear evidence that the M25 gene is both necessary and sufficient for the induction of cell rounding. First, MCMV virus mutants lacking the M25 gene failed to induce cell rounding.  $\Delta$ M25-infected cells maintained a typical fibroblast morphology with finger-like protrusions at early stages of infection, whereas wild type MCMV-infected cells demonstrated a decreased cell size and reduced protrusions. At final stages of infection,  $\Delta$ M25-infected cells still formed protrusions whereas wild type MCMV-infected cells obtained a completely round cell shape with accumulated cortical actin. Second, the re-insertion of the M25 gene into the MCMV  $\Delta$ M25 genome restored the ability to induce morphological changes to the reconstituted virus. Third, the expression of the M25 gene from an expression vector, outside the context of the viral genome, was sufficient to induce cell rounding in fibroblasts.

Having identified M25 as a key factor in MCMV induced cell rounding, two different experiments showed that M25 transcripts and proteins were present at early stages of MCMV infection correlating with the onset of induced cell rounding. Northern blot analysis demonstrated the presence of an M25 early transcript in RNA extracted from wild type MCMV-infected cells at six hours after infection and a second M25 transcript expressed during late stages, after 24 hours of infection. Immunoblotting of M25 proteins revealed the expression of multiple proteins from the M25 ORF. A 105 kDa protein was the predominant protein species at early times of infection, whereas the expression of additional M25 proteins was detected at later stages. These results support the view that cytomegalovirus-induced cell rounding is caused by an early viral protein [Albrecht et al., 1983].



## In Vitro Growth Properties of the $\Delta$ M25 Virus

Wild type MCMV-like growth properties of the  $\Delta$ M25 virus indicates that cell rounding is a direct consequence of the lack of the M25 protein and not due to delayed replication kinetics.

The infection of cells with virus mutants either lacking multiple genes including M25 ( $\Delta$ M24-m25.2) or the single M25 ORF ( $\Delta$ M25) or parts of the M25 sequence (M25 $\Delta$ conserved or M25 $\Delta$ non-conserved) did not manifest in a tiny and rounded cell shape. It was considered possible that the absence of the M25 gene leads to delayed growth of the viral mutants in vitro and thus makes the lack of cell rounding an effect of the delayed growth kinetics of a slower replicating virus. This was proven not to be the case. Consistent with the study from Zhan et al. that revealed similar titres of a virus mutant with a transposon inserted in the M25 locus to those of the wild type MCMV [Zhan et al., 2000], in the present study only slightly lower titres were measured in general of the  $\Delta$ M25 virus compared to those of the wild type MCMV. Viral proteins of different kinetic classes were present in  $\Delta$ M25 virus-infected cells concluding that the respective genes were correctly expressed. The results obtained from independent experiments were however not uniform. A higher abundance of viral proteins were detected in  $\Delta$ M25-infected cells compared to wild type MCMV was found in one experiment whereas in a second experiment the protein abundance was higher in wild type MCMV infected cells. Analysis of the growth properties of the  $\Delta$ M25 virus revealed no difference in one experiment but slightly lower titres of the  $\Delta$ M25 virus compared to those of wild type MCMV in additional experiments.

This could be explained by the limitations in determining the exact values of the titres of the viruses used in these experiments. The actual value of the titre of a virus can be measured with a certain accuracy only. In the above described experiments the titre of one virus might be closer to the true value and the titre of the second virus might be more distant from the true value. Hence, the infection of cells with either of these viruses will manifest in a different number of infected cells. Based on long experimental experience, it is estimated that the true value of a MCMV titre can be determined within the range of about one order of magnitude by the applied method. Although a variability between single experiments existed it did not change the main statement of the experiments.

The correct synthesis of viral proteins of specific kinetic classes and the maintenance of a typical fibroblast cell shape in  $\Delta$ M25-infected cells indicated that viral growth is not strictly dependent on the presence of the M25 gene and cell rounding is not an effect of an altered viral gene expression. The results obtained in this study suggest that the induction of cell rounding is conserved as an accessory viral mechanism since viral gene expression and virus particle production did not strictly depend on this process.

## Characterisation of M25 Transcripts

The observation that two M25 transcripts are present during MCMV infection, one transcript at early stages and the other at late stages of infection indicated that the 105 kDa-M25 protein at five hours after infection results from an early transcript.

Previous analysis of M25 transcripts by Dallas et al. and Zhan et al. identified a single M25 RNA at 16 hours and 24 hours after MCMV infection [Dallas et al., 1994, Zhan et al., 2000]. The expression of this transcript was blocked in the presence of PAA treatment indicating that viral DNA synthesis is required for its generation [Dallas et al., 1994]. The present study detected M25 proteins at five hours after infection suggesting the presence of a corresponding mRNA. Supporting this hypothesis, a 2.8 kb M25 mRNA was detected at six hours after infection in Northern Blot analysis. This mRNA was also identified at 24 hours after infection together with a second 3.1 kb M25 mRNA. The detection of the late M25 transcript is consistent with the results of others [Dallas et al., 1994, Zhan et al., 2000]. In contrast, the early M25 transcript was identified for the first time in the present study.

Mapping the M25 transcript ends and transcript start sites revealed that both transcripts share the same 3'-end but differ in their 5'-ends.

The 5'-end of the early M25 transcript was mapped to the M25 ORF, 313 nt downstream of the 5'-end of the late transcript. The same 3'-end position was identified for both transcripts. Thus both transcripts were initiated within the M25 ORF and the late transcript covers the complete sequence of the early M25 transcript. The calculated size of the transcripts, of 2.7 kb and 2.4 kb, and poly(A) tailing matched approximately the observed sizes of the transcripts detected in Northern blotting. Analysis of the DNA sequence for the M25 gene and its flanking regions identified a single core promoter element, a TATA-box, 31 nt upstream of the late transcript start and a single poly(A) signal downstream of the transcript end suggesting that both M25 transcripts share the same poly(A) signal.

Although there is no evidence of a GC-box characteristic for TATA-less promoters, a second, yet unidentified, TATA-less promoter might drive transcription of the early transcript. Initiation of transcription is highly regulated through binding of transcription factors to enhancer and repressor elements proximal or distal to the core promoter element thereby influencing the formation of the transcription initiation complex and so the activity of the RNA polymerase II.

Repressors possibly bind to proximal promoter elements and prevent transcription of the larger transcript during the early phase of viral gene expression but do not influence the transcription of the short M25 transcript. At late stages of viral gene expression the repressor may dissociate from the promoter region allowing the synthesis of both transcripts.

## Kinetics of M25 Protein Expression

Analysis of M25 protein expression revealed the presence of multiple protein species expressed from the M25 ORF. Four major proteins of approximately 130, 105, and 80 kDa were detected. The detection of this M25 protein pattern in M25HA-virus infected cell lysates is consistent with the M25 protein pattern identified in previous publications [Farrell and Shellam, 1990, Wu et al., 1999]. In the present study, at five hours after infection the 105 kDa-M25 protein was detected in a high abundance together with low amounts of the 130 and 80 kDa proteins. The abundance of these proteins in infected cells did not change until 18 hours after infection. From this time point on the abundance of all three protein species, especially those of the 130 and 80 kDa proteins increased reaching the highest abundance at 36 hours after infection.

Whereas the presence of M25 proteins in the late phase of infection are consistent with the results from Wu et al., the onset of M25 protein expression and the presence of additional M25 proteins during the early phase of viral gene expression are controversial. In the present study, the 105 kDa protein species was synthesised with early kinetics, starting already at five hours after infection, whereas Wu et al. detected the 105 kDa protein at nine hours after infection in lysates of wild type MCMV-infected cells [Wu et al., 1999]. The discrepancy between the results obtained in this study and the published data for the detection of the 105 kDa protein could be attributed to the different infection doses used in the experiments. In the current study, a high infection dose of five PFU/cell was used for infection whereas the infection dose utilised in the earlier publications is not mentioned but was possibly lower than five PFU/cell. The more virus particles are present and able to express their genes, the higher the expected expression of viral proteins.

The virus isolate, investigated in the previous publications is the MCMV K181 strain and not the MCMV Smith strain used in the present study. The alignment of the M25 amino acid sequence from both strains revealed 99% similarity. This supports the finding of the same pattern of M25 proteins in both MCMV isolates but it is possible that functional differences between other viral proteins of the strains K181 and the Smith strain influence M25 gene expression and could also explain the temporal differences of M25 protein expression.

In addition to the 105 kDa protein, in this study, low levels of a 130 and 80 kDa-M25 proteins were also detected at early stages of infection. The low abundance of the 130 kDa-M25 protein may originate from incoming virus particles since the 130 kDa-M25 protein species has been detected in purified virions [Wu et al., 1999, Kattenhorn et al., 2004]. The increase of the 130 kDa protein abundance at late stages of infection, after 18 hours, indicated that it is made from a mRNA that is synthesised with late kinetics. Indeed, the generation of a 130 kDa-M25 protein in wild type MCMV infected cells is prevented when the expression of late viral genes is blocked [Wu et al., 1999]. It is very likely that the 2.8 kb M25 mRNA detected in wild type MCMV infected cells at 6 hours and 24 hours after infection results in the synthesis

of the 105 kDa-M25 protein whereas translation of the 3.1 kb M25 mRNA identified at 24 hours after infection results in the 130 kDa protein.

The origin of the 80 kDa-M25 protein that was present in a low abundance at early stages of infection remains unclear. Protein expression from different M25 plasmids did not result in a 80 kDa-M25 species whereas the synthesis of the 105 and 130 kDa-M25 proteins was initiated at specific start codons. Thus, the 80 kDa-M25 protein is likely a degradation or cleavage product of the 130 or 105 kDa-M25 proteins.

### **Identification of the Translation Initiation Sites for the Synthesis of the 105 and 130 kDa-M25 Proteins**

Protein synthesis from different M25 constructs provided evidence that the 105 and 130 kDa-M25 proteins were synthesised starting from different ATGs and resulting in two distinct N-terminal domains.

Several proteins were shown to be expressed from the M25 gene and several potential translation initiation sites are present in frame within the M25 ORF. The 6th ATG within the M25 ORF is the potential translation initiation codon of the early 2.8 kb M25 transcript since it is the first ATG downstream of the 5'-end of the transcript. The 2nd ATG of the M25 ORF is the first start codon of the late 3.1 kb transcript where protein synthesis could possibly start. The predicted sizes of the proteins that would result from the various ATGs within the M25 ORF did not match with the size of any of the detected M25 proteins suggesting that the proteins were posttranslationally modified. Analysis of protein expression from successively shortened M25 ORF constructs revealed that translation initiated at the 6th ATG predominantly produced an approximately 105 kDa protein, and a 130 kDa protein is the major product when translation is initiated at the 2nd ATG. The 5th ATG that is proposed to be the translation initiation codon for M25 proteins [Dallas et al., 1994] was excluded, based on the results of the present study, since the protein produced from the 5th ATG did not match to any of the M25 proteins detected during infection. Translation initiation sites generating the 80 kDa protein could not be identified suggesting that this proteins did not originate from unique translation events.

Replacing the 2nd and 6th methionine with similar non-polar amino acids followed by the analysis of M25 protein expression would be an alternative method to show at which ATG the synthesis of the M25 protein variants starts. A second alternative would be to apply a translation assay coupled with a primer-extension assay as described [Kozak, 1997]. In this system, the M25 mRNA would be analysed using an in vitro translation system containing ribosomes and inhibitors to block elongation. The 80s ribosomal subunit would bind to the favoured physiological ATG. This ATG start site would then be identified using a primer extension inhibition assay in which a radiolabeled M25 specific primer would anneal to the

M25 mRNA downstream from all potential initiator codons and would be extended by reverse transcriptase up to the bound ribosome.

### **The 105 kDa-M25 Protein is a Potential Effector of Cell Rounding**

Comparing wild type MCMV-induced cell rounding to  $\Delta$ M25-induced cell rounding over the course of a complete MCMV replication cycle revealed that cell rounding is not induced in the absence of the M25 gene.

The onset of cell rounding was observed in cells infected with wild type MCMV at five hours after infection and completely round and tiny cells were present at 24 hours after infection. The finding that  $\Delta$ M25-infected cells did not round up during the course of a viral replication cycle suggested that MCMV-induced cell rounding is dependent on the M25 protein and no other viral protein substitutes for the M25 protein.

The presence of the 80, 105 and 130 kDa proteins in M25HA-virus infected cell lysates at five hours after infection made them potential candidates for the induction of cell rounding. Previous studies revealed that viral protein synthesis is required for virus-induced cell rounding [Furukawa et al., 1973, Hirai et al., 1977]. Cell rounding was inhibited in the presence of the protein synthesis inhibitor cycloheximide when added to cells one hour before or after infection with HCMV whereas the drug did not prevent cell rounding when added two hours after infection or later [Furukawa et al., 1973]. The fact that UV-light affects the ability of viral particles to induce cell rounding [Hirai et al., 1977] supports the hypothesis that a newly synthesised viral protein is required. UV-irradiation of infectious particles prevents the de-novo synthesis of viral proteins due to DNA damage of the viral DNA. The number of rounded cells and the presence of HCMV early antigens decreased after infection with UV-irradiated virus particles in a dose-dependent manner whereas the amount of nuclei-associated HCMV DNA was not affected [Hirai et al., 1977]. The 105 kDa-M25 protein fulfils the requirements of two criteria to be a candidate for the induction of cell rounding: First, its presence at five hours after infection correlates with the onset of cell rounding observed at the same time. Second, the 105 kDa protein is not present in MCMV virions, thus must be newly synthesised during infection.

### **Subcellular Localisation of M25 Proteins**

The finding that M25 proteins were localised in distinct cellular compartments at different stages during infection led to the speculation that the distinct N-terminal domains of the 105 and 130 kDa-M25 proteins determines their localisation and their function.

The M25 signal was followed in epithelial cells infected with a M25HA-tagged virus by immunofluorescence. M25 proteins were associated with the nucleus at early stages of infection

and accumulated outside, at one site of the nucleus, in the cytoplasm during late stages of infection. Additionally, at both early and late times after infection, a diffuse M25 signal was detected in the cytoplasm. Comparison of the data obtained from M25 immunofluorescence with those of M25 protein synthesis suggests that the signal observed at early stages of infection is due to the 105 kDa protein whereas the signal detected at late stages of infection could reflect the presence of both the 105 as well as the 130 kDa protein.

The work of others suggests that the 130 kDa-M25 protein is a tegument protein. At early stages of infection, the 105 kDa protein was detected exclusively in the nuclear fraction of MCMV-infected cells whereas the 130 kDa protein was the major protein in the cytoplasmic fraction and both proteins were present to some degree in both the nuclear and cytoplasmic fractions at late stages of infection [Wu et al., 1999]. In addition, the 130 kDa protein but not the 105 kDa protein was detected in purified virions by the same authors. Further, a M25-specific antibody labeled with gold particles localised to electron dense material in the nucleus and to individual virions and multicapsid structures in the cytoplasm. In the cytoplasmic virions, the immunogold particles localised to the viral tegument.

Further evidence for a 130 kDa-M25 tegument protein was provided since a monoclonal antibody raised against MCMV antigens reacted with a structural MCMV protein of 130 kDa size [Dallas et al., 1994]. Screening of a MCMV cDNA library with this monoclonal antibody identified a reactive clone. The insert of this clone exclusively hybridised to a fragment of the MCMV genome that was mapped to be the M25 ORF. Considering all these points, it is most likely that the 130 kDa structural protein detected by the monoclonal antibody is a component of the viral tegument. Many tegument proteins are phosphorylated. Consistent with this, the M25 protein sequence contains several serines, threonines and tyrosine throughout the sequence that were predicted to be phosphorylated.

The tegumentation of virus capsids is thought to take place at the Trans-Golgi-Network (TGN) by budding into transport vesicles constricted from the TGN-cisternae [Eickmann et al., 2006]. The cytoplasmic staining of M25, observed at late stages of infection resembles the localisation of at least three other known HCMV tegument proteins, pp150, pUL24 and pUL43 during the late phase of infection [Sanchez et al., 2000, Adair et al., 2002].

Co-localisation studies using markers for Golgi and tegument proteins in addition to the detection of M25 would reveal whether the M25 staining observed in this study at late stages of infection reflects the tegumentation of viral capsids.

The 105 kDa-M25 protein is possibly a nuclear protein. The size of the 105 kDa protein indicates that it must have been actively transported into the nucleus. Only proteins smaller than 60 kDa can diffuse through the nuclear pore [Nigg, 1997]. This implies the presence of a nuclear localisation signal (NLS) that is required for the nuclear import by cargo proteins. A NLS with similarity to the NLS of the SV40 large T antigen was predicted within the M25

protein indicating the possibility of active nuclear import. However, the function of this signal has yet to be experimentally verified. A passive translocation to the nucleus by interaction of M25 with cytoplasmic proteins that actively translocate to the nucleus is also possible. Further studies on the localisation of the M25 protein variants synthesised from the M25 plasmids, especially the 105 and 130 kDa proteins, would help to understand whether additional viral proteins are required or cellular proteins are sufficient to translocate the M25 proteins to the nucleus.

The unique 89 amino acids present at the N-terminus of the 130 kDa protein that are missing in the 105 kDa protein could influence the properties of the protein. An accumulated sequence of threonines and serines within this N-terminal segment is predicted to be phosphorylated, and thus could have an impact on the localisation and the function of the 130 kDa M25 protein. The additional N-terminal amino acids could also alter the secondary structure of the protein possibly exposing interaction domains not present in the 105 kDa M25 protein. For instance, one of the two predicted M25 homologs in HCMV, the ORF UL35, encodes two proteins that are synthesised from two different transcripts. The N-terminus of the 22 and 75 kDa UL35 proteins has been suggested to determine their localisation and function [Liu and Biegalke, 2002]. The 22 kDa protein is localised in the nucleus and inhibits activation of the MIEP, whereas the 75 kDa protein is localised exclusively in the cytoplasm, is packaged in virions and is important for particle formation [Liu and Biegalke, 2002, Schierling et al., 2005].

The analysis of morphological changes induced by the M25ATG2 or M25ATG6 proteins, in fibroblasts will help to identify whether the 130 kDa or the 105 kDa M25 protein is crucial for the induction of cell rounding, possibly determined by their N-termini.

## **M25-induced Cell Rounding Outside the Context of the Viral Genome**

Having shown that M25 is able to induce morphological changes during MCMV infection it was considered possible that M25 could also induce cell rounding without the help of additional viral proteins.

Indeed, M25 protein expression was sufficient to induce morphological changes in transfected cells. The GFP-expression from the bicistronic M25 transcript made it easy to identify transfected cells and allowed the characterisation of their cellular morphology. The transfection of two vectors expressing N- or C-terminally HA-tagged M25 variants yielded in each case about two times more rounded cells than transfection of the empty vector concluding that a direct interaction between the M25 protein and cellular factors without additional viral proteins is sufficient to induce cell rounding. The presence of round cells after transfection of the empty vector is possibly related to stress-induced rounding due to the transfection proce-

dure. Rounded cells were also observed when other transfection reagents were tested. The cloning of M25 into a retrovirus vector and the infection of cells with these M25-expressing retroviruses would be an alternative method to the transfection approach that could possibly reduce the background of rounded cells.

## M25 Homologs in HCMV

Based on the sequence conservation of the C-terminal domain between the MCMV M25 protein and the HCMV UL25 and UL35 proteins, it was speculated whether these proteins may also share functional homology.

The UL25 and UL35 are the only members of the HCMV UL25 gene family [Chee et al., 1990]. Similar to the proteins expressed from the MCMV M25 ORF, several proteins are expressed from the HCMV UL25 and UL35 ORFs that localise to the nucleus or are detected in the cytoplasm of infected cells and individual UL25 and UL35 proteins have been identified in purified virions [Baldick and Shenk, 1996, Battista et al., 1999, Zini et al., 1999, Liu and Biegalka, 2002, Schierling et al., 2005].

No differences in cellular morphology between fibroblasts infected with a UL35 deletion virus and wild type HCMV have been described suggesting that the UL35 protein is functionally distinct from the M25 protein [Schierling et al., 2005]. The infection of fibroblasts with a HCMV  $\Delta$ UL25 virus resulted in cell rounding similar to cell infected with wild type HCMV suggesting that the M25 protein is not a functional equivalent to the UL25 protein (personal communication, Corinna Benkartek).

During evolution of MCMV and HCMV, functional domains might have been lost and/or new functional domains were gained. Herpesviruses may have captured a number of their genes from the cellular genome repertoire during co-evolution with their host [Shackelton and Holmes, 2004]. Other viral genes are likely to have been passed vertically from viral ancestors. If conserved domains, important for the function of a gene, are lacking after the transfer, these genes may no longer retain their original function but might instead obtain new functions. This happened to be the case for the HCMV UL72 protein that represents the ortholog of a cellular dUTPase [Davison and Stow, 2005]. Due to the loss of conserved motifs this protein lacks dUTPase activity. As members of the UL25 family, the M25, UL25 and UL35 proteins could have a common origin in a viral ancestor or in the genome of a cellular host but have obtained distinct functions during evolution of the viruses. This might explain why cell rounding is (still) induced by the MCMV M25 gene products but not by the HCMV UL25 or UL35 proteins.

Perhaps M25 is unique to MCMV and provides a specialised function for the induction of cell rounding in MCMV whereas in HCMV other factors may account for the same function.



## Possible Mechanisms of M25-induced Cell Rounding

Combining the obtained data from the present study and the published data about M25, several scenarios are plausible to explain the M25-mediated cell rounding. The role of M25 in two scenarios, that are described in the following, will be investigated in future experiments.

The M25 proteins may directly influence the regulation of the cytoskeleton. Exploiting the GFP-expressing viruses and visualising actin filaments during infection led to the observation that the absence of the M25 gene affects cellular morphology during infection. Three types of cytoskeletal filaments, actin filaments, microtubules and intermediate filaments, determine the spatial organisation and the structural framework of a cell. Factors that regulate the dynamics of these cytoskeletal filaments represent putative M25 interaction partners. Cdc42, Rho and Rac, members of the Rho GTPase family, are key regulators of the actin cytoskeleton and determine the formation of cellular protrusions, e.g. filopodia and lamellipodia [Hall, 1998, Mattila and Lappalainen, 2008].

Several members of the herpesviruses have been shown to directly or indirectly interact with Rho GTPases. The expression of Rac1 and Cdc42 mutants did not influence binding, internalisation and transport of HSV-1 particles but affected infectivity [Hoppe et al., 2006]. Activation of Rho GTPases during HHV-8 entry results in a reorganisation of the actin cytoskeleton [Sharma-Walia et al., 2004]. The activity of Rho GTPases is stimulated by integrin engagement [DeMali et al., 2003]. RhoA protein levels decrease during HCMV infection, possibly through integrin-mediated signalling [Wang et al., 2005] and integrins have been identified as HCMV entry receptors mediating HCMV internalisation [Feire et al., 2004]. Cell rounding is also induced via Rho GTPases by other pathogens that infect epithelial cells. Glycosylation of Rho proteins by *Clostridium difficile* Toxin A and Toxin B causes actin re-organisation resulting in rounded epithelial cells and fibroblasts [Gerhard et al., 2008, Halabi-Cabazon et al., 2008].

In the present study, filopodia and lamellipodia have been observed in fibroblasts infected with the  $\Delta$ M25 virus whereas wild type infected cells did not exhibit protrusions but in contrast altered their morphology towards a rounded cell shape. This points to a potential, direct or indirect M25-mediated effect on the Rho GTPase proteins. M25 proteins might induce cell rounding by affecting the activity of these Rho GTPases. Stimulation of these Rho GTPases upon infection may in turn stimulate downstream effectors that are involved in effecting changes in the actin cytoskeleton. Altered protein levels have been detected, among others, of the actin regulators Connexin-43, Paxillin and the protein Eg5 upon HCMV infection [Stanton et al., 2007]. It cannot be ruled out that, besides actin filaments, the breakdown of microtubules or intermediate filaments caused the cell rounding in CMV-infection. Investigation of the MCMV-induced CPE and the  $\Delta$ M25-induced CPE after treatment with inhibitors of actin polymerisation or with microtubule disrupting agents will help to identify the cytoskeletal filaments involved. Pull-down assays from cells expressing Rho GTPases using

M25 as the bait or MCMV infection of cells expressing dominant-negative Rho GTPases would help to understand the mechanism of M25-induced changes in cellular morphology.

In the second scenario, M25 proteins may indirectly induce cell rounding by interacting with cellular factors that control the host cell cycle. The cell cycle is a complex and controlled process that prepares a cell for its division during the mitotic phase. A hallmark of mitosis is cell rounding. The molecular mechanisms of the morphological changes during mitosis are not fully understood.

HCMV and MCMV can infect cells throughout the cell cycle [Salvant et al., 1998, Wiebusch et al., 2008]. HCMV stimulates cellular proliferative pathways by activating synthesis-phase promoting pathways and mitosis-phase promoting complexes [Salvant et al., 1998, Sanchez et al., 2003 Dec]. Increased protein levels of a key regulatory factor, cyclin E, have been measured during HCMV infection [Salvant et al., 1998]. Cyclin E is expressed in the G1 phase of the cell cycle and associates with cyclin-dependent kinase 2. This complex is required for the progression into the S-phase. The effect of HCMV on cyclin E is at the transcriptional level by upregulating cyclin E mRNA [Salvant et al., 1998]. Both, HCMV or MCMV infection inhibits cellular DNA synthesis resulting in a deregulated cell cycle in infected cells [Bresnahan et al., 1996, Petrik et al., 2006, Wiebusch et al., 2008]. Although cellular DNA synthesis is inhibited, other features of the S-phase such as an active nucleotide metabolism and the expression of replication factors are induced to ensure proper viral replication. It is conceivable that the cell cycle is further stimulated towards the mitotic phase. Notably, pseudo-mitotic cells have been reported in HCMV-infected cells [Hertel et al., 2007]. In this regard, MCMV-induced cell rounding might be the result of the interaction of M25 proteins with cell cycle regulators.

Further experiments are required to investigate whether MCMV wild type infected cells resemble mitotic cells.

### **Possible Contribution of Cell Rounding to Viral Dissemination**

Cytomegaloviruses manipulate target cells in various ways in order to disseminate efficiently. These include virus-encoded chemokines that recruit leukocytes to sites of infection, the suppression of cell death and the interferon response, as well as the subversion of host immune responses. The induction of cell rounding may also contribute to viral dissemination within the host.

The observation that plaque formation was not only present in a fibroblast cell line but also in primary mouse embryonic fibroblasts suggested that cell rounding is not only an *in vitro* effect but is probably also present *in vivo*. Notably, cell rounding and plaque formation was also induced in epithelial cells indicating that virus-induced cell rounding is not restricted to fibroblasts. In fact, circulating HCMV-infected endothelial cells have been found in the

peripheral blood of immunosuppressed patients with lytic HCMV infection and have been associated with CMV dissemination [Percivalle et al., 1993, Gerna et al., 1998, Salzberger et al., 1997]. Thus, endothelial cells might round up upon CMV infection and move from the vascular endothelium into the blood stream. These infected cells, circulating in the blood stream, may provide a means for dissemination of the virus.

Bentz et al. report of an actin stress fibre breakdown in HCMV-infected endothelial cells [Bentz et al., 2006]. The induction of these cytoskeletal alterations together with the degradation of lateral junction proteins in HCMV-infected endothelial cells, described by the same group, is suggested to increase the permeability of the endothelium upon infection with HCMV. HCMV is further shown to increase the permeability of the endothelium which in turn increased the number of naïve monocytes that migrated through the infected endothelial cell layer [Bentz et al., 2006]. A small percentage of these monocytes becomes infected during their trans-endothelial passage. In an in vivo scenario these infected monocytes would migrate into the surrounding tissue and disseminate the virus. These data imply that HCMV-induced morphological changes of the endothelium play a role in dissemination of the virus.



## Bibliography

- R. Adair, E. R. Douglas, J. B. Maclean, S. Y. Graham, J. D. Aitken, F. E. Jamieson, and D. J. Dargan. The products of human cytomegalovirus genes UL23, UL24, UL43 and US22 are tegument components. *J Gen Virol*, 83(Pt 6):1315–1324, 2002.
- K. Aktories and J. T. Barbieri. Bacterial cytotoxins: targeting eukaryotic switches. *Nat Rev Microbiol*, 3(5):397–410, 2005.
- B. Alberts, A. Johnson, J. Lewis, M. Raff, K. Roberts, and P. Walter. Cell Junctions, Cell Adhesion, and the Extracellular Matrix. In *Molecular Biology of the Cell*, chapter 19. Garland Science, 4th edition, 2002.
- T. Albrecht, T. Cavallo, N. L. Cole, and K. Graves. Cytomegalovirus: development and progression of cytopathic effects in human cell culture. *Lab Invest*, 42(1):1–7, 1980.
- T. Albrecht, D. J. Speelman, and O. S. Steinsland. Similarities between cytomegalovirus-induced cell rounding and contraction of smooth muscle cells. *Life Sci*, 32(19):2273–2278, 1983.
- S. F. Altschul, W. Gish, W. Miller, E. W. Myers, and D. J. Lipman. Basic local alignment search tool. *J Mol Biol*, 215(3):403–410, 1990.
- D. G. Anders, J. A. Kerry, and G. S. Pari. CMV DNA synthesis and late viral gene expression. In E. S. Mocarski, editor, *Human Herpesviruses: Biology, Therapy and Immunoprophylaxis*, chapter 19, pages 295–310. Cambridge University Press, 2007.
- A. Angulo, P. Ghazal, and M. Messerle. The major immediate-early gene ie3 of mouse cytomegalovirus is essential for viral growth. *J Virol*, 74(23):11129–11136, 2000.
- C. J. J. Baldick and T. Shenk. Proteins associated with purified human cytomegalovirus particles. *J Virol*, 70(9):6097–6105, 1996.
- J. F. J. Bale and M. E. O’Neil. Detection of murine cytomegalovirus DNA in circulating leukocytes harvested during acute infection of mice. *J Virol*, 63(6):2667–2673, 1989.
- M. Baltesen, M. Messerle, and M. J. Reddehase. Lungs are a major organ site of cytomegalovirus latency and recurrence. *J Virol*, 67(9):5360–5366, 1993.

- M. C. Battista, G. Bergamini, M. C. Boccuni, F. Campanini, A. Ripalti, and M. P. Landini. Expression and characterization of a novel structural protein of human cytomegalovirus, pUL25. *J Virol*, 73(5):3800–3809, 1999.
- G. L. Bentz, M. Jarquin-Pardo, G. Chan, M. S. Smith, C. Sinzger, and A. D. Yurochko. Human cytomegalovirus HCMV infection of endothelial cells promotes naive monocyte extravasation and transfer of productive virus to enhance hematogenous dissemination of HCMV. *J Virol*, 80(23):11539–11555, 2006.
- N. Blom, S. Gammeltoft, and S. Brunak. Sequence and structure-based prediction of eukaryotic protein phosphorylation sites. *J Mol Biol*, 294(5):1351–1362, 1999.
- E.-M. Borst and M. Messerle. Analysis of human cytomegalovirus oriLyt sequence requirements in the context of the viral genome. *J Virol*, 79(6):3615–3626, 2005.
- E. M. Borst, S. Mathys, M. Wagner, W. Muranyi, and M. Messerle. Genetic evidence of an essential role for cytomegalovirus small capsid protein in viral growth. *J Virol*, 75(3):1450–1458, 2001.
- E. M. Borst, C. Benkartek, and M. Messerle. Use of bacterial artificial chromosomes in generating targeted mutations in human and mouse cytomegaloviruses. *Curr Protoc Immunol*, Chapter 10:Unit 10.32, 2007.
- E. M. Borst, K. Wagner, A. Binz, B. Sodeik, and M. Messerle. The essential human cytomegalovirus gene UL52 is required for cleavage-packaging of the viral genome. *J Virol*, 82(5):2065–2078, 2008.
- W. A. Bresnahan, I. Boldogh, E. A. Thompson, and T. Albrecht. Human cytomegalovirus inhibits cellular DNA synthesis and arrests productively infected cells in late G1. *Virology*, 224(1):150–160, 1996.
- W. Britt. Manifestations of human cytomegalovirus infection: proposed mechanisms of acute and chronic disease. *Curr Top Microbiol Immunol*, 325:417–470, 2008.
- W. J. Britt. Cytomegalovirus. In B. N. Fields, D. M. Knipe, and P. M. Howley, editors, *Fields Virology*, volume 2, chapter 77, pages 2493–2523. Lippincott Williams & Wilkins, 3rd edition, 1996.
- W. J. Britt. CMV maturation and egress. In E. S. Mocarski, editor, *Human Herpesviruses: Biology, Therapy and Immunoprophylaxis*, chapter 20, pages 311–323. Cambridge University Press, 2007.

- L. Brocchieri, T. N. Kledal, S. Karlin, and E. S. Mocarski. Predicting coding potential from genome sequence: application to betaherpesviruses infecting rats and mice. *J Virol*, 79(12): 7570–7596, 2005.
- J. M. Brown, H. Kaneshima, and E. S. Mocarski. Dramatic interstrain differences in the replication of human cytomegalovirus in SCID-hu mice. *J Infect Dis*, 171(6):1599–1603, 1995.
- W. Brune, H. Hengel, and U. H. Koszinowski. A mouse model for cytomegalovirus infection. *Curr Protoc Immunol*, Chapter 19:Unit 19.7.1–19.7.13, 1999.
- W. Brune, C. Menard, J. Heesemann, and U. H. Koszinowski. A ribonucleotide reductase homolog of cytomegalovirus and endothelial cell tropism. *Science*, 291(5502):303–305, 2001.
- W. Brune, M. Wagner, and M. Messerle. Manipulating Cytomegalovirus Genomes by BAC Mutagenesis: Strategies and Applications. In M. J. Reddehase, editor, *Cytomegaloviruses*, chapter 4, pages 63–89. Caister Academic Press, 2006.
- I. Bubic, M. Wagner, A. Krmpotic, T. Saulig, S. Kim, W. M. Yokoyama, S. Jonjic, and U. H. Koszinowski. Gain of virulence caused by loss of a gene in murine cytomegalovirus. *J Virol*, 78(14):7536–7544, 2004.
- A. H. Buck, J. Santoyo-Lopez, K. A. Robertson, D. S. Kumar, M. Reczko, and P. Ghazal. Discrete clusters of virus-encoded micrnas are associated with complementary strands of the genome and the 7.2-kilobase stable intron in murine cytomegalovirus. *J Virol*, 81(24): 13761–13770, 2007.
- B. Bühler, G. M. Keil, F. Weiland, and U. H. Koszinowski. Characterization of the murine cytomegalovirus early transcription unit e1 that is induced by immediate-early proteins. *J Virol*, 64(5):1907–1919, 1990.
- S. J. Butcher, J. Aitken, J. Mitchell, B. Gowen, and D. J. Dargan. Structure of the human cytomegalovirus B capsid by electron cryomicroscopy and image reconstruction. *J Struct Biol*, 124(1):70–76, 1998.
- J. Chambers, A. Angulo, D. Amaratunga, H. Guo, Y. Jiang, J. S. Wan, A. Bittner, K. Frueh, M. R. Jackson, P. A. Peterson, M. G. Erlander, and P. Ghazal. DNA microarrays of the complex human cytomegalovirus genome: profiling kinetic class with drug sensitivity of viral gene expression. *J Virol*, 73(7):5757–5766, 1999.

- W. L. W. Chang and P. A. Barry. Cloning of the full-length rhesus cytomegalovirus genome as an infectious and self-excisable bacterial artificial chromosome for analysis of viral pathogenesis. *J Virol*, 77(9):5073–5083, 2003.
- T. L. Chapman and P. J. Bjorkman. Characterization of a murine cytomegalovirus class I major histocompatibility complex (MHC) homolog: comparison to MHC molecules and to the human cytomegalovirus MHC homolog. *J Virol*, 72(1):460–466, 1998.
- M. S. Chee, A. T. Bankier, S. Beck, R. Bohni, C. M. Brown, R. Cerny, T. Horsnell, C. A. r. Hutchison, T. Kouzarides, and J. A. Martignetti. Analysis of the protein-coding content of the sequence of human cytomegalovirus strain AD169. *Curr Top Microbiol Immunol*, 154:125–169, 1990.
- D. H. Chen, H. Jiang, M. Lee, F. Liu, and Z. H. Zhou. Three-dimensional visualization of tegument/capsid interactions in the intact human cytomegalovirus. *Virology*, 260(1):10–16, 1999.
- P. P. Cherepanov and W. Wackernagel. Gene disruption in *Escherichia coli*: TcR and KmR cassettes with the option of Flp-catalyzed excision of the antibiotic-resistance determinant. *Gene*, 158(1):9–14, 1995.
- L. Cicin-Sain, Z. Ruzsics, J. Podlech, I. Bubic, C. Menard, S. Jonjic, M. J. Reddehase, and U. H. Koszinowski. Dominant-negative FADD rescues the *in vivo* fitness of a cytomegalovirus lacking an antiapoptotic viral gene. *J Virol*, 82(5):2056–2064, 2008.
- G. M. Ciocco-Schmitt, Z. Karabekian, E. W. Godfrey, R. M. Stenberg, A. E. Campbell, and J. A. Kerry. Identification and characterization of novel murine cytomegalovirus M112-113 (e1) gene products. *Virology*, 294(1):199–208, 2002.
- T. M. Collins, M. R. Quirk, and M. C. Jordan. Biphasic viremia and viral gene expression in leukocytes during acute cytomegalovirus infection of mice. *J Virol*, 68(10):6305–6311, 1994.
- T. Compton, D. M. Nowlin, and N. R. Cooper. Initiation of human cytomegalovirus infection requires initial interaction with cell surface heparan sulfate. *Virology*, 193(2):834–841, 1993.
- P. B. Dallas, P. A. Lyons, J. B. Hudson, A. A. Scalzo, and G. R. Shellam. Identification and characterization of a murine cytomegalovirus gene with homology to the UL25 open reading frame of human cytomegalovirus. *Virology*, 200(2):643–650, 1994.
- K. A. Datsenko and B. L. Wanner. One-step inactivation of chromosomal genes in *Escherichia coli* K-12 using PCR products. *Proc Natl Acad Sci U S A*, 97(12):6640–6645, 2000.



- N. J. Davis-Poynter, D. M. Lynch, H. Vally, G. R. Shellam, W. D. Rawlinson, B. G. Barrell, and H. E. Farrell. Identification and characterization of a G protein-coupled receptor homolog encoded by murine cytomegalovirus. *J Virol*, 71(2):1521–1529, 1997.
- A. J. Davison and D. Bhella. Comparative genome and virion structure. In E. S. Mocarski, editor, *Human Herpesviruses*, chapter 14, pages 177–204. Cambridge University Press, 2007.
- A. J. Davison and N. D. Stow. New genes from old: redeployment of dUTPase by herpesviruses. *J Virol*, 79(20):12880–12892, 2005.
- K. A. DeMali, K. Wennerberg, and K. Burridge. Integrin signaling to the actin cytoskeleton. *Curr Opin Cell Biol*, 15(5):572–582, 2003.
- L. Dölken, J. Perot, V. Cognat, A. Alioua, M. John, J. Soutschek, Z. Ruzsics, U. Koszinowski, O. Voinnet, and S. Pfeffer. Mouse cytomegalovirus microRNAs dominate the cellular small RNA profile during lytic infection and show features of posttranscriptional regulation. *J Virol*, 81(24):13771–13782, 2007.
- W. Dunn, C. Chou, H. Li, R. Hai, D. Patterson, V. Stolc, H. Zhu, and F. Liu. Functional profiling of a human cytomegalovirus genome. *Proc Natl Acad Sci U S A*, 100(24):14223–14228, 2003.
- M. Dworsky, M. Yow, S. Stagno, R. F. Pass, and C. Alford. Cytomegalovirus infection of breast milk and transmission in infancy. *Pediatrics*, 72(3):295–299, 1983.
- M. E. Ehsani, T. W. Abraha, C. Netherland-Snell, N. Mueller, M. M. Taylor, and B. Holwerda. Generation of mutant murine cytomegalovirus strains from overlapping cosmid and plasmid clones. *J Virol*, 74(19):8972–8979, 2000.
- M. Eickmann, D. Gicklhorn, and K. Radsak. Glycoprotein Trafficking in Virion Morphogenesis. In M. J. Reddehase, editor, *Cytomegaloviruses*, chapter 13, pages 245–264. Caister Academic Press, 2006.
- S. Etienne-Manneville and A. Hall. Rho GTPases in cell biology. *Nature*, 420(6916):629–635, 2002.
- P. J. Fannin Rider, W. Dunn, and F. Liu. Human cytomegalovirus micrornas. In T. Shenk and M. F. Stinski, editors, *Human Cytomegalovirus*. Current Topics in Microbiology and Immunology, 2008.
- H. E. Farrell and G. R. Shellam. Characterization of neutralizing monoclonal antibodies to murine cytomegalovirus. *J Gen Virol*, 71 ( Pt 3):655–664, 1990.

- A. L. Feire, H. Koss, and T. Compton. Cellular integrins function as entry receptors for human cytomegalovirus via a highly conserved disintegrin-like domain. *Proc Natl Acad Sci U S A*, 101(43):15470–15475, 2004.
- A. Fioretti, T. Furukawa, D. Santoli, and S. A. Plotkin. Nonproductive infection of guinea pig cells with human cytomegalovirus. *J Virol*, 11(6):998–1003, 1973.
- P. Fleming, N. Davis-Poynter, M. Degli-Esposti, E. Densley, J. Papadimitriou, G. Shellam, and H. Farrell. The murine cytomegalovirus chemokine homolog, m131/129, is a determinant of viral pathogenicity. *J Virol*, 73(8):6800–6809, 1999.
- T. Furukawa, A. Fioretti, and S. Plotkin. Growth characteristics of cytomegalovirus in human fibroblasts with demonstration of protein synthesis early in viral replication. *J Virol*, 11(6):991–997, 1973.
- R. Gerhard, S. Nottrott, J. Schoentaube, H. Tatge, A. Olling, and I. Just. Glucosylation of rho GTPases by *Clostridium difficile* toxin A triggers apoptosis in intestinal epithelial cells. *J Med Microbiol*, 57(Pt 6):765–770, 2008.
- G. Gerna, D. Zipeto, E. Percivalle, M. Parea, M. G. Revello, R. Maccario, G. Peri, and G. Milanesi. Human cytomegalovirus infection of the major leukocyte subpopulations and evidence for initial viral replication in polymorphonuclear leukocytes from viremic patients. *J Infect Dis*, 166(6):1236–1244, 1992.
- G. Gerna, M. Zavattoni, F. Baldanti, M. Furione, L. Chezzi, M. G. Revello, and E. Percivalle. Circulating cytomegalic endothelial cells are associated with high human cytomegalovirus (HCMV) load in AIDS patients with late-stage disseminated HCMV disease. *J Med Virol*, 55(1):64–74, 1998.
- W. Gibson. Assembly and Maturation of the Capsid. In M. J. Reddehase, editor, *Cytomegaloviruses*, chapter 12, pages 231–243. Caister Academic Press, 2006.
- V. S. Goldmacher. Cell death suppression by cytomegaloviruses. *Apoptosis*, 10(2):251–265, 2005.
- V. S. Goldmacher, L. M. Bartle, A. Skaletskaya, C. A. Dionne, N. L. Kedersha, C. A. Vater, J. W. Han, R. J. Lutz, S. Watanabe, E. D. Cahir McFarland, E. D. Kieff, E. S. Mocarski, and T. Chittenden. A cytomegalovirus-encoded mitochondria-localized inhibitor of apoptosis structurally unrelated to Bcl-2. *Proc Natl Acad Sci U S A*, 96(22):12536–12541, 1999.
- F. D. Goodrum, C. T. Jordan, K. High, and T. Shenk. Human cytomegalovirus gene expression during infection of primary hematopoietic progenitor cells: a model for latency. *Proc Natl Acad Sci U S A*, 99(25):16255–16260, 2002.

- G. Hahn, M. G. Revello, M. Patrone, E. Percivalle, G. Campanini, A. Sarasini, M. Wagner, A. Gallina, G. Milanese, U. Koszinowski, F. Baldanti, and G. Gerna. Human cytomegalovirus UL131-128 genes are indispensable for virus growth in endothelial cells and virus transfer to leukocytes. *J Virol*, 78(18):10023–10033, 2004.
- I. Halabi-Cabezón, J. Huelsenbeck, M. May, M. Ladwein, K. Rottner, I. Just, and H. Genth. Prevention of the cytopathic effect induced by Clostridium difficile Toxin B by active Rac1. *FEBS Lett*, 582(27):3751–3756, 2008.
- A. Hall. Rho GTPases and the actin cytoskeleton. *Science*, 279(5350):509–514, 1998.
- M. Hasan, A. Krmpotic, Z. Ruzsics, I. Bubic, T. Lenac, A. Halenius, A. Loewendorf, M. Messerle, H. Hengel, S. Jonjic, and U. H. Koszinowski. Selective down-regulation of the NKG2D ligand H60 by mouse cytomegalovirus m155 glycoprotein. *J Virol*, 79(5):2920–2930, 2005.
- L. Hertel, S. Chou, and E. S. Mocarski. Viral and cell cycle-regulated kinases in cytomegalovirus-induced pseudomitosis and replication. *PLoS Pathog*, 3(1):e6, 2007.
- K. Hirai, M. Fumiko, and Y. Watanabe. Expression of Early Virus Functions in Human Cytomegalovirus Infected HEL Cells: Effect of Ultraviolet Light-Irradiation of the Virus. *J Gen Virol*, 38:121–133, 1977.
- R. Holtappels, V. Bohm, J. Podlech, and M. J. Reddehase. CD8 T-cell-based immunotherapy of cytomegalovirus infection: "proof of concept" provided by the murine model. *Med Microbiol Immunol*, 197(2):125–134, 2008.
- M. Homman-Loudiyi, K. Hultenby, W. Britt, and C. Soderberg-Naucler. Envelopment of human cytomegalovirus occurs by budding into Golgi-derived vacuole compartments positive for gB, Rab 3, trans-golgi network 46, and mannosidase II. *J Virol*, 77(5):3191–3203, 2003.
- R. W. Honess and B. Roizman. Regulation of herpesvirus macromolecular synthesis. I. Cascade regulation of the synthesis of three groups of viral proteins. *J Virol*, 14(1):8–19, 1974.
- S. Hoppe, M. Schelhaas, V. Jaeger, T. Liebig, P. Petermann, and D. Knebel-Morsdorf. Early herpes simplex virus type 1 infection is dependent on regulated Rac1/Cdc42 signalling in epithelial MDCKII cells. *J Gen Virol*, 87(Pt 12):3483–3494, 2006.
- S. Ihara, K. Hirai, and Y. Watanabe. Temperature-sensitive mutants of human cytomegalovirus: isolation and partial characterization of DNA-minus mutants. *Virology*, 84(1):218–221, 1978.

- S. Ihara, S. Saito, and Y. Watanabe. Suppression of fibronectin synthesis by an early function(s) of human cytomegalovirus. *J Gen Virol*, 59:409–413, 1982.
- S. Ihara, M. Takekoshi, N. Mori, S. Sakuma, J. Hashimoto, and Y. Watanabe. Identification of mutation sites of a temperature-sensitive mutant of HCMV DNA polymerase activity. *Arch Virol*, 137(3-4):263–275, 1994.
- A. Irmiere and W. Gibson. Isolation and characterization of a noninfectious virion-like particle released from cells infected with human strains of cytomegalovirus. *Virology*, 130(1):118–133, 1983.
- A. C. Iskenderian, L. Huang, A. Reilly, R. M. Stenberg, and D. G. Anders. Four of eleven loci required for transient complementation of human cytomegalovirus DNA replication cooperate to activate expression of replication genes. *J Virol*, 70(1):383–392, 1996.
- G. Jahn, B. C. Scholl, B. Traupe, and B. Fleckenstein. The two major structural phosphoproteins (pp65 and pp150) of human cytomegalovirus and their antigenic properties. *J Gen Virol*, 68 ( Pt 5):1327–1337, 1987.
- N. L. Jones, J. C. Lewis, and B. A. Kilpatrick. Cytoskeletal disruption during human cytomegalovirus infection of human lung fibroblasts. *Eur J Cell Biol*, 41(2):304–312, 1986.
- S. Jonjic, W. Mutter, F. Weiland, M. J. Reddehase, and U. H. Koszinowski. Site-restricted persistent cytomegalovirus infection after selective long-term depletion of CD4<sup>+</sup> T lymphocytes. *J Exp Med*, 169(4):1199–1212, 1989.
- I. Jurak and W. Brune. Induction of apoptosis limits cytomegalovirus cross-species infection. *EMBO J*, 25(11):2634–2642, 2006.
- L. M. Kattenhorn, R. Mills, M. Wagner, A. Lomsadze, V. Makeev, M. Borodovsky, H. L. Ploegh, and B. M. Kessler. Identification of proteins associated with murine cytomegalovirus virions. *J Virol*, 78(20):11187–11197, 2004.
- G. M. Keil, A. Ebeling-Keil, and U. H. Koszinowski. Temporal regulation of murine cytomegalovirus transcription and mapping of viral RNA synthesized at immediate early times after infection. *J Virol*, 50(3):784–795, 1984.
- G. Kemble, G. Duke, R. Winter, and R. Spaete. Defined large-scale alterations of the human cytomegalovirus genome constructed by cotransfection of overlapping cosmids. *J Virol*, 70(3):2044–2048, 1996.
- K. S. Kim and R. I. Carp. Growth of murine cytomegalovirus in various cell lines. *J Virol*, 7(6):720–725, 1971.

- 
- V. N. Kim. MicroRNA biogenesis: coordinated cropping and dicing. *Nat Rev Mol Cell Biol*, 6 (5):376–385, 2005.
- M. Kozak. How do eucaryotic ribosomes select initiation regions in messenger RNA? *Cell*, 15 (4):1109–1123, 1978.
- M. Kozak. An analysis of 5'-noncoding sequences from 699 vertebrate messenger RNAs. *Nucleic Acids Res*, 15(20):8125–8148, 1987.
- M. Kozak. An analysis of vertebrate mRNA sequences: intimations of translational control. *J Cell Biol*, 115(4):887–903, 1991.
- M. Kozak. Recognition of AUG and alternative initiator codons is augmented by G in position +4 but is not generally affected by the nucleotides in positions +5 and +6. *EMBO J*, 16 (9):2482–2492, 1997.
- M. Kozak. Initiation of translation in prokaryotes and eukaryotes. *Gene*, 234(2):187–208, 1999.
- M. Kozak. Pushing the limits of the scanning mechanism for initiation of translation. *Gene*, 299(1-2):1–34, 2002.
- C. A. Kulesza and T. Shenk. Human cytomegalovirus 5-kilobase immediate-early RNA is a stable intron. *J Virol*, 78(23):13182–13189, 2004.
- C. A. Kulesza and T. Shenk. Murine cytomegalovirus encodes a stable intron that facilitates persistent replication in the mouse. *Proc Natl Acad Sci U S A*, 103(48):18302–18307, 2006.
- R. L. Lafemina and G. S. Hayward. Differences in cell-type-specific blocks to immediate early gene expression and DNA replication of human, simian and murine cytomegalovirus. *J Gen Virol*, 69 ( Pt 2):355–374, 1988.
- L. A. Lagenaur, W. C. Manning, J. Vieira, C. L. Martens, and E. S. Mocarski. Structure and function of the murine cytomegalovirus sgg1 gene: a determinant of viral growth in salivary gland acinar cells. *J Virol*, 68(12):7717–7727, 1994.
- D. Lembo, M. Donalizio, A. Hofer, M. Cornaglia, W. Brune, U. Koszinowski, L. Thelander, and S. Landolfo. The ribonucleotide reductase R1 homolog of murine cytomegalovirus is not a functional enzyme subunit but is required for pathogenesis. *J Virol*, 78(8):4278–4288, 2004.
- A. E. Lilja, W. L. W. Chang, P. A. Barry, S. P. Becerra, and T. E. Shenk. Functional genetic analysis of rhesus cytomegalovirus: Rh01 is an epithelial cell tropism factor. *J Virol*, 82(5): 2170–2181, 2008.

- B. Liu and M. F. Stinski. Human cytomegalovirus contains a tegument protein that enhances transcription from promoters with upstream ATF and AP-1 cis-acting elements. *J Virol*, 66(7):4434–4444, 1992.
- Y. Liu and B. J. Biegalke. The human cytomegalovirus UL35 gene encodes two proteins with different functions. *J Virol*, 76(5):2460–2468, 2002.
- K. M. Lockridge, G. Sequer, S. S. Zhou, Y. Yue, C. P. Mandell, and P. A. Barry. Pathogenesis of experimental rhesus cytomegalovirus infection. *J Virol*, 73(11):9576–9583, 1999.
- A. Loewendorf, C. Kruger, E. M. Borst, M. Wagner, U. Just, and M. Messerle. Identification of a mouse cytomegalovirus gene selectively targeting CD86 expression on antigen-presenting cells. *J Virol*, 78(23):13062–13071, 2004.
- C. Mack, A. Sickmann, D. Lembo, and W. Brune. Inhibition of proinflammatory and innate immune signaling pathways by a cytomegalovirus RIP1-interacting protein. *Proc Natl Acad Sci U S A*, 105(8):3094–3099, 2008.
- B. W. J. Mahy and M. H. V. van Regenmortel, editors. *Encyclopedia of Virology*, volume 1. Academic Press, 3rd edition, 2008.
- W. C. Manning and E. S. Mocarski. Insertional mutagenesis of the murine cytomegalovirus genome: one prominent alpha gene (*ie2*) is dispensable for growth. *Virology*, 167(2):477–484, 1988.
- W. C. Manning, C. A. Stoddart, L. A. Lagenaur, G. B. Abenes, and E. S. Mocarski. Cytomegalovirus determinant of replication in salivary glands. *J Virol*, 66(6):3794–3802, 1992.
- M. J. Masse, M. Messerle, and E. S. Mocarski. The location and sequence composition of the murine cytomegalovirus replicator (*oriLyt*). *Virology*, 230(2):350–360, 1997.
- S. Mathys, T. Schroeder, J. Ellwart, U. H. Koszinowski, M. Messerle, and U. Just. Dendritic cells under influence of mouse cytomegalovirus have a physiologic dual role: to initiate and to restrict t cell activation. *J Infect Dis*, 187(6):988–999, 2003.
- P. K. Mattila and P. Lappalainen. Filopodia: molecular architecture and cellular functions. *Nat Rev Mol Cell Biol*, 9(6):446–454, 2008.
- T. Mayer, M. Meyer, A. Janning, A. C. Schiedel, and A. Barnekow. A mutant form of the rho protein can restore stress fibers and adhesion plaques in v-src transformed fibroblasts. *Oncogene*, 18(12):2117–2128, 1999.

- D. J. McGeoch, M. A. Dalrymple, A. J. Davison, A. Dolan, M. C. Frame, D. McNab, L. J. Perry, J. E. Scott, and P. Taylor. The complete DNA sequence of the long unique region in the genome of herpes simplex virus type 1. *J Gen Virol*, 69:1531–1574, 1988.
- C. Ménard, M. Wagner, Z. Ruzsics, K. Holak, W. Brune, A. E. Campbell, and U. H. Koszinowski. Role of murine cytomegalovirus US22 gene family members in replication in macrophages. *J Virol*, 77(10):5557–5570, 2003.
- J. A. Mercer and D. H. Spector. Pathogenesis of acute murine cytomegalovirus infection in resistant and susceptible strains of mice. *J Virol*, 57(2):497–504, 1986.
- M. Messerle, G. M. Keil, and U. H. Koszinowski. Structure and expression of murine cytomegalovirus immediate-early gene 2. *J Virol*, 65(3):1638–1643, 1991.
- M. Messerle, B. Bühler, G. M. Keil, and U. H. Koszinowski. Structural organization, expression, and functional characterization of the murine cytomegalovirus immediate-early gene 3. *J Virol*, 66(1):27–36, 1992.
- M. Messerle, I. Crnkovic, W. Hammerschmidt, H. Ziegler, and U. H. Koszinowski. Cloning and mutagenesis of a herpesvirus genome as an infectious bacterial artificial chromosome. *Proc Natl Acad Sci U S A*, 94(26):14759–14763, 1997.
- T. C. Mettenleiter, B. G. Klupp, and H. Granzow. Herpesvirus assembly: a tale of two membranes. *Curr Opin Microbiol*, 9(4):423–429, 2006.
- S. Mitaku and T. Hirokawa. Physicochemical factors for discriminating between soluble and membrane proteins: hydrophobicity of helical segments and protein length. *Protein Eng*, 12(11):953–957, 1999.
- E. Mocarski, T. Shenk, and R. Pass. Cytomegaloviruses. In D. Knipe and P. Howley, editors, *Fields Virology*, volume 2, chapter 69, pages 2703–2773. Lippincott Williams & Wilkins, 2007.
- E. S. Mocarski, M. Bonyhadi, S. Salimi, J. M. McCune, and H. Kaneshima. Human cytomegalovirus in a SCID-hu mouse: thymic epithelial cells are prominent targets of viral replication. *Proc Natl Acad Sci U S A*, 90(1):104–108, 1993.
- T. Murata, F. Goshima, T. Daikoku, H. Takakuwa, and Y. Nishiyama. Expression of herpes simplex virus type 2 US3 affects the Cdc42/Rac pathway and attenuates c-Jun N-terminal kinase activation. *Genes Cells*, 5(12):1017–1027, 2000.

- C.-H. Nagel, K. Dohner, M. Fathollahy, T. Strive, E. M. Borst, M. Messerle, and B. Sodeik. Nuclear egress and envelopment of herpes simplex virus capsids analyzed with dual-color fluorescence HSV1(17+). *J Virol*, 82(6):3109–3124, 2008.
- K. Nakai and P. Horton. PSORT: a program for detecting sorting signals in proteins and predicting their subcellular localization. *Trends Biochem Sci*, 24(1):34–36, 1999.
- E. A. Nigg. Nucleocytoplasmic transport: signals, mechanisms and regulation. *Nature*, 386(6627):779–787, 1997.
- S. Noda, S. A. Aguirre, A. Bitmansour, J. M. Brown, T. E. Sparer, J. Huang, and E. S. Mocarski. Cytomegalovirus mck-2 controls mobilization and recruitment of myeloid progenitor cells to facilitate dissemination. *Blood*, 107(1):30–38, 2006.
- D. M. Nowlin, N. R. Cooper, and T. Compton. Expression of a human cytomegalovirus receptor correlates with infectibility of cells. *J Virol*, 65(6):3114–3121, 1991.
- K. Ogawa-Goto, K. Tanaka, W. Gibson, E. Moriishi, Y. Miura, T. Kurata, S. Irie, and T. Sata. Microtubule network facilitates nuclear targeting of human cytomegalovirus capsid. *J Virol*, 77(15):8541–8547, 2003.
- P. E. Pellett and B. Roizman. The Family Herpesviridae: A Brief Introduction. In D. M. Knipe and P. M. Howley, editors, *Fields Virology*, volume 2, chapter 66, pages 2479–2499. Lippincott Williams & Wilkins, 2007.
- E. Percivalle, M. G. Revello, L. Vago, F. Morini, and G. Gerna. Circulating endothelial giant cells permissive for human cytomegalovirus (HCMV) are detected in disseminated HCMV infections with organ involvement. *J Clin Invest*, 92(2):663–670, 1993.
- G. Pesole, G. Grillo, A. Larizza, and S. Liuni. The untranslated regions of eukaryotic mRNAs: structure, function, evolution and bioinformatic tools for their analysis. *Brief Bioinform*, 1(3):236–249, 2000.
- D. T. Petrik, K. P. Schmitt, and M. F. Stinski. Inhibition of cellular DNA synthesis by the human cytomegalovirus IE86 protein is necessary for efficient virus replication. *J Virol*, 80(8):3872–3883, 2006.
- M. C. Pizzorno and G. S. Hayward. The IE2 gene products of human cytomegalovirus specifically down-regulate expression from the major immediate-early promoter through a target sequence located near the cap site. *J Virol*, 64(12):6154–6165, 1990.



- D. Poncet, A.-L. Pauleau, G. Szabadkai, A. Voza, S. R. Scholz, M. Le Bras, J.-J. Briere, A. Jalil, R. Le Moigne, C. Brenner, G. Hahn, I. Wittig, H. Schagger, C. Lemaire, K. Bianchi, S. Souquere, G. Pierron, P. Rustin, V. S. Goldmacher, R. Rizzuto, F. Palmieri, and G. Kroemer. Cytopathic effects of the cytomegalovirus-encoded apoptosis inhibitory protein vMIA. *J Cell Biol*, 174(7):985–996, 2006.
- N. J. Proudfoot, A. Furger, and M. J. Dye. Integrating mrna processing with transcription. *Cell*, 108(4):501–512, 2002.
- K. Radtke, K. Dohner, and B. Sodeik. Viral interactions with the cytoskeleton: a hitchhiker's guide to the cell. *Cell Microbiol*, 8(3):387–400, 2006.
- W. D. Rawlinson, H. E. Farrell, and B. G. Barrell. Analysis of the complete DNA sequence of murine cytomegalovirus. *J Virol*, 70(12):8833–8849, 1996.
- M. J. Reddehase, M. Baltesen, M. Rapp, S. Jonjic, I. Pavic, and U. H. Koszinowski. The conditions of primary infection define the load of latent viral genome in organs and the risk of recurrent cytomegalovirus disease. *J Exp Med*, 179(1):185–193, 1994.
- S. R. Riddell, P. Reusser, and P. D. Greenberg. Cytotoxic T cells specific for cytomegalovirus: a potential therapy for immunocompromised patients. *Rev Infect Dis*, 13 Suppl 11:S966–73, 1991.
- L. Rohrschneider and S. Reynolds. Regulation of cellular morphology by the Rous sarcoma virus src gene: analysis of fusiform mutants. *Mol Cell Biol*, 5(11):3097–3107, 1985.
- B. J. Ryckman, M. A. Jarvis, D. D. Drummond, J. A. Nelson, and D. C. Johnson. Human cytomegalovirus entry into epithelial and endothelial cells depends on genes UL128 to UL150 and occurs by endocytosis and low-pH fusion. *J Virol*, 80(2):710–722, 2006.
- B. J. Ryckman, B. L. Rainish, M. C. Chase, J. A. Borton, J. A. Nelson, M. A. Jarvis, and D. C. Johnson. Characterization of the human cytomegalovirus gH/gL/UL128-131 complex that mediates entry into epithelial and endothelial cells. *J Virol*, 82(1):60–70, 2008.
- T. Sacher, J. Podlech, C. A. Mohr, S. Jordan, Z. Ruzsics, M. J. Reddehase, and U. H. Koszinowski. The major virus-producing cell type during murine cytomegalovirus infection, the hepatocyte, is not the source of virus dissemination in the host. *Cell Host Microbe*, 3(4):263–272, 2008.
- N. Saederup, S. A. Aguirre, T. E. Sparer, D. M. Bouley, and E. S. Mocarski. Murine cytomegalovirus CC chemokine homolog MCK-2 (m131-129) is a determinant of dissemination that increases inflammation at initial sites of infection. *J Virol*, 75(20):9966–9976, 2001.

- B. S. Salvant, E. A. Fortunato, and D. H. Spector. Cell cycle dysregulation by human cytomegalovirus: influence of the cell cycle phase at the time of infection and effects on cyclin transcription. *J Virol*, 72(5):3729–3741, 1998.
- B. Salzberger, D. Myerson, and M. Boeckh. Circulating cytomegalovirus (CMV)-infected endothelial cells in marrow transplant patients with CMV disease and CMV infection. *J Infect Dis*, 176(3):778–781, 1997.
- V. Sanchez, E. Sztul, and W. J. Britt. Human cytomegalovirus pp28 (UL99) localizes to a cytoplasmic compartment which overlaps the endoplasmic reticulum-golgi-intermediate compartment. *J Virol*, 74(8):3842–3851, 2000.
- V. Sanchez, A. K. McElroy, and D. H. Spector. Mechanisms governing maintenance of Cdk1/cyclin B1 kinase activity in cells infected with human cytomegalovirus. *J Virol*, 77(24):13214–13224, 2003 Dec.
- P. Sarnow, C. L. Jopling, K. L. Norman, S. Schutz, and K. A. Wehner. MicroRNAs: expression, avoidance and subversion by vertebrate viruses. *Nat Rev Microbiol*, 4(9):651–659, 2006.
- V. Scaria, M. Hariharan, S. Maiti, B. Pillai, and S. K. Brahmachari. Host-virus interaction: a new role for microRNAs. *Retrovirology*, 3:68, 2006.
- K. Schierling, C. Buser, T. Mertens, and M. Winkler. Human cytomegalovirus tegument protein ppUL35 is important for viral replication and particle formation. *J Virol*, 79(5):3084–3096, 2005.
- M. Schmelz, B. Sodeik, M. Ericsson, E. J. Wolffe, H. Shida, G. Hiller, and G. Griffiths. Assembly of vaccinia virus: the second wrapping cisterna is derived from the trans golgi network. *J Virol*, 68(1):130–147, 1994.
- M. Scholz, H. W. Doerr, and J. Cinatl. Human cytomegalovirus retinitis: pathogenicity, immune evasion and persistence. *Trends Microbiol*, 11(4):171–178, 2003.
- D. Schumacher, B. K. Tischer, S. Trapp, and N. Osterrieder. The protein encoded by the US3 orthologue of Marek's disease virus is required for efficient de-envelopment of perinuclear virions and involved in actin stress fiber breakdown. *J Virol*, 79(7):3987–3997, 2005.
- L. A. Shackelton and E. C. Holmes. The evolution of large DNA viruses: combining genomic information of viruses and their hosts. *Trends Microbiol*, 12(10):458–465, 2004.
- N. Sharma-Walia, P. P. Naranatt, H. H. Krishnan, L. Zeng, and B. Chandran. Kaposi's sarcoma-associated herpesvirus/human herpesvirus 8 envelope glycoprotein gB induces the

- integrin-dependent focal adhesion kinase-Src-phosphatidylinositol 3-kinase-rho GTPase signal pathways and cytoskeletal rearrangements. *J Virol*, 78(8):4207–4223, 2004.
- C. Sinzger, A. Grefte, B. Plachter, A. S. Gouw, T. H. The, and G. Jahn. Fibroblasts, epithelial cells, endothelial cells and smooth muscle cells are major targets of human cytomegalovirus infection in lung and gastrointestinal tissues. *J Gen Virol*, 76:741–750, 1995.
- C. Sinzger, M. Digel, and G. Jahn. Cytomegalovirus cell tropism. *Curr Top Microbiol Immunol*, 325:63–83, 2008.
- D. F. Smee, A. Colletti, H. A. Alaghamandan, and L. B. Allen. Evaluation of continuous cell lines in antiviral studies with murine cytomegalovirus. *Arch Virol*, 107(3-4):253–260, 1989.
- G. A. Smith and L. W. Enquist. A self-recombining bacterial artificial chromosome and its application for analysis of herpesvirus pathogenesis. *Proc Natl Acad Sci U S A*, 97(9):4873–4878, 2000.
- L. M. Smith, A. R. McWhorter, L. L. Masters, G. R. Shellam, and A. J. Redwood. Laboratory strains of murine cytomegalovirus are genetically similar to but phenotypically distinct from wild strains of virus. *J Virol*, 82(13):6689–6696, 2008.
- M. G. Smith. Propagation of salivary gland virus of the mouse in tissue cultures. *Proc Soc Exp Biol Med*, 86(3):435–440, 1954.
- L. Soroceanu, A. Akhavan, and C. S. Cobbs. Platelet-derived growth factor- $\alpha$  receptor activation is required for human cytomegalovirus infection. *Nature*, 455(7211):391–395, 2008.
- R. J. Stanton, B. P. McSharry, C. R. Rickards, E. C. Y. Wang, P. Tomasec, and G. W. G. Wilkinson. Cytomegalovirus destruction of focal adhesions revealed in a high-throughput Western blot analysis of cellular protein expression. *J Virol*, 81(15):7860–7872, 2007.
- N. Stern-Ginossar, N. Elefant, A. Zimmermann, D. G. Wolf, N. Saleh, M. Biton, E. Horwitz, Z. Prokocimer, M. Prichard, G. Hahn, D. Goldman-Wohl, C. Greenfield, S. Yagel, H. Hengel, Y. Altuvia, H. Margalit, and O. Mandelboim. Host immune system gene targeting by a viral miRNA. *Science*, 317(5836):376–381, 2007.
- M. F. Stinski and J. L. Meier. Immediate-early viral gene regulation and function. In E. S. Mocarski, editor, *Human Herpesviruses: Biology, Therapy and Immunoprophylaxis*, chapter 17, pages 241–263. Cambridge University Press, 2007.

- Q. Tang and G. G. Maul. Mouse cytomegalovirus immediate-early protein 1 binds with host cell repressors to relieve suppressive effects on viral transcription and replication during lytic infection. *J Virol*, 77(2):1357–1367, 2003.
- Q. Tang and G. G. Maul. Mouse cytomegalovirus crosses the species barrier with help from a few human cytomegalovirus proteins. *J Virol*, 80(15):7510–7521, 2006.
- Q. Tang, L. Li, and G. G. Maul. Mouse cytomegalovirus early M112/113 proteins control the repressive effect of IE3 on the major immediate-early promoter. *J Virol*, 79(1):257–263, 2005.
- Q. Tang, E. A. Murphy, and G. G. Maul. Experimental confirmation of global murine cytomegalovirus open reading frames by transcriptional detection and partial characterization of newly described gene products. *J Virol*, 80(14):6873–6882, 2006.
- T. A. Tatusova and T. L. Madden. Blast 2 sequences, a new tool for comparing protein and nucleotide sequences. *FEMS Microbiol Lett*, 174(2):247–250, 1999.
- J. Tooze, M. Hollinshead, B. Reis, K. Radsak, and H. Kern. Progeny vaccinia and human cytomegalovirus particles utilize early endosomal cisternae for their envelopes. *Eur J Cell Biol*, 60(1):163–178, 1993.
- B. L. Trus, W. Gibson, N. Cheng, and A. C. Steven. Capsid structure of simian cytomegalovirus from cryoelectron microscopy: evidence for tegument attachment sites. *J Virol*, 73(3):2181–2192, 1999.
- B. L. Trus, J. B. Heymann, K. Nealon, N. Cheng, W. W. Newcomb, J. C. Brown, D. H. Kedes, and A. C. Steven. Capsid structure of Kaposi's sarcoma-associated herpesvirus, a gammaherpesvirus, compared to those of an alphaherpesvirus, herpes simplex virus type 1, and a betaherpesvirus, cytomegalovirus. *J Virol*, 75(6):2879–2890, 2001.
- J. W. Upton, W. J. Kaiser, and E. S. Mocarski. Cytomegalovirus M45 cell death suppression requires receptor-interacting protein (RIP) homotypic interaction motif (RHIM)-dependent interaction with RIP1. *J Biol Chem*, 283(25):16966–16970, 2008.
- G. Van Minnebruggen, H. W. Favoreel, L. Jacobs, and H. J. Nauwynck. Pseudorabies virus US3 protein kinase mediates actin stress fiber breakdown. *J Virol*, 77(16):9074–9080, 2003.
- S. M. Varnum, D. N. Streblow, M. E. Monroe, P. Smith, K. J. Auberry, L. Pasa-Tolic, D. Wang, D. G. n. Camp, K. Rodland, S. Wiley, W. Britt, T. Shenk, R. D. Smith, and J. A. Nelson. Identification of proteins in human cytomegalovirus (HCMV) particles: the HCMV proteome. *J Virol*, 78(20):10960–10966, 2004.

- M. Wagner, S. Jonjic, U. H. Koszinowski, and M. Messerle. Systematic excision of vector sequences from the BAC-cloned herpesvirus genome during virus reconstitution. *J Virol*, 73(8):7056–7060, 1999.
- D. Wang and T. Shenk. Human cytomegalovirus virion protein complex required for epithelial and endothelial cell tropism. *Proc Natl Acad Sci U S A*, 102(50):18153–18158, 2005a.
- D. Wang and T. Shenk. Human cytomegalovirus UL131 open reading frame is required for epithelial cell tropism. *J Virol*, 79(16):10330–10338, 2005b.
- X. Wang, D. Y. Huang, S.-M. Huong, and E.-S. Huang. Integrin alphavbeta3 is a coreceptor for human cytomegalovirus. *Nat Med*, 11(5):515–521, 2005.
- A. P. Warren, C. N. Owens, L. K. Borysiewicz, and K. Patel. Down-regulation of integrin alpha 1/beta 1 expression and association with cell rounding in human cytomegalovirus-infected fibroblasts. *J Gen Virol*, 75:3319–3325, 1994.
- M. P. Weiner, G. L. Costa, W. Schoettlin, J. Cline, E. Mathur, and J. C. Bauer. Site-directed mutagenesis of double-stranded DNA by the polymerase chain reaction. *Gene*, 151(1-2):119–123, 1994.
- U. Welsch. Epithelgewebe. In *Lehrbuch Histologie*, chapter 3.1, pages 86–108. Urban & Fischer, Elsevier München, 2 edition, 2006.
- E. White and D. H. Spector. Early CMV gene expression and function. In E. S. Mocarski, editor, *Human Herpesviruses: Biology, Therapy and Immunoprophylaxis*, chapter 18, pages 264–294. Cambridge University Press, 2007.
- L. Wiebusch, A. Neuwirth, L. Grabenhenrich, S. Voigt, and C. Hagemeyer. Cell cycle-independent expression of immediate-early gene 3 results in G1 and G2 arrest in murine cytomegalovirus-infected cells. *J Virol*, 82(20):10188–10198, 2008.
- C. A. Wu, M. E. Carlson, S. C. Henry, and J. D. Shanley. The murine cytomegalovirus M25 open reading frame encodes a component of the tegument. *Virology*, 262(2):265–276, 1999.
- X. Zhan, M. Lee, G. Abenes, I. Von Reis, C. Kittinunvorakoon, P. Ross-Macdonald, M. Snyder, and F. Liu. Mutagenesis of murine cytomegalovirus using a Tn3-based transposon. *Virology*, 266(2):264–274, 2000.
- F.-C. Zhou, Y.-J. Zhang, J.-H. Deng, X.-P. Wang, H.-Y. Pan, E. Hettler, and S.-J. Gao. Efficient infection by a recombinant Kaposi's sarcoma-associated herpesvirus cloned in a bacterial artificial chromosome: application for genetic analysis. *J Virol*, 76(12):6185–6196, 2002.

- Z. H. Zhou, B. V. Prasad, J. Jakana, F. J. Rixon, and W. Chiu. Protein subunit structures in the herpes simplex virus A-capsid determined from 400 kV spot-scan electron cryomicroscopy. *J Mol Biol*, 242(4):456–469, 1994.
- A. Zimmermann and H. Hengel. Cytomegalovirus Interference with Interferons. In M. J. Reddehase, editor, *Cytomegaloviruses*, chapter 16, pages 321–340. Caister Academic Press, 2006.
- A. Zimmermann, M. Trilling, M. Wagner, M. Wilborn, I. Bubic, S. Jonjic, U. Koszinowski, and H. Hengel. A cytomegaloviral protein reveals a dual role for STAT2 in IFN- $\gamma$  signaling and antiviral responses. *J Exp Med*, 201(10):1543–1553, 2005.
- N. Zini, M. C. Battista, S. Santi, M. Riccio, G. Bergamini, M. P. Landini, and N. M. Maraldi. The novel structural protein of human cytomegalovirus, pUL25, is localized in the viral tegument. *J Virol*, 73(7):6073–6075, 1999.

# A Anhang

## Primers used for the Generation of a Library of MCMV Mutants

Upper case letters designate the homology to the wild type MCMV Smith strain, lower case letters designate homology to the pGP704-kan plasmid. [deleted MCMV genes] (genomic positions of the deletion)

[ $\Delta$ m01-m17] (479...16,951)

Delta1.for

5'- CAC GTG TTA GCA TAG GAA TCC AGA CGC GCG CTC GCC TGA gcgtcgtggaatgccttcgaattc -3'

Delta1.rev

5'- CTT TGA AAT CGG ACG ACC GAT CAG AAC GTC CGC CTT CGA GA aacaaggacgacgacgacaagtaa -3'

[ $\Delta$ m18-m23.1] (19,225...24,975)

m18.for

5'- CCG CTC TGC GCG AGC CGG TGG TCG TCT CCA CAG GCC CTC CGT TCA ATA AA aggacgacgacgacaagtaa -3'

m23.1.rev

5'- AAA GGC CGA GGG ACG CCC ACC CAC GAC CGA CCC ATC GTC TCG AGC TCG AA caggaacacttaacgcctga -3'

[ $\Delta$ M24-m25.2] (25,685...30,751)

M24.for

5'- CCG ATC TCG ATG GGG CCT GCC GTG CAG TGA ATC GGA TAA AAA TAT CTG AA aggacgacgacgacaagtaa -3'

m25.2.rev

5'- CTA CGA CCC GGC GCC CTA CGG GGG ACT ATA TAG GCT TGC CAA CAC TAT GA caggaacacttaacgcctga -3'

[ $\Delta$ M28-M31] (34,489...38,826)

A4.for

5'-CTG GCG GGA TAA CTG CAA GAG AGG GGA AAA GCG GTC GAT CCC AGC CGT CA ctacaggacgacgacgacaagtaa -3'

A4.rev

5'-CGG GGA GAT CAG CGA GAG GCG GAT GGG GCT CTG CGG GCG CCA GAC CGT CA gtgacacaggaacacttaacggctga -3'

[ $\Delta$ m29-M31] (36,339...38,442)

m29.for

5'- CCG CTC GGA GCG GCG CTT TTC GCT GGA GCA CGC GAG CAT TTT ATT CAT AA aggacgacgacgacaagtaa -3'

M31.rev

5'- TGC CGC CGT CCA CGA CGT ACA TGC TCT CGA CGT TGA TAC CGG CCT CGA AA caggaacacttaacgcctga -3'

[ $\Delta$ M33] (41,656...42,586)

M33.for

5'- TAA ATG ATT GAT ATC CGT CTA TCT TCG GTG TCC GGT GTC TAT CCC CAC AA aggacgacgacgacaagtaa -3'

M33.rev

5'- CGC CGA CTG AAG AGC TTG CCA GTT ATG CAT TGC ATG AAG CGT TTG TTG AA caggaacacttaacggctga -3'

## A Anhang

---

[**ΔM35-M37**] (45,969...50,165)

M35.for

5'- CGA CGG AGG AAG ACC CCA GAC GCG ACA CGA GTC TGA TGA TAA ACG AGA GA aggacgacgacgacaagtaa -3'

M37.rev

5'- AGC TGT CAA GAT GCC TTC ACG TTG GTC AGT ACC TGG TTC GGC AAG GTT AA caggaacacttaacggctga -3'

[**Δm39-m40**] (53,319...52,841)

m40.rev (KnR is inserted in reverse orientation)

5'- GGG CCT GGT TCG CGT ACA ACA TCT ACG CCG TTA GAC GTG AAT TCG TTC GA aggacgacgacgacaagtaa -3'

m39.for

5'- TGC ACG GTG GGA GAA AGT GCC TCG TCC GAG TAC CAT TTC TTC CTG AGA AA caggaacacttaacggctga -3'

[**Δm42-M43**] (54,471...57,001)

m42.for (KnR cassette is inserted in reverse orientation)

5'- GGA CAC ACA GAC TCC GAC CGT GAT GGC GGT CCA CTG AAA CTC TTT ATC CA caggaacacttaacggctga -3'

M43.rev

5'- GAC GGA ACA TCA CCA GCG TCC CCG CGC CGT TCT CTA TGT ATC CCG AAC GA aggacgacgacgacaagtaa -3'

[**ΔM45**] (59,674...62,907)

M45.for

5'- AAG CCG ATG GCG ACG GGC AGC GAC TGC GCA TGG TCG ACG AAC GGC TGT CT aggacgacgacgacaagtaa -3'

M45.rev

5- GAG GCC AGC AGA CCG CCA CCA CCG CTG CCG GGG GAG CCT TCG GGG TGG GT caggaacacttaacgcctga -3'

[**Δm106-m108**] (153,916...162,771)

A2.for

5'- GTT TTC TGA CAT GAG TCT GTG TGT TTA TTT ATT AAT TAT CTG TCA GTT CA ctacaggacgacgacgacaagtaa -3'

A2.rev

5'- CTG GGC GCC GAG GCC AGT AAT GTG CCT GTC TCC CCG GAC CCG CCT AGC AG gtgacacaggaacacttaacggctga -3'

[**ΔM116**] (167,452...168,980)

M116.for

5'- CGC TCA GGA CGA ACG GCC CGT ATT TCG CGG GGC AGT ACC TGC GAG TGC AT aggacgacgacgacaagtaa -3'

M116.rev

5'- CTC CGT GAC CTC CAA GCA GCC GAG CAT ACC CAA ACA GCC CAA GCT GGA TA caggaacacttaacgcctga -3'

[**Δm117-m120**] (169,217...174,574)

A3.for

5'- GTG TCC GAG AGG TTA AAT AGT TGA TGG GGG TGA CGG GGA AAA ACT CGC TAC ctacaggacgacgacgacaagtaa -3'

A3.rev

5'- GTA CGA GTC CGT GAC CGC GTC CCT CCC GCT CTT TCT CGT CTA CCC GAC CA gtgacacaggaacacttaacggctga -3'

[**ΔM121**] (175,903...177,674)

M121.for

5'- ATG CGT ATC GAT TTC CGG TTC ACC TGA GAC CAC GGG GAG AAG GTC GAC CA aggacgacgacgacaagtaa -3'

M121.rev

5'- TGT TGG CGC GCG GTG GCG GTG GTG CAG AGA GTG CCG CTC AAG TGA CTA AC caggaacacttaacgcctga -3'



---

[**Δm128-m138**] (168,085...193,943)

A1.for

5'- CCG GGG GCG TGA GGG ACG CGA CTG CTC ACG GTT CTG TTT GTC TGT AGA T ctacaggacgacgacgacaagtaa -3'

A1.rev

5'- CAG AGC GCG AGC TCA AGT CGC CAT CAT CTC TCG GTC GGC AGA GCC GAG GCG gtagacacaggaacacttaacggctga -3'

[**Δm139-m141**] (194,494...199,182)

m139.for

5'- GCC TCT TCG CCT CGC TCA CGT TCG ACA GGG CCA CGC CGT CCT GCA ACC GC aggacgacgacgacaagtaa -3'

m141.rev

5'- ATG GAG AGG CCG GTG ACG GCG AAC GCC ATC TCC GCG TAC AAG CGG GTG AT caggaacacttaacgcctga -3'

[**Δm144-m158**] (203,001...217,799)

Delta6.for

5'- AGC GCC GTC CGA ACC TCC TAC GCG TCT TCC TCT GTT CCT TG aggacgacgacgacaagtaa -3'

Delta6.rev

5'- CTA CCG TCT CCT CGA ATG GCA GAG AGG CGA TCT CGT ACC TCT AAC C aggaacacttaacggctga -3'

[**Δm159-m170**] (218,173...229,997)

Delta7S1.for

5'- AAC TGG AAA ATA TAG TTA GCA CCG TTA GAG AGG GCG ACA GAT TTC GAT CA ctacaggacgacgacgacaagtaa -3'

DeltaS3.rev

5'- ATG TGC TCG GTT AAC GAG TTG GCC TTC GTC CGG CTG TCC GGC ACG ACT AC gtagacacaggaacacttaacggctga -3'

[**HCMV ΔUL25**] (on the basis of the HCMV TB40/E strain, Refseq EF999921 )

UL21.5-25ko.for

5'- TAA CGT GAT TGT GAA CGC GGT TAT CGT GTT TTT GCA GCG TGA CGG TGG AA gaaaagtgccacctgcagat -3'

UL21.5-25ko.rev

5'- TGA AGG CGT CCT GCT GAC GCA CGA CGC GTA AAA AGT CAA ACA ACG caggaacacttaacggctga -3'

## Primer Sequences for the generation of Probes used for Northern Blotting

### **m106 probe**

sonde m106.for 5'- GAC GCT GAT CGC GAC GAC GA -3'

sonde m106.rev 5'- GAT CGT CCC ATG TGG ACA CA -3'

### **intron probe**

sonde intron.for 5'- GCG GTC GCG TAG ACT ATA CA -3'

sonde intron.rev 5'- GCA TCG TTG ATG ACG TGA CA -3'

### **M25 probe**

sonde M25.for 5'-AAC GCC AAC GAC GAC GAT GA-3' (original name: M25sequenzierung VI.for)

sonde M25.rev 5'-TGC GCG GCG GGG TCA TCA GA-3' (original name: 5' RACE M25 SP1.rev)

## 5'- /3'-RACE

### **M25 RACE**

(M25-1) 5'- GGA TTA TCG CGT ATC CGT CC -3'

(M25-2) 5'- CTG TCC GCC GTA CCT ATT GC -3'

(M25-3) 5'- GAG CCG GTC CTG ACC AAG AA -3'

**m108 RACE**

(108-1) 5'- CCG TAC GCC GTA TAC TTA CA -3'

(108-2) 5'- TTC GGG CGG TTG CTC GTG AA -3'

(108-3) 5'- CGG TCC GAT CGG CTC GAT GA -3'

**m106 RACE**

(106-1) 5'- GGT ATA GGA CGG GGA TTC AA -3'

(106-2) 5'- CGG CGA CGT TGT CAT CGA GA -3'

**m107 RACE**

(107-1) 5'- CGG TCC GAT CGG CTC GAT GA -3'

(107-2) 5'- GAC CGC TCG TTC ACG AGC AA -3'

## Primers for the Generation of Additional Mutants within the M24-m25.2 Region of the MCMV Genome

[ $\Delta$ M24-m25.1]

M24.for

5'- CCG ATC TCG ATG GGG CCT GCC GTG CAG TGA ATC GGA TAA AAA TAT CTG AA aggacgacgacgacaagtaa -3'

m25.1.rev

5'- GTC AAG ATC CGC AAG GGA TGG CGG ATG CCG CTG ACC TGG CCC AAG AAT TA caggaacacttaacgcctga -3'

[ $\Delta$ M24]

M24end.for

5'- TGG CGC CGA TGC CGA CGA AGC CCG GGA TCG AGT CGG CTA TGA GAT AGT AA aggacgacgacgacaagtaa -3'

M24start.rev

5'- TTC GGC CGT TTC TAC TGT TAT CGC GGG CCC CCG GAC GAC GCC ATC TAC TA caggaacacttaacgcctga -3'

[ $\Delta$ m25.1]

m25.1end.for

5'- AGG CAA CGT AAG GTG CTG TTC TCC CCA CAG AGA TCT TGT CCT GTG AAG AA aggacgacgacgacaagtaa -3'

m25.1.rev

5'- GTC AAG ATC CGC AAG GGA TGG CGG ATG CCG CTG ACC TGG CCC AAG AAT TA caggaacacttaacgcctga -3'

[ $\Delta$ M25]

M25start.for

5'- TCG CGA CAC GTC GTC GTG GAC GAC GAC GAC GAC GGA GAT TAT GAT TCA CA aggacgacgacgacaagtaa -3'

M25end.rev

5'- GAG TAG CCT TCG AAG CCT GCC TCT TCC ATG GCC GCG CAC TTG ATC AGA TA caggaacacttaacgcctga -3'

[ $\Delta$ M25non-conserved]

M25non-conserved.for

5'- CGT GCC AGC CGT CCT ATT CCC CGT GCC GGC GCG TCC CTT TCG ACC TCG AA aggacgacgacgacaagtaa -3'

M25non-conserved.rev

5'- TCG ATC ACC ATG GCG GTG GCG GAT ATC GGG GTC TCG TAT AGA TGA TTA TT caggaacacttaacgcctga -3'

---

### [ΔM25conserved]

A stop-codon (underlined) was added at the 3'-end of the 5'-M25conserved.for primer in order to preserve M25-protein expression from the M25 gene in the mutant.

M25conserved.for

5'- GGC ATC GTC GTC GAC TCC TCA TCG CAC CCA GCC TCT GCC CGT CCC ACC G TAG aggacgacgacgacaagtaa -3'

M25conserved.rev

5'- CGT GTG GCT AAG TGC TAA GTG CTT TTG GGG TTG GTT ATT CTG CTG ATT AA caggaacacttaacggctga -3'

## Primers for the generation of the pIRESM25CHA and pIRESM25NHA vectors

(EcoRI or PstI restriction sites, hemagglutinin tag)

### pIRESM25CHA

M25CHA-PstI.for

5'- aactgcagaa CTA CGCGTAGTCCGGCACGTCGTACGGGTA CAG AAA GGT ACG CTT GGA GTA C-3')

M25CHA-EcoRI.rev

5'- cggaattccggccgccATG AGC CAG TTC GTA CAG CAC GTC G -3')

### pIRESM25NHA

HANM25-EcoRI.rev

5'- ggaattcctgatcATG TACCCGTACGACGTGCCGGACTACCGC GAC CCC CCG GAG ACG ACG TCG TCG TCG TCA -3'

HANM25-PstI.for

5'- aactgcagaaTTA CAG AAA GGT ACG CTT GGA GTA C -3'

**Primers for the Shortening of the M25 ORF within the pIRES2AcGFP1 Vector PstI restriction site)**

Primer HMIEP 5'-GCG GAT CTG ACG GTT CAC TA-3'

ATG N°2 5'- tgcaactgcagCTC GAA CGC CTG TCC GAG AA -3'

(ATG N° 4/5) 5'- tgcaactgcagCGT CAC CGA CGA CTC GTC GGA TGA -3'

(ATG N° 6) 5'- tgcaactgcagGAG GAA CTA AAC GGC GAA GA -3'

(ATG N°7/8) 5'- tgcaactgcagCTT ATG CGG ACC CGG CCG ATG TGA GA -3'

(ATG N° 9) 5'- tgcaactgcagCGA CGA CGA CGG AGA TTA TGA -3'

(ATG N°10) 5'- tgcaactgcagCGT GTC GAT CAC ACG GAG AA -3'

## Primers for the Generation of Hemagglutinin-tagged viruses

(The sequence coding for the hemagglutinin-tag is underlined)

### M25HA-tagged virus

M25CHA.for

5'- CTC CTC CCC CGG CCG CCG GAG GGC CAA AGT ACT CCA AGC GTA CCT TTC TG-

TAC CCG TAC GAC GTG CCG GAC TAC GCG TAG aggacgacgacgacaagtaa -3'

M25CHA.rev

5'- CGT GTG GCT AAG TGC TAA GTG CTT TTG GGG TTG GTT ATT CTG CTG ATT AA caggaacacttaacggctga -3'

### m108HA-tagged virus

m108CHA.rev

5'- GAG CAC CCG TTC GCT TCG ATC GAG CGG TCG TGG CGT TCG CGG CAA TCA AA-

TAC CCG TAC GAC GTG CCG GAC TAC GCG TAG caggaacacttaacggctga -3'

m108CHA.for

5'- CTT CGA CCG ACC CCT CGT AGC GAC CGA CCG CTC GCT TCG ATT ACC CGC TC caggacgacgacgacaagtaa -3'

## Additional Mutants within the m106-m108 Region

### [ $\Delta$ m106]

A1.for

5'- CCG GGG GCG TGA GGG ACG CGA CTG CTC ACG GTT CTG TTT GTC TGT AGA T ctacaggacgacgacgacaagtaa -3'

m106.rev

5'- CCC GCA TCT GTA CGC AAT TTT CTG GTC TCA CGG GAG TCG AGG TCT CAC GG caggaacacttaacggctga -3'

### [ $\Delta$ intron]

RVSS25.for

5'- GCCGAATCTGTGGTTGTCCCCTCACACGCTTTGTTACGGTTCGGATAAA aggacgacgacgacaagtaa -3'

RVSS25.rev

5'- GAG CGC CTC GGG TAT GCT ATA TGT CCC CCT TTT TGT ACC TGT GTC ATT AA caggaacacttaacggctga -3'

### [ $\Delta$ m107-m108]

m107.for

5'- TCC AGG TAT CCT ACC TAG CGC GGT CAC GTC CGA CGC CGC AAA GTA TAA TA aggacgacgacgacaagtaa -3'

A2.rev

5'- CTG GGC GCC GAG GCC AGT AAT GTG CCT GTC TCC CCG GAC CCG CCT AGC AG gtgacacaggaacacttaacggctga -3'

### [ $\Delta$ 7.2kb RNA]

delta7.2kbRNAsplicedonor.for

5'- ACG ATA AAA GAG GAC AGT AGA TAA AGA TTG ATT TAG TGT ACA CAC GTT GT aggacgacgacgacaagtaa -3'

delta7.2kbRNAsplicedonor.rev

5'- AGG CCG AGG AGG CGG CGG CGG AGG TGA CGG CGT CCC GAA GGC CCG GAG CT caggaacacttaacggctga -3'

### [m108mutATG]

m108mutATG.for (nucleotides that have been exchanged, CAT → TCA are marked in bold letters)

5'-C TCG TGC ATG TCG GCG GTC CGC GGT GAG GTT ATA GAC **TCA** CTG CTA GGC G aggacgacgacgacaagtaa -3'

m108start.rev

5'- CAC GCC TAG GCT GGG CGC CGA GGC CAG TAA TGT GCC TGT CTC CCC GGA CC caggaacacttaacggctga -3'

### [ $\Delta$ m108]

m108middle.for

5'- CAC ATT TCG GGC GGT TGC TCG TGA ACG AGC GGT CGC TCG TCA CGG CGA TA aggacgacgacgacaagtaa -3'

m108middlel.rev

5'- CGT CGA GCG GGT GTC CGA AGA GGG GTT TTC CCG GTC CGA TCG GCT CGA TG caggaacacttaacggctga -3'

### [m108 $\Delta$ miRNA]

miRNAm108ko.for

5'- GTA CGT AGG GAG GTG CTC CAT CGG CGG CCT GAC CGA CGC TC -3'

miRNAm108-1ko.rev

5'- GTT ACG CAC GTG TAA GTA TAC GGC GTA CGG AGC TCC GTT C-3'

### [m108 $\Delta$ intron]

m108middle.for

5'-CAC ATT TCG GGC GGT TGC TCG TGA ACG AGC GGT CGC TCG TCA CGG CGA TA-3'

m108start.rev

5'-CAC GCC TAG GCT GGG CGC CGA GGC CAG TAA TGT GCC TGT CTC CCC GGA CC-3'

# Curriculum Vitae

**Dipl. Biol. Sarah Sengstake**

Adresse: Stolzestrasse 45, 30171 Hannover

Geburtsdatum: 24.06.1978 in Bremen

Staatsangehörigkeit: deutsch

email: sengstakesarah@gmail.com

---

## Hochschulausbildung

- |             |  |
|-------------|--|
| 2005 – 2009 | Medizinische Hochschule Hannover<br>Doktorandin, Institut für Virologie, AG Messerle   |
| 2005 – 2008 | Stipendiatin des DFG-Graduiertenkollegs 745<br>"Mukosale Erreger-Wirt Interaktionen"   |
| 1998 – 2004 | Universität Konstanz<br>Diplom im Fach Biologie<br>Titel der Diplomarbeit: "Regulation of Activation-Induced CD21-Shedding" angefertigt am Biotechnologie Institut Thurgau an der Universität Konstanz, Schweiz. Betreuer: Harald Illges |
| 1998        | Universität Hamburg<br>Chemiestudium   |
- 

## Schulbildung

- |             |                                       |
|-------------|---------------------------------------|
| 1989 – 1997 | Gymnasium Tonndorf, Hamburg<br>Abitur |
| 1985 – 1989 | Grundschule Darne, Lingen (Ems)       |

---

## Publikationen

Sarah Sengstake, Corinna Benkartek, Mandy Glass and Martin Messerle  
**MCMV M25-induced cell rounding**, in preparation

Sarah Sengstake, Eva-Maria Boneberg and Harald Illges  
**CD21 and CD62L-shedding are both inducible via P2X7Rs**  
Int Immunol. 2006 Jul;18(7):1171-8

---

## Vorträge und Poster zu der vorliegenden Arbeit

Sarah Sengstake and Martin Messerle  
**Maintenance of normal cell morphology in cells infected with mouse cytomegalovirus**  
European Congress of Virology, Nürnberg, 2007 (Vortrag)

Sarah Sengstake and Martin Messerle  
**Identification of viral factors for the epithelial cell tropism of mouse cytomegalovirus and virus induced cell rounding**  
Klausurtagung des DFG-Graduiertenkollegs 745, Ruthe, 2007 (Vortrag)

Sarah Sengstake and Martin Messerle  
**Investigation of the infection of epithelial cells with mouse cytomegalovirus.**  
Klausurtagung des DFG-Graduiertenkollegs 745, Bergkirchen, 2006 (Vortrag)

Sarah Sengstake, Corinna Benkartek, Andreas Busche and Martin Messerle  
**Characterisation of a gene involved in mouse CMV-induced cell rounding.**  
International Herpesvirus Workshop, Estoril, Portugal, 2008 (Poster)

Sarah Sengstake, Corinna Benkartek, Martin Messerle  
**Investigation of the infection of epithelial cells with mouse cytomegalovirus.**  
Workshop der Gesellschaft für Zellbiologie "Cell Biology of Viral Infections ",  
Deidesheim, 2006 (Poster)

Sarah Sengstake, Corinna Benkartek, Martin Messerle  
**Investigation of the infection of epithelial cells with mouse cytomegalovirus.**  
Fachtagung der Gesellschaft für Virologie, München, 2006 (Poster)